SPRAY CHARACTERIZATION FOR WATER-in-DIESEL EMULSIONS

A Thesis Submitted to
the Graduate School of Engineering and Science of
İzmir Institute of Technology
in Partial Fulfillment of the Requirements for the Degree of

MASTER OF SCIENCE
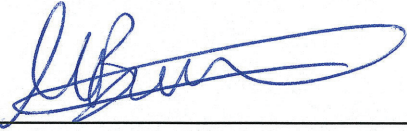
in Mechanical Engineering

by
Seven Burçin ÇELLEK

July 2019
İZMİR

We approve the thesis of **Seven Burçin ÇELLEK**

Examining Committee Members:

Assoc. Prof. Dr. Ünver ÖZKOL
Department of Mechanical Engineering, İzmir Institute of Technology
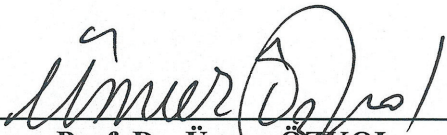

Assoc. Prof. Dr. Murat BARIŞIK
Department of Mechanical Engineering, İzmir Institute of Technology

Assist. Prof. Dr. Levent BİLİR
Department of Engineering, Yaşar University

11 July 2019

Assoc. Prof. Dr. Ünver ÖZKOL
Supervisor, Department of Mechanical Engineering
İzmir Institute of Technology

Prof. Dr. Sedat AKKURT
Head of the Department of Mechanical
Engineering

Prof. Dr. Aysun SOFUOĞLU
Dean of the Graduate School of
Engineering and Science

ABSTRACT

SPRAY CHARACTERIZATION FOR WATER-in-DIESEL EMULSIONS

As we consider the pollutions caused by combustion engines, they have a big impact on several problems like global warming, acid rain, etc. Engineers and scientists are willing to control the pollutants and to reduce them as low as possible. There are some possible solutions to reduce environmental problems such as diesel particulate filters, high pressure fuel injection equipment, and sophisticated piezo injectors and associated control systems. However, all mentioned solutions need a modification on the current engine system to be used. Because of high costs of modification, recently, fuel-based solutions are more popular. This study investigates one of the possible fuel-based solutions which is water-in-diesel emulsions.

Through the work, spray characteristics such as spray penetration and spray angle have been examined and compared with neat diesel spray. In order to achieve the purpose of this research, experiments have been carried out in a constant volume combustion chamber and all have been recorded by the help of a high-speed camera. A Matlab algorithm has been developed to analyse the recorded data. It was found that, due to lower volatility of the water, water-in-diesel emulsion has longer and wider spray when compared to neat diesel spray. According to the literature, this results in better fuel-air mixing for combustion process, hence cleaner exhaust gas.

ÖZET

SU İÇEREN DİZEL EMÜLSİYONLARI İÇİN PÜSKÜRTME KARATERİZASYONU

Yanma motorlarından kaynaklanan çevre kirlilikleri düşünürsek, küresel ısınma, asit yağmurları gibi birçok problemler üzerinde büyük etkileri var. Mühendisler ve bilim insanları çevre kirliliklerini kontrol etmek ve onları olabildiğince azaltmayı istiyorlar. Çevresel problemleri azaltmanın dizel partikül filtresi, yüksek basınçlı yakıt enjeksiyon ekipmanları, ve piezo enjektörler ve ilgili kontrol sistemleri gibi olası çözümleri var. Fakat, bütün bahsedilen çözümlerin kullanılabilmesi için mevcut motor sisteminde modifikasyon yapılması gerekir. Modifikasyonun yüksek maliyetleri yüzünden, son zamanlarda, yakıt-bazlı çözümler daha popülerdir. Bu çalışma yakıt-bazlı çözümlerden bir tanesi olan su içeren dizel emülsiyonlarını inceler.

Çalışma boyunca, sprey uzunluğu ve sprey açısı gibi sprey karakterizasyonları incelendi ve saf dizel sprey ile karşılaştırıldı. Çalışmanın amacını başarabilmek için, sabit hacimli yanma odasında deneyler gerçekleştirildi ve hepsi yüksek hızlı kamera yardımı ile kaydedildi. Kaydedilen datayı analiz edebilmek için bir Matlab algoritması geliştirildi. Suyun alçak uçuculuğundan ötürü, su içeren dizel emülsiyonu saf dizel spreyi ile kıyaslandığında daha uzun ve daha geniş spreye sahip olduğu bulunmuştur. Literatüre göre, bu durum yanma prosesi için daha iyi yakıt-hava karışımı ile sonuçlanır, böylelikle daha temiz eksoz gazı oluşur.

TABLE OF CONTENTS

LIST OF FIGURES

LIST OF TABLES

LIST OF ABBREVIATIONS/SYMBOLS

SI	Spark-Ignition
CI	Compression-Ignition
BDC	Bottom Dead Center
TDC	Top Dead Center
ECU	Engine Control Unit
TPS	Throttle Position Sensor
FIE	Fuel Injection Equipment
AFR	Air/Fuel Ratio
VCO	Valve Covered Orifice
bsfc	Brake Specific Fuel Consumption
HLB	Hydrophilic-Lipophilic Balance
ULSD	Ultra Low Sulphur Diesel
PID	Pressure Ignition Delay
LID	Luminous Ignition Delay
CVCC	Constant Volume Combustion Chambe
T	Temperature
P	Pressure
PCV	Pressure Control Valve
VCV	Volume Control Valve
WiDE	Water-in-Diesel Emulsion

NOMENCLATURE

Oh	Ohnesorge Number
We	Weber Number
Re	Reynolds Number
ρ	Density of the Fluid (kg/m^3)
ϑ	Velocity of the Fluid (m/s)
L	Characteristic Length, typically the droplet diameter (m)
σ	Surface Tension (N/m)
u	Velocity of the Fluid with respect to the object (m/s)
μ	Dynamic Viscosity of the Fluid (Pa.s)
HLB_{comb}	Final HLB value
HLB_{Si}	Surfactant HLB value
W_{Si}	Mass Ratio of the Surfactant
$(H_2O)_i$	Initial Water Content
$(H_2O)_f$	Final Water Content
P	Partial Pressure in bar
V	Volume of the chamber which is 0.00205 m^3
R	Universal gas constant which is 8.314 J/ (K mol)
T	Temperature of chamber which is 298 K
n	Actual mol number of the reactants
x	Actual total mol number of the reactants
M_{C2H2}	Molar mass of acetylene which is 26 kg/kmol

M_{O2} Molar mass of oxygen which is 32 kg/kmol

M_{N2} Molar mass of nitrogen which is 28 kg/kmol

M_{Ar} Molar mass of argon which is 39.95 kg/kmol

d   Density of the reactants which is 5 kg/m^3

I.P.   Indicated Power (kW)

P_m Indicated Mean Effective Pressure (Pa)

l   Length of Stroke (m)

A   Piston Area (m^2)

N   Engine Speed (rpm)

k   Constant (k=1 for 2-cylinder engine, k=2 for 4-cylinder engine)

B.P.   Brake Power (kW)

T   Engine Torque (Nm)

F.P.   Fuel Power (kW)

η_{it} Indicated Thermal Efficiency

$\dot{m}_f$ Mass Fuel Rate (kg/sec)

C.V.   Calorific Value of Fuel (J/kg)

η_{bt} Brake Thermal Efficiency

Bsfc   Brake Specific Fuel Consumption (kg/kWh)

CHAPTER 1

INTRODUCTION

The number of automobiles is rising dramatically day by day around the world. One of the drawbacks of internal combustion engines is their effect on pollutants. Environment is highly influenced due to pollutants produced by internal combustion engines. In order to avoid high pollutant emission levels, there are strict regulations and requirements about pollutant levels. As a result of strict regulations, many alternative fuels for diesel engines have been investigated by many researchers. The idea of this research has been arisen from the alternative fuel types. Water-in-diesel emulsions are one the alternative fuels. The main focus of this research is spray characterization of water-in-diesel emulsions.

In Chapter 2, an overview of internal combustion engines and fuel injection equipment are introduced firstly. To understand the spray characteristics, brief information is given about spray formation. The effect of injection pressure on spray characteristics is explained. Additionally, alternative fuel types, which are biodiesel and water-in-diesel emulsions are introduced. Furthermore, preparation of emulsion and its effect on combustion process are explained briefly.

In Chapter 3, detailed information about the test rig used in the study is given. How the emulsified fuel is prepared is explained through the chapter. High-speed optical system is introduced. Image processing steps are explained and Matlab algorithm is clarified.

In Chapter 4, results and discussion section is introduced. In-depth discussion of the results is provided. Image processing provides an opportunity to comment on the results.

In Chapter 5, conclusion and future works are presented.

CHAPTER 2

LITERATURE SURVEY

The internal combustion engine is a heat engine where the burning of the mixture of a fuel and an oxidizer occurs in a combustion chamber. It is divided into two categories according to the formation of combustion process: Spark-Ignition (SI) Engines and Compression-Ignition (CI) Engines. There are four-stroke cycles for both engine types in order to complete the combustion. These are intake, compression, ignition, and exhaust. SI engines and CI engines differ in both intake and ignition cycles. Additionally, they use different types of fuels. Gasoline is used as a fuel in SI engines. Diesel is used as a fuel in CI engines. In SI engines, the mixture of gasoline fuel and air is introduced into the chamber during the intake cycle. Intake cycle lasts until the piston reaches bottom dead center (BDC). The mixture is compressed by the help of a piston until it reaches top dead center (TDC). Visual representation of BDC and TDC is given in Figure 2.1.
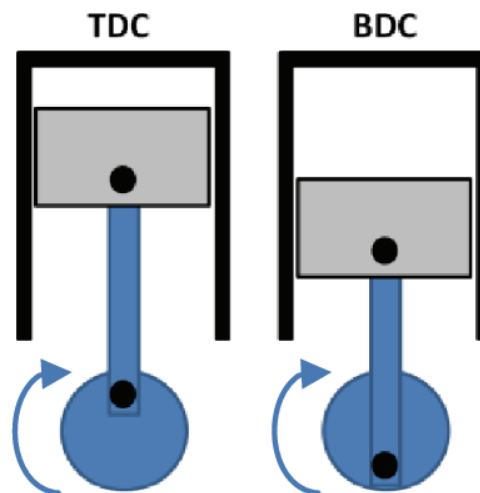
Figure 2. 1. Piston Positions (Source: (92))

When the compression is finished, the compressed air-fuel mixture is ignited by a spark plug and combustion occurs. Exhaust cycle follows combustion cycle in order to exhaust all the combustion products. In CI engines, only air is introduced into the chamber during the intake cycle. Air is compressed by the help of a piston. As

compression is finished, diesel fuel is introduced into the chamber by the help of an injector. When compressed air comes across the diesel fuel, combustion occurs. After that, exhaust cycle takes place. When combustion process in CI engines is examined in more detail, there are four stages of combustion shown in Figure 2.2. These are ignition delay period, premixed combustion phase, mixing-controlled combustion phase, and late combustion phase.
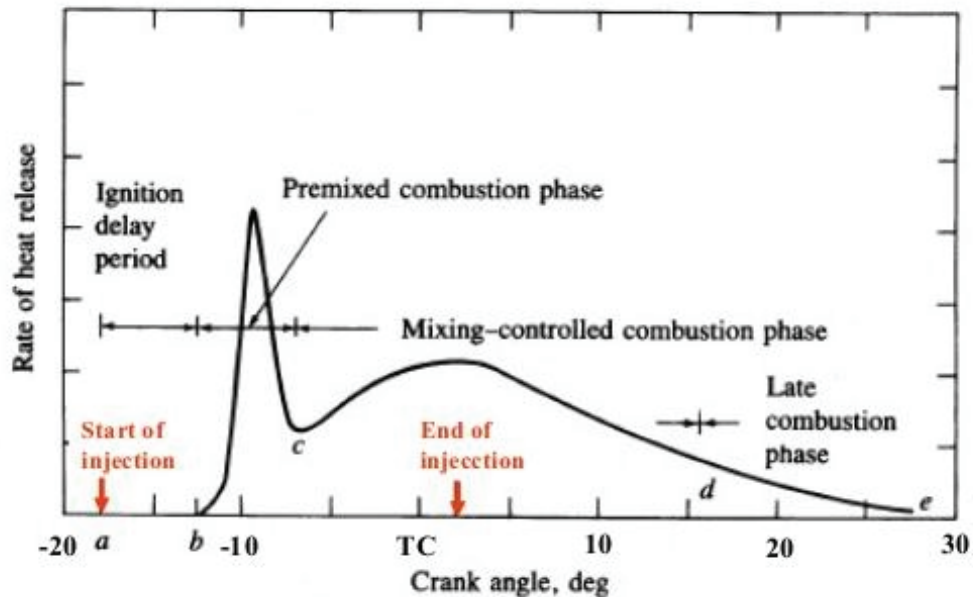
Figure 2. 2. Four Stages of Combustion in CI Engines (Source: (1))

The fuel ignites with a delay when it is injected into the chamber. The ignition delay period is the period between the start of injection and the start of combustion which is shown in Figure 2.2. The ignition delay period decreases as the engine speed increases. Figure 2.3 represents the cylinder pressures for retarded and advanced ignition timing as a function of crank angle.

If there is no delay, the fuel will start igniting at the injector and there will not be sufficient oxygen around the injector to complete the combustion. So, it results in incomplete combustion. On the other hand, if ignition delay period is too long, the amount of fuel availability for simultaneous explosion will be too much. So, it results in rapid pressure rise, hence knocking occurs. Ignition delay is composed of physical delay and chemical delay. These delays take place almost at the same time. Physical delay involves atomisation, vaporisation, and mixing of air-fuel. It depends on the fuel type,

mixture temperature, and pressure. Chemical delay involves precombustion reactions. Ignition delay is very important because of its effect on both engine performance and emission formations. Premixed combustion period is the period between the start of combustion and the point of maximum pressure. It is the combustion of the entered fuel which has mixed with air within flammability limits. It affects both soot formation and NO_x formation. Mixing-controlled period is the period that combustion is controlled by injection rate. It lasts until the maximum temperature occurs. Late combustion period is counted as the combustion of the unburnt fuel particles left.
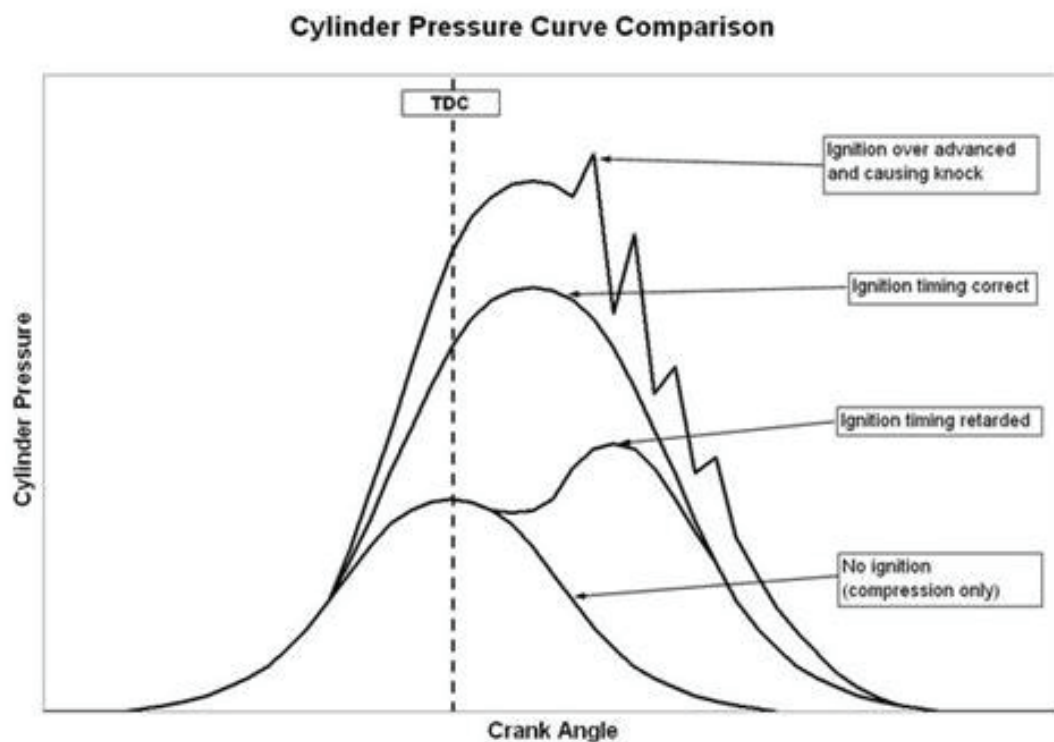
Figure 2. 3. Effect of Different Ignition Timing (Source: (2))

Differences between the SI and CI engines cause differences in engine performance and in emission rates. In order to achieve compression ignition in CI engines, higher compression ratio is needed. That means CI engines have greater torque produced and greater thermal efficiency than SI engines. Therefore, CI engines are more preferable especially for heavy duty vehicles. On the other hand, considering the pollutants produced by internal combustion engines, these have a big impact on several problems like global warming, acid rain, etc.

Engineers and scientists are willing to control the pollutants and to reduce them as low as possible. In order to do that, there are some possible solutions such as diesel

4

particulate filters, high pressure fuel injection equipment, and sophisticated piezo injectors and associated control systems. Since a modification needs to be applied to the existing engines in order to use these solutions, it is going to be expensive. So, fuel-based solutions can be cheaper and more proper possibilities because they can be used in existing engines. Biodiesel fuel is one of the oldest alternative fuels for compression ignition engines. Because of its higher viscosity, there are disadvantages of using it as a fuel as well as advantages. Its properties, its effect on pollutants, and its effect on spray characterization will be given in details in the following sections. Another alternative fuel is water-in-diesel emulsion which is the main focus of this review. Its properties, its effect on pollutants, and its effect on spray characterization will be given in details in the following sections. For better understanding of spray characterization, spray properties will be introduced at first.

2.1. Fuel Injection Equipment

Fuel injection is defined as the fuel introduction into the combustion chamber by the help of an injector. The amount (by weight) of fuel required by the engine can be determined by the amount (by weight) of air entrained into the chamber. This information is provided via a mass flow sensor, the sensor sends the required signals to the Engine Control Unit (ECU). In addition to this information, ECU can use the amount of required power output (engine load), which is provided via a Throttle Position Sensor (TPS), while calculating the amount of fuel needed. Right after the information transfer is completed, fuel is transported from the fuel tank by the help of fuel lines and pressurised up to the desired pressure by using fuel pumps. Fuel pressure regulator adjusts the correct amount of fuel pressure. The fuel is supplied equally into the required number of cylinders by the help of a common rail. A schematic of the Fuel Injection Equipment (FIE) is represented in Figure 2.4 given below. Since it affects the engine performance and emission rate, it is important to understand how fuel injection system works. There are two important parameters that affect the engine performance and the emission rate: injection pressure and injection timing. They are explained in detail below.
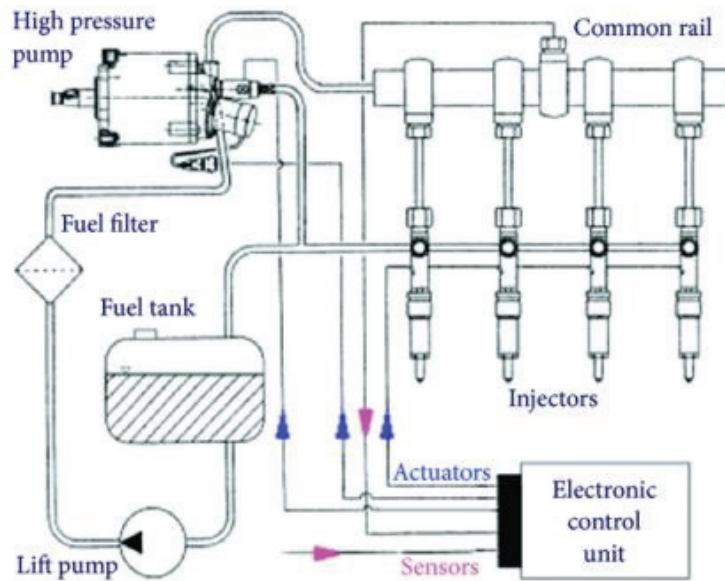
Figure 2. 4. Schematic of Fuel Injection Equipment (Source: (3))

2.1.1. Effect of Injection Pressure and Injection Timing

The purpose behind the development of the fuel injection system is to obtain sufficient evaporation of fuel in a shortest time by achieving a high degree of fuel atomisation and to utilise the air/fuel charge by achieving the sufficient spray penetration. It is developed to enhance the efficiency with higher injection pressure.

In order to calculate the efficiency, three concepts of power - which are fuel power, indicated power, and brake power - should be understood clearly. Fuel power is the power of fuel which can be calculated as multiplication of calorific value of fuel with fuel consumed (by mass). Calorific value of fuel is defined as the amount of heat released when 1 kilogram of fuel is burned completely. Indicated power is the power produced in the chamber. It can be considered as the power left from the fuel power when removing the heat loss from the fuel power. Brake power is the power produced at the crank shaft. It can be considered as the power left from indicated power when removing the friction loss from the indicated power. By means of these, indicated thermal efficiency is the ratio of indicated power and fuel power, and brake thermal efficiency is the ratio of brake power and fuel power. Another parameter to compare the

efficiency is the brake specific fuel consumption (bsfc). Brake specific fuel consumption is the ratio of the fuel mass flow rate and the engine output power (brake power).

$$I.P. = \frac{P_m lAN}{60000 * k}$$

$$B.P. = \frac{2\pi NT}{60000}$$

$$F.P. = I.P. - B.P.$$

$$\eta_{it} = \frac{I.P.}{\dot{m}_f * C.V.}$$

$$\eta_{bt} = \frac{B.P.}{\dot{m}_f * C.V.}$$

$$bsfc = \frac{\dot{m}_f}{B.P.}$$

If the injection pressure is low, fuel spray droplet size will increase, hence the ignition delay period. It ends up with higher piston pressure and lower brake thermal efficiency. If the injection pressure is extremely high, fuel spray droplet size will extremely decrease, hence the ignition delay period. It ends up with inhomogeneous mixture inside the chamber and brake thermal efficiency decreases. The spray formation will be explained in detail at the spray formation section. So, it is crucial to adjust the injection pressure accurately.

Furthermore, fuel injection system optimises the Air/Fuel Ratio (AFR) which is the mass ratio of Air to Fuel presented in the combustion chamber. It depends on the AFR whether the mixture inside the chamber is combustible or not. Depending on that, the amount of energy released and the amount of pollutants produced alter. It decides whether the complete combustion occurs. Complete combustion means cleaner combustion. So, it is important to adjust the injection pressure accurately (4).

In addition to that, it is important to inject the fuel at the right time. Injection timing has a great influence on both the engine performance and emission rates. It directly affects the ignition delay period. For earlier injection timing, the ignition delay

will increase due to the lower temperature and pressure of air. For later injection timing, the ignition delay will decrease due to the higher temperature and pressure of air.
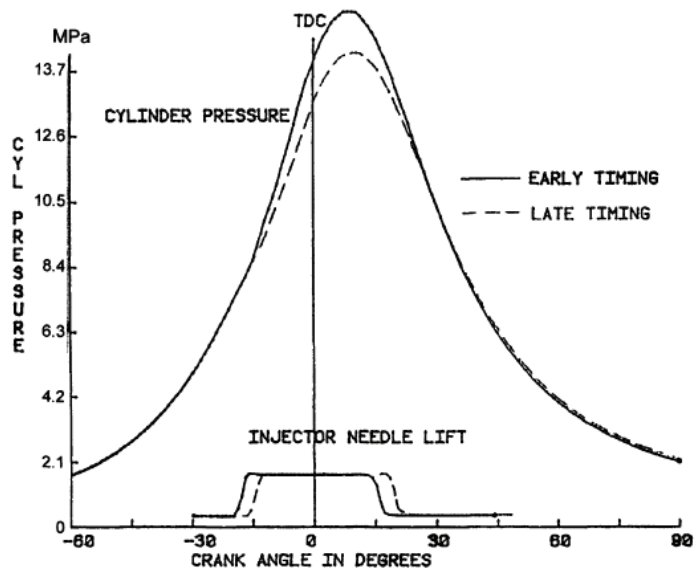
Figure 2. 5. In-cylinder Pressure Due to Different Injection Timings (Source: (5))

As it can be noticed from Figure 2.5, for early injection timing, combustion starts earlier which results in higher in-cylinder pressure.
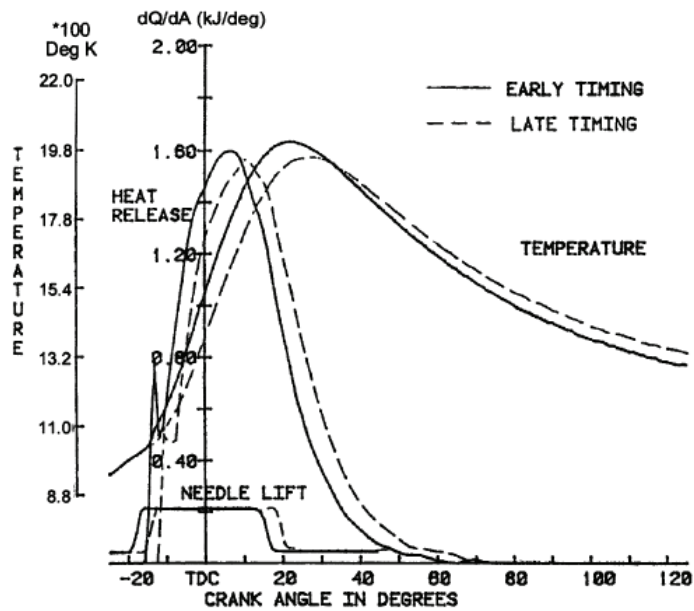
Figure 2. 6. Combustion Analysis of Different Injection Timings (Source: (5))

Figure 2.6 shows us the combustion analysis of different injection timings. As it can be seen from the graph, for early injection timing, cylinder temperature increases sharply as soon as the heat release begins. Therefore, it reaches a higher peak value and results in higher NO_x production. Additionally, if the definition of heat release is considered, the area under the heat release curve gives the amount of fuel burned. According to this, more fuel is burned before TDC for early injection timing. However, more fuel is burned later in the expansion stroke for late injection timing. Because of expansion, temperature decreases. At the same time, as the combustion continues, heat is still supplied which increases the cylinder temperature. At the end, it results in higher exhaust temperature, hence higher soot formation.

Additionally, the initial heat release peak occurs as a result of premixed combustion of fuel injected during the ignition delay period. As the ignition delay period increases, more fuel will premix and burn. Ignition delay period increases as a result of lower temperature. For early injection timing, injection starts at a lower temperature, so ignition delay period lasts longer and more fuel is ignited in the premixed combustion phase. Consequently, due to both higher peak cylinder temperature and more premixed burning, NO_x emission is higher for early injection timing (5).

2.1.2. Spray Formation

Spray characteristics such as spray pattern, spray angle, drop size, and spray impact are significantly affected by the nozzle type (6). A spray nozzle is responsible for dispersion of liquid into a spray. The nozzle is used for the following purposes:

> ➢ It should atomize the fuel because it is important to obtain better air-fuel mixing.
> ➢ It should distribute the fuel over an area within the combustion chamber.
> ➢ It should prevent the occurrence of fuel striking on the walls because it causes unburned hydrocarbons on the walls which is an unwanted situation.

Briefly, regardless of the type of the fuel injection system, all nozzles must fulfil the engine performance requirements by producing correct fuel spray. Additionally, they

should be designed accurately to prevent fuel leakage on the common rail type of fuel injection system. There should be no dripping on the rail system. They should be designed by considering the fatigue strength requirements on the unit injector/unit pump type of fuel injection system to resist the pressure pulsing conditions. They should be designed to obtain minimal hydraulic dead volume on the pump-line-nozzle type of fuel injection system (7, 8).

There are 4 main types of nozzles being used in internal combustion (IC) engines. These are single-hole nozzle, multi-hole nozzle, pintle nozzle, and pintaux nozzle. Figure 2.7 shows us the visual representative of nozzle types.
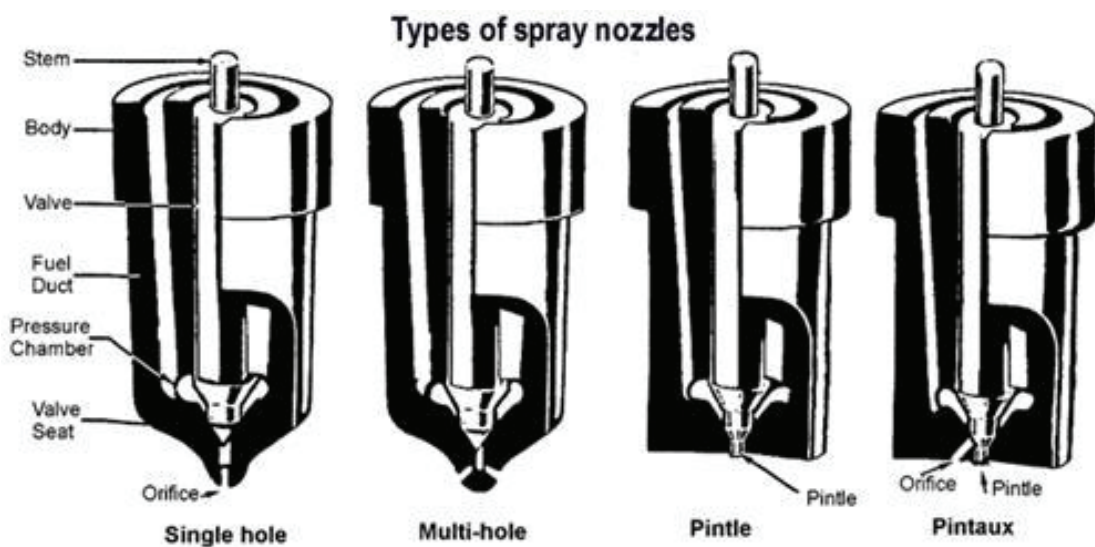
Figure 2. 7. Types of Spray Nozzle (Source: (8))

Single-hole type of nozzle has a single hole at the center of the body which is closed by the nozzle valve. The diameter of the hole is about 0.2 mm. Spray can be pressurized up to 10 MPa and spray angle is about 15 degrees for this type of nozzle. It must be used in higher velocities in order to achieve better air-fuel mixture for combustion. Additionally, it has a disadvantage of dribbling.

Multi-hole type of nozzle has multiple holes varied from 4 to 18 in the tip of the nozzle. The diameter of the holes is in between 35 and 200 micrometers. Injection pressure is about 18 MPa and spray angle is about 20 degrees. It has an advantage of distributing fuel properly.

Pintle type of nozzle has an extended stem of nozzle valve, called as a pin or a pintle, which protrudes through the mouth of the nozzle. The shape and dimensions of

the pintle depends on the requirements. Injection pressure is about 10 MPa and spray angle is about 60 degrees. It prohibits weak injection and dribbling as well as the carbon deposition on the nozzle hole.

Pintaux type of nozzle has an auxiliary hole drilled, which is called as orifice, in the nozzle body differently from pintle type of nozzle. A small amount of fuel is injected through orifice slightly before the main injection. At low speeds, most of the fuel is injected through orifice because the needle valve does not lift fully. This type of nozzle has both advantage and disadvantage. It has a better cold starting performance. However, injection characteristics are worse than multi-hole type of nozzle (8).

Additionally, there are 2 main types of nozzle in direct injection diesel engines: the sac hole nozzle and the valve covered orifice (VCO). Figure 2.8 represents us these nozzle types.
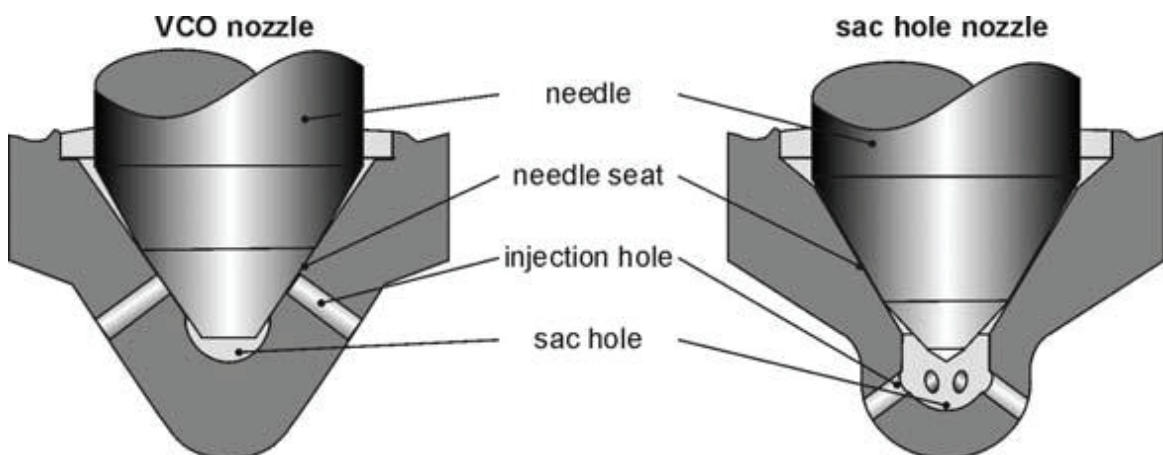
Figure 2. 8. Nozzle Types in Direct Injection Diesel Engines (Source: (9))

As it can be noticed from Figure 2.8, the sac hole nozzle has an additional volume below the needle seat. This volume causes the increased distance between needle seat and injection hole. As a result, it ends up with a very symmetric spray because the eccentricity of the needle tip does not have an effect on the mass flow through the different holes. Besides this advantage, it has a disadvantage of increased hydrocarbon emissions due to the same reason. Because of the increased distance between injection hole and needle seat, the fuel collected at this volume can enter the chamber, which causes the soot formation, after the end of the injection. That's why; this volume should be kept as small as possible which leads us to VCO nozzle. However, it has also a disadvantage of lower spray quality. Because an eccentricity of

the needle tip causes an uncontrollable variation of the discharge through the different nozzle holes, additional structural actions should be taken to prevent the radial motion of the nozzle tip (9).
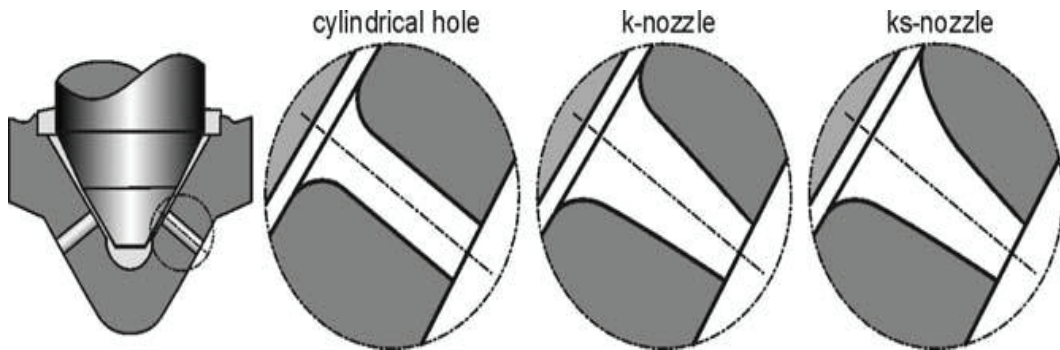
Figure 2. 9. Nozzle Hole Geometries (Source: (9))

For improved inflow conditions and abrasion produced in advance, the inlets of the nozzle holes are usually rounded. Figure 2.9 shows us the different nozzle hole geometries that are being used according to the application types. The strongest cavitation is produced in cylindrical hole and it ends up with an increased spray breakup with a large spray divergence near the nozzle. The cavitation effect decreases by reducing the effective cross-sectional area along the hole in axis-symmetric conical nozzle (k-nozzle). Spray penetration increases in conical type of nozzle. If the reduction of cross-sectional area depends on the distribution of mass flow to completely suppress the cavitation, it is the conical and flow optimized nozzle (ks-nozzle) (9).

As it is mentioned above, besides spray angle, spray pattern also depends on the type of the nozzle. There are 4 main spray patterns: Solid Stream, Hollow Cone, Full Cone, and Flat Spray. Figure 2.10 shows us the visual representative of the spray patterns.
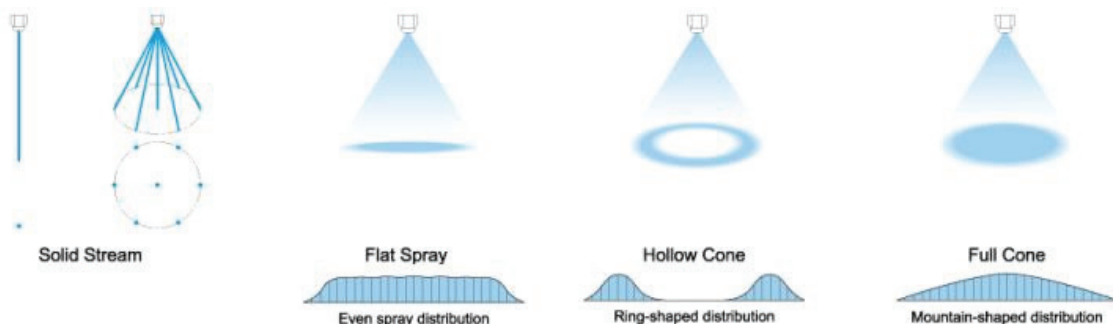
Figure 2. 10. Spray Patterns (Source: (12))

Solid stream type of spray pattern is mostly used in cleaning applications because of its high impact per unit area. Tank-cleaning nozzles can be given as an example of this type of spray pattern. Flat spray is shaped by an elliptical or a round orifice on a deflective surface that is tangent to the exit orifice. Based on the uniformity of the spray, it is divided into 2 categories: tapered and even. Tapered flat spray patterns are useful for overlapping patterns between multiple nozzle headers. Even flat spray patterns are used for creating a uniform spray pattern. Hollow cone spray is produced by an orifice that is tangent to a cylindrical swirl chamber opened at one end or by a spiral design of the nozzle. It provides better atomization of liquids at low pressure, smaller droplet size, and supplies quick heat transfer. In order to create full cone spray, liquid is swirled within the nozzle and mixed with non-spinning liquid before exiting through an orifice. It provides a uniform spray pattern of medium to large droplet size (6).

Diesel engine sprays usually have full-cone type of the spray pattern. Diesel spray formation is shown in Figure 2.11. As the liquid is injected, starting from the nozzle exit, firstly, intact liquid core exists. A few nozzle diameters further downstream, there are ligaments which are the large droplets. After that, ligaments start to break up into smaller droplets in the thick zone. Thick zone is the zone where volume fraction and mass fraction of the liquid phase are high. For further downstream, the breakup of the liquid continues, meanwhile the surrounding gas keeps being entrained into the spray area. The thin zone and the dilute zone follow the thick zone, respectively. The thin zone is the zone where volume fraction of the liquid phase is low and mass fraction of the liquid is still high. The dilute zone is the zone where both volume fraction and mass fraction of the liquid are negligible (4).

There are two main breakup regimes of the spray: Primary Breakup and Secondary Breakup. Figure 2.12 represents us the schematic of spray breakup regimes. Primary breakup is the breakup of the intact core liquid into ligaments. Cavitation and turbulence are the main breakup mechanisms. They are produced inside the injection holes due to high injection pressures. They are explained in detail at below section. Primary breakup is the mechanism which determines the size of the droplets, hence evaporation behaviour and starting point of secondary breakup. Secondary breakup is the breakup of droplets into smaller droplets (4).
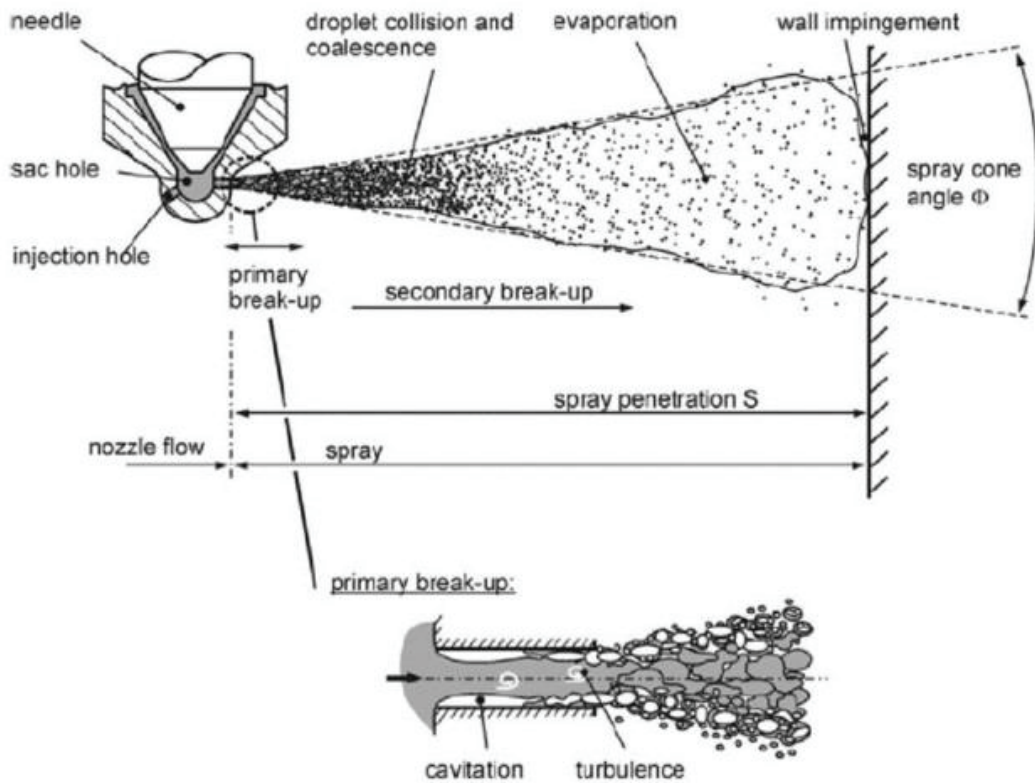
Figure 2. 11. Spray Formation (Source: (4))
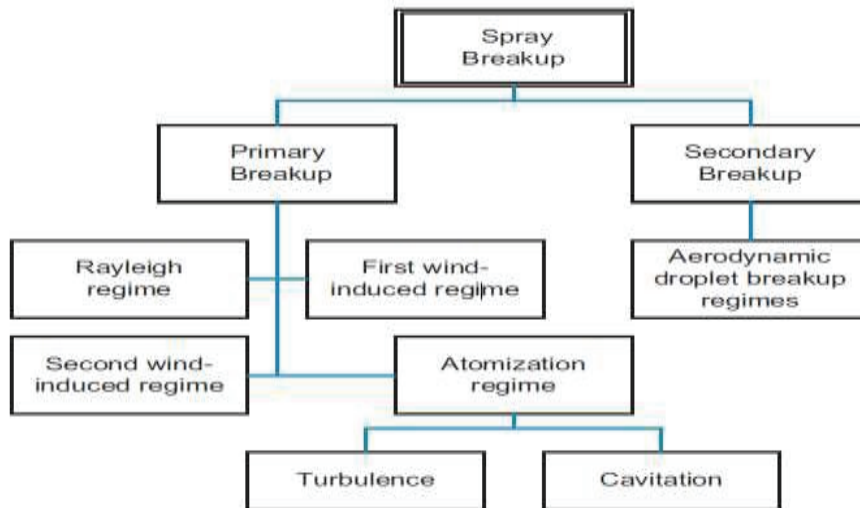
Figure 2. 12. Spray Breakup Regimes (Source: (4))

As it can be noticed from the schematic above, primary breakup is divided into 4 regimes: Rayleigh Regime, First Wind-Induced Regime, Second Wind-Induced Regime, and Atomization Regime. In order to understand the regimes clearly, there are 3 important quantity defined in the literature: Ohnesorge Number (Oh), Weber Number

(We), and Reynolds Number (Re). Ohnesorge number represents the effect of viscosity and surface tension in the context of spray breakup. Oh number is introduced as:

$$Oh = \frac{\sqrt{We}}{Re}$$

Weber number is the ratio of inertial forces to surface tension forces. Reynolds number refers to the ratio of injected liquid inertia to its viscous forces. Weber number and Reynolds number are defined as follows:

$$We = \frac{\rho \vartheta^2 L}{\sigma} \qquad\qquad Re = \frac{\rho u L}{\mu}$$

So, Ohnesorge number become as follows:

$$Oh = \frac{\mu}{\sqrt{\sigma \rho L}}$$
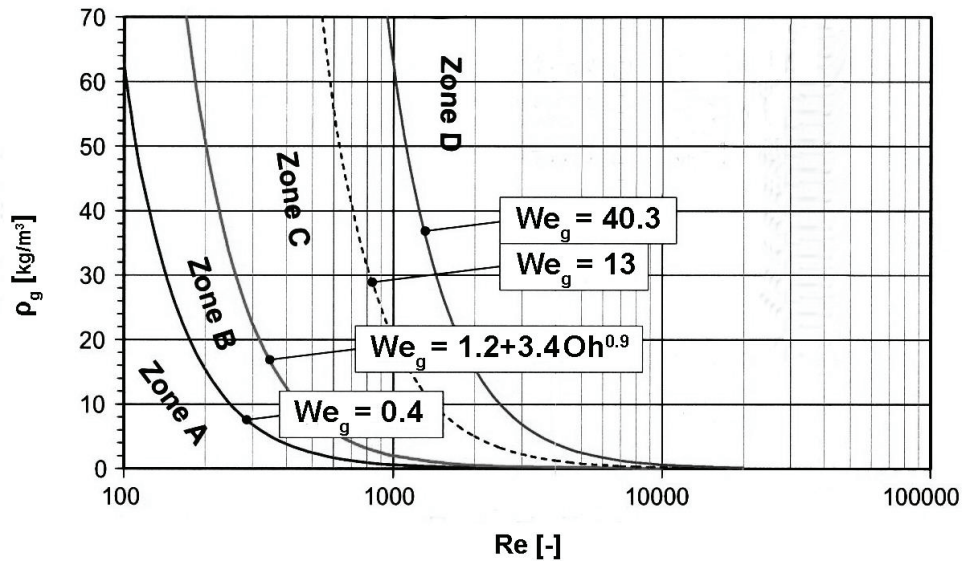
Figure 2. 13. Primary Breakup Regimes (Source: (13))

Figure 2.13 indicates us the distribution of 4 regimes of primary breakup as a function of Re number. Zone A represents Rayleigh regime. Zone B represents first wind-induced regime. Zone C refers to second wind-induced regime. Zone D refers to atomization regime. Figure 2.14 shows us the spray structure for these regimes. As it can be noticed from Figure 2.13, the higher Weber number is, the more intensive the breakup is. Therefore, the breakup ranges from Rayleigh regime to atomization regime.

15

According to the literature, General Weber number goes beyond the highest limit of regime switch, so atomization regime is the regime that characterizes the breakup process of engine sprays (13).
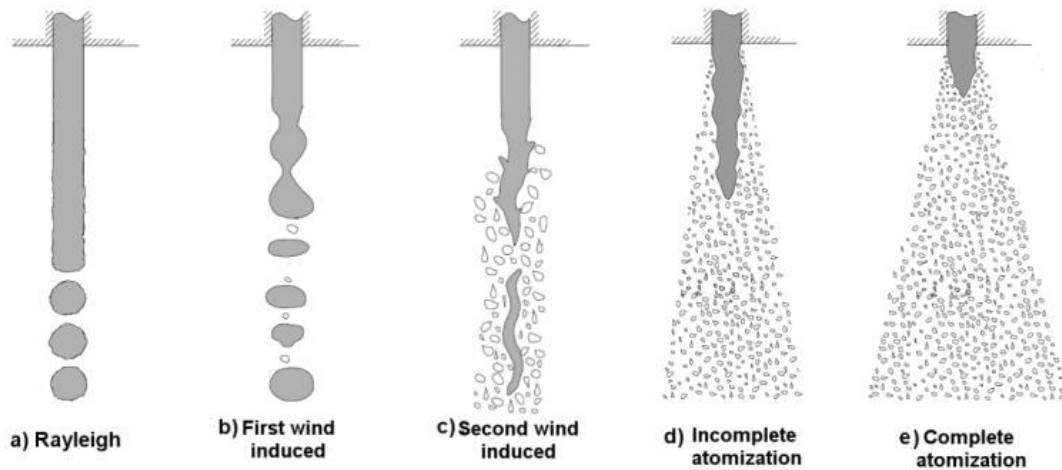
Figure 2. 14. Spray Structure of Breakup Regimes (Source: (14))

Rayleigh regime is for low injection velocities and defined as the breakup initiated by liquid inertia and surface tension forces. It leads to the generation of uniform size droplets. Droplet diameters are higher than the nozzle outlet diameter. This regime has been discussed by many researchers including Rayleigh, Yuen, Nayfey, and Rutland and Jameson (15, 16, 17, 18).

In first wind-induced regime, aerodynamic forces lead to stepping up the relevant forces of the Rayleigh regime. The occurrence of the first oscillations in the liquid surface due to surface tension increases as a result of higher velocities. Droplet diameters are similar to the nozzle outlet diameter. Reitz and Bracco have been investigated this regime in detail (19).

Second wind-induced regime leads to lower breakup lengths and smaller droplet size. The flow in the nozzle is turbulent. In this regime, because of the separation of small droplets from the surface, two breakup lengths should be taken into account: intact surface length and core length. Intact surface length is described as the beginning of surface breakup. Core length is described as the end of jet breakup. Reitz and Bracco have been analysed this regime in detail (19).

Atomization regime occurs if the intact core length is almost zero. As a result of this regime, a conical spray is occurred, and breakup starts near the nozzle exit. A few nozzle diameters further downstream, a dense core, which includes large liquid fragments, can still be exist. That's why, it characterises the breakup process of engine sprays. Droplet size is much lower when compared to the nozzle outlet diameter and shows a non-uniform distribution. It is much harder to describe this regime theoretically when compared to the other regimes because flow conditions inside the nozzle hole, which are usually unknown, affects extremely the disintegration process (4, 9, 14).
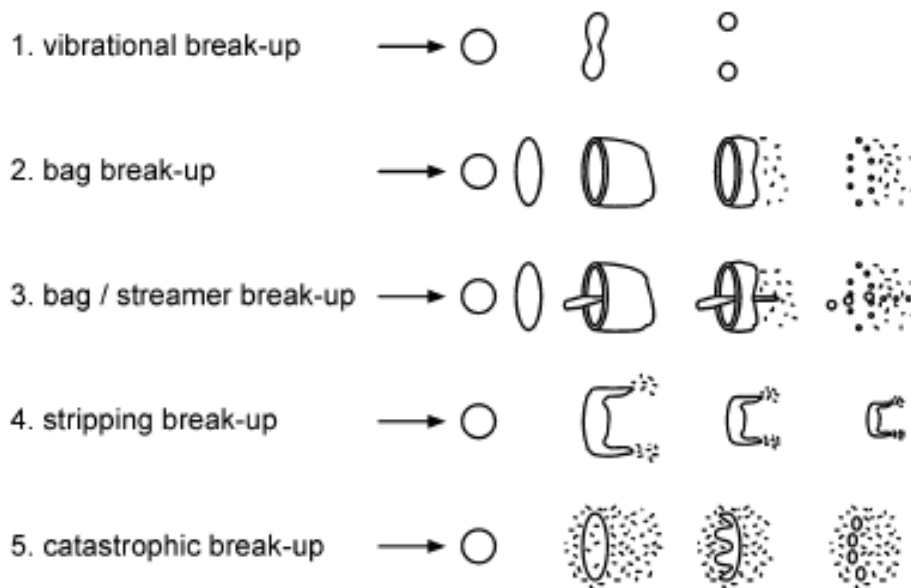
Figure 2. 15. Secondary Breakup Regimes according to Wierzba (Source: (20))

Figure 2.15 indicates the secondary breakup regimes. The concern of secondary breakup is the breakup of droplets affected by aerodynamic forces induced by the interaction between droplet and surrounding gases. As a result of the aerodynamic forces, disintegration and smaller droplet formation occur. Conversely, the surface tension forces stand against the aerodynamic forces to keep the droplet spherical. As the droplet become smaller, the surface tension become higher which leads to higher chance of the occurrence of an instable droplet deformation and disintegration. According to the literature, this behaviour can be described with the help of the Weber number. Due to the change in Weber number, different droplet breakup regimes occur. These regimes are given in

Figure 2.15. There are some inconsistencies in the literature about the transition Weber numbers (21, 22, 23).

According to Wierzba (20), if Weber number is lower than 12, droplet deformation does not end up with breakup. If it is around 12, vibrational breakup occurs. Bag breakup occurs if Weber number is in between 12 and 20. It causes a disintegration of the droplets as a result of bag-like disintegration. Bag/streamer breakup occurs if Weber number is in between 20 and 50. In bag/streamer breakup regime, an additional jet occurs. The rim breaks up into larger droplets when compared to the rest of the bag breakup. If Weber number is in between 50 and 100, stripping breakup happens. Because of the shear forces, very small droplets separate from the boundary layer and droplet diameter decreases progressively. If Weber number is higher than 100, catastrophic breakup occurs. It has 2 phases occurred at the same time: 1) Larger droplets occur as a result of breakups of the droplets which have surface waves with long wavelengths, 2) Smaller droplets occur as a result of breakups of the droplets which have surface waves with short wavelengths.

All of these breakup regimes happen in engine sprays. Weber number is high near the nozzle, that's why most of the disintegrations occur near the nozzle. Further downstream, Weber number becomes smaller due to the smaller droplets and due to the smaller relative velocity (9).

2.1.3. Cavitation and Turbulence

There are two main breakup mechanisms of primary breakup which are shown in Figure 2.16: Turbulence-Induced Disintegration and Cavitation-Induced Disintegration.

Turbulence-induced primary breakup is one of the most important breakup mechanisms of high-pressure sprays. Droplets, which are able to break through the surface tension, start swirling and leaving the jet as a result of strong radial turbulent velocity fluctuations inside the jet.
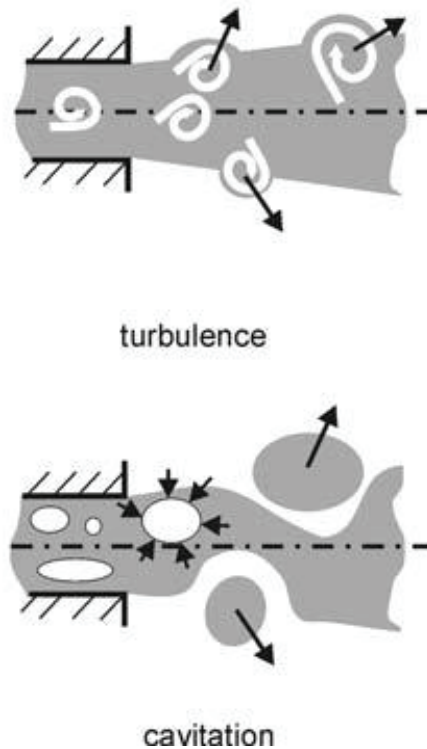
Figure 2. 16. Mechanisms of Primary Breakup (Source: (9))

Cavitation-induced primary breakup is another most important breakup mechanism of high-pressure sprays. Strong acceleration of the liquid at the outlet of the nozzle causes a decrease in static pressure. This situation results in development of cavitation structures inside the nozzle hole. High ambient pressure inside the cylinder leads to imploding of these structures. The turbulence level and the intensity of the spray disintegration are increased by implosion of these structures inside the nozzle hole. Both mechanisms happen simultaneously.

Hiroyasu et al., Soteriou et al., and Tamaki et al. have discussed experimentally the effect of the transition from a pure turbulent to a cavitation. They have resulted in an increase in spray angle and in a decrease in spray penetration (24, 25, 26).

2.1.4. Spray Characteristics

Spray characteristics are investigated under two topics: Macroscopic Scale and Microscopic Scale. Spray penetration and spray angle are the parameters of

macroscopic scale. Droplet size is the parameter of microscopic scale. Figure 2.17 represents the spray parameters.
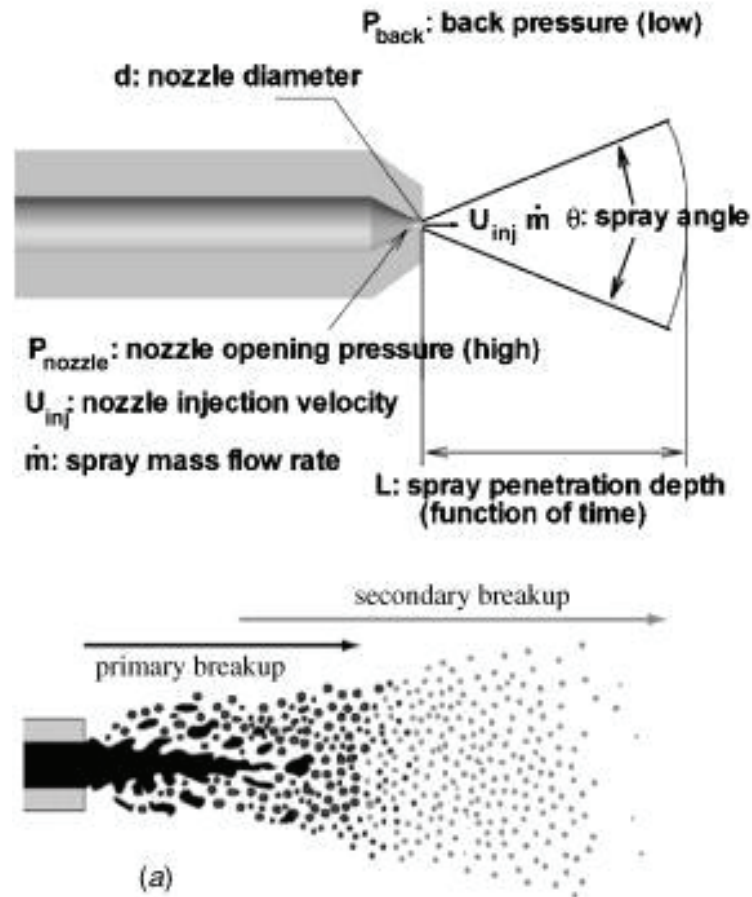
Figure 2. 17. Spray Characteristics (Source: (27))

Maximum distance measured from the injector to the spray tip is defined as spray penetration. It depends on injection pressure, fuel properties, and nozzle geometry. Spray penetration increases as injection pressure increases. In order to understand the effect of fuel properties on spray penetration, fuel density is counted as a reference property. As fuel density decreases, spray penetration decreases.

The angle between two straight lines starting from the orifice exit of the nozzle is called as spray angle. These lines are tangent to the spray outline. Nozzle geometry, fuel properties, and air density are the main parameters that affect the spray angle. As the temperature of the working fluid decreases, spray angle increases. Similarly, as injection pressure increases, spray angle increases.

Droplet size is calculated on the average by Sauter Mean Diameter (SMD). Average droplet size depends on injection pressure, working fluid temperature, and fuel properties. As injection pressure increases, droplet size decreases in general. Since working fluid temperature and fuel properties affect the evaporation rate, they also affect the droplet size (4, 9).

2.2. Alternative Fuel Types

Two different fuel types which are Biodiesel and Water-in-Diesel Emulsion is going to be explained in the following sections.

2.2.1. Biodiesel

Preparation of biodiesel, physical properties of biodiesel, and its effect on emissions is going to be explained briefly.

2.2.1.1. Preparation of Biodiesel

Biodiesel is one of the alternative fuels being used in compression ignition engines. There are 3 generation of biodiesel. These are first generation biodiesel, second generation biodiesel, and third generation biodiesel.

First generation biodiesel can be produced by using vegetable oil, animal oil, and waste cooking oil. First generation biodiesel is produced through a chemical process called as transesterification. It is a process which separates the glycerin from the fat or vegetable oil. The products of this chemical process are methyl esters and glycerin. Glycerin is used in soaps and other products. Methyl ester is the chemical name for biodiesel (28, 29).

Second generation biodiesel is derived from wasted food crops, non-food crops such as wood, seed crops, and grasses. Since the feedstock used in second generation

21

biodiesels are different than first generation biodiesels, the process to extract the energy from them is different. There are 2 steps to produce second generation biodiesel: thermochemical conversion and biochemical conversion. Thermochemical conversion consists of 3 routes: gasification, pyrolysis, and torrefaction. Gasification is used for wood, black liquor, brown liquor, and other feedstock to produce biodiesel. Carbon monoxide, hydrogen, and carbon dioxide are produced by carbon-based products through gasification. The gas produced is called as syngas. Fischer-Tropsch process is used to convert syngas into liquid. After that, it can be used to produce energy. Pyrolysis is preferred when there is lack of oxygen and an inert gas like halogen. Two products are produced through pyrolysis process: tars and char. Torrefaction is similar to pyrolysis but is carried out at lower temperatures. Biochemical conversion can be defined as a number of biological and chemical processes adapted to convert biomass to liquid (30).

Third generation biodiesel is derived from algae. Various fuel types can be produced by using algae. Algae have two main characteristics to be used as feedstock. First one is that, oil produced by algae can easily be refined into diesel. Second one is that, they have a special talent which is used to produce everything such as ethanol, butanol, and even diesel fuel directly (30).

2.2.1.2. Physical Properties of Biodiesel and Its Effect on Emissions

Biodiesel has lower calorific value than diesel fuel. It has higher cloud and pour points which may cause problems during cold weather. Additionally, it has higher viscosity and density. High viscosity causes poor atomization, incomplete combustion, choking of the injectors, ring carbonization, and accumulation of the fuel in the lubricating oils. In order to lower the viscosity and density of biodiesel, the mixture of biodiesel and diesel fuel is used (31, 32).

Usage of biodiesel fuel in compression ignition engines increases the engine efficiency. Since biodiesel fuel has higher flash points, it is safer to store. Its fatty compounds suitable as diesel fuel because it is an oxygenated fuel. More complete combustion and lower emission rates are achieved due to its oxygenated and sulphur-

free structure. As a result of its sulphur-free content, there is a decrease in soot, CO_2 emission, and hydrocarbon (HC) emission. However, there is a slight increase in NO_x emission. It needs an Exhaust Gas Recirculation (EGR) to handle NO_x emission (32).

2.2.1.3. Spray Characterization of Biodiesel

Spray characteristics such as atomization, penetration, and cone angle get highly influenced by viscosity and surface tension. According to the literature, higher density of biodiesel fuel leads to decreasing in nozzle outlet velocity due to the increase in friction losses. Higher viscosity of biodiesel fuel decreases the amount of fuel injected and its penetration. Moreover, instabilities in a liquid jet which are essential for better atomization are reduced due to higher viscosity of biodiesel fuel. Higher surface tension of biodiesel fuel causes a reduction in droplet formation (31).

Spray characteristics get influenced by internal injector flow, as well. According to the literature, researchers have investigated the effect of internal injector flow both numerically and experimentally. They all agreed on a reduction in cavitation effect when biodiesel fuel was used as a fuel. This is because of the lower vapour pressure of biodiesel. Reduced injection velocity and cavitation effect resulted in poor air-fuel mixture for combustion (31, 33, 34, 35, 36).

2.2.2. Water-in-Diesel Emulsions

The mixture of two or more immiscible liquids is called as emulsion. One liquid is dispersed into the other one by the help of a surface agents called as surfactants. Main surfactant characteristics are explained in the following section. There are two main types of emulsification: two-phase emulsions and three-phase emulsions. Two-phase emulsions are also called as primary emulsions. They contain one dispersed phase liquid and one continuous phase liquid. Three-phase emulsions are also called as secondary emulsions. They contain one continuous phase liquid and two or more dispersed phase liquids.

Water-in-diesel emulsion is one of the fuel-based solutions. In order to improve the engine performance, Hopkinson (37) suggested a brand new method which deals with addition of water into the engine combustion chamber in 1913. After that suggestion, several techniques were applied to introduce water into the chamber such as water injection in inlet manifold, water-in-diesel emulsions, etc. However, these techniques were not useful and practicable enough until they found out what micro-explosion phenomena is in 1965. Micro-explosion of water-in-diesel emulsions improves the small-scale atomization of the droplets which is especially lacking from the biodiesels.

The usage of water-in-diesel emulsion as a fuel in compression ignition engines can help with the reduction of adiabatic flame temperature due to water content, hence particulate matter-NO_x trade off as well as the improvement of the combustion efficiency. Due to the vaporization of the liquid water, the temperature of the combustion products decreases and it ends up with the reduction in NO_x emission. The existence of water inside the combustion chamber leads to an increase in oxidation of soot particles which results in a decrease in PM emissions. The effects of water-in-diesel emulsion on engine performance and emissions have discussed by many researches (38, 39, 40, 41, 42, 43). They will be discussed in detail in the following sections.

2.2.2.1. Emulsification Techniques

Two- and Three- Phase Emulsions are going to be explained in this section.

2.2.2.1.1. Two-Phase Emulsion

There are two types of two-phase emulsions depending on the dispersed and continuous phases: oil-in-water emulsions and water-in-oil emulsions. The illustration of three-phase emulsions is given at Figure 2.19.
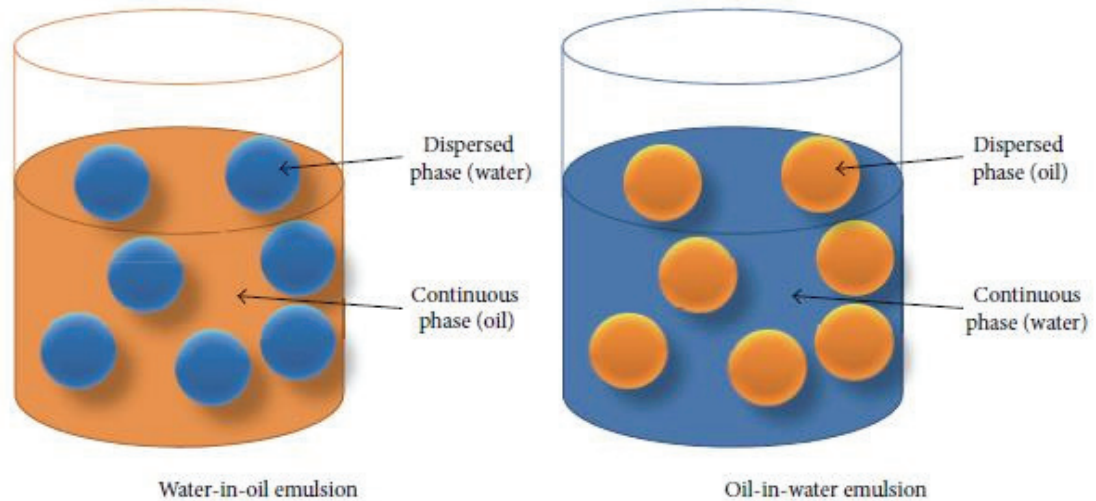
Figure 2. 18. Two-Phase Emulsions (Source: (38))

Water is the dispersed phase in water-in-oil emulsions while oil is the dispersed phase in oil-in-water emulsions. There are 3 basic conditions required to produce two-phase emulsions:

➢ The liquids must be immiscible at normal conditions.
➢ Surfactants must be used to make the liquids mix.
➢ The duration of the mechanical agitation must be long enough to ensure the stability of the emulsion.

In addition to the requirements given above, surfactants must be chosen carefully. They should not change the physicochemical properties of the fuel. They should not affect the combustion properties and the emission rates (48, 49).

Since the concern of this investigation is water-in-diesel emulsions which are categorised under two-phase emulsions. The preparation and stabilization of water-in-diesel emulsions are explained in detail in the following section.

2.2.2.1.2. Three-Phase Emulsion

There are two types of three-phase emulsions depending on the dispersed and continuous phases: oil-in-water-in-oil emulsions and water-in-oil-in-water emulsions. The illustration of three-phase emulsions is given at Figure 2.18.
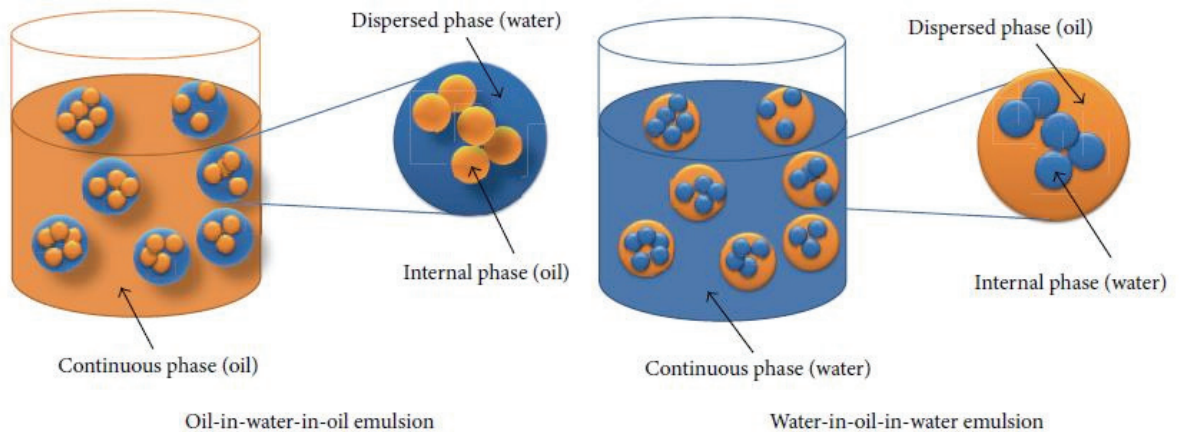
25

Figure 2. 19. Three-Phase Emulsions (Source: (38))

Oil-in-water-in-oil emulsions are proper for fueling purposes in internal combustion engines; however, there is a limited literature available. Water-in-oil-in-water emulsions are proper for cosmetics applications, food applications, or pharmaceutical manufacturing. There are three ways to produce three-phase emulsions: phase inversion, mechanical agitation, and two-stage emulsion (44). The most common type is two-stage emulsification (44, 45, 46, 47). Both lipophilic and hydrophilic surfactants are used in this technique. Firstly, a mechanical homogenizer and a hydrophilic type of surfactant are used to produce two-phase oil-in-water emulsion. After that, three-phase oil-in-water-in-oil emulsion is produced by using a lipophilic type of surfactant.

Lin et al. (44) have studied the fuel properties of three-phase emulsions by changing homogenizer speed, hydrophilic-lipophilic balance (HLB) value, and water amount. They have used Tween 80 and Span 80 as surfactants. They have recorded a decrease in droplet size with an increase in stirring speed. As the water amount at the inner phase increased, viscosity increased. More stable three-phase emulsion was obtained for higher surfactant volume with HLB value of 6-8.

Lin et al. (45) have studied the effect of three-phase emulsion on engine performance and emission rates of four-cylinder four stroke marine diesel engine. They have run the experiments with regular diesel, two-phase emulsion, and three-phase emulsion. Because higher water amount caused lower calorific values, higher brake specific fuel consumption (bsfc) obtained when compared to the neat diesel. Three-phase emulsion had lower bsfc than two-phase emulsion. Three-phase emulsion had

higher exhaust temperature, lower CO and NO_x emissions when compared to two-phase emulsion.

Lin and Chen (46) have compared the fuel characteristics and emission rates of two- and three-phase emulsions. They have used four-cylinder four stroke marine diesel engine as a test rig. They have performed two different emulsification methods while preparing the emulsions: ultrasonically vibrating and mechanically homogenizing. They have observed lower fuel consumption rate, lower bsfc, and lower CO emission, and larger black smoke opacity for the emulsions prepared by the ultrasonic vibrator. Regardless of the preparation method, two-phase emulsion had lower fuel consumption rate, bsfc, CO, and lower black smoke opacity than three-phase emulsion.

It should be noted that three-phase emulsions require two-stage emulsification process, and therefore it would be more expensive to prepare three-phase emulsions. According to the literature mentioned above, three-phase emulsions have advantages when comparing to two-phase emulsions. Despite the advantages of three-phase emulsions over two-phase emulsions, it is still unclear the differences between the process cost, emulsion characteristics, emulsified fuel properties, engine performance, and emission rates. Besides, it is still unclear how micro-explosion phenomena is affected when three-phase emulsions are used as fuel in the internal combustion engines (38).

2.2.2.2. Preparation and Stabilization of Water-in-Diesel Emulsions

Emulsion is a special type of mixture made by combining the liquids which are immiscible at normal conditions. Water and diesel are combined by the help of a surfactant. The surfactants are divided into two groups: hydrophilic and hydrophobic surfactants. In order to weaken the surface tension between water and oil phases, these surfactants are added into the mixture. The hydrophilic ones go towards the water and the hydrophobic ones go towards the oil so that the surface tension is removed (38, 50). It is important to achieve the most proper hydrophilic-lipophilic balance (HLB) for the surfactants so that the most stable emulsion is obtained. High HLB values are desired to

have oil-in-water emulsion. Low HLB values are desired to have water-in-oil emulsion (38, 50). HLB values are calculated by using the formula given below.

$$HLB_{comb} = \sum_i (HLB_{Si} * W_{Si})$$

It is important to select the suitable type of surfactant so that the surfactant does not affect the physiochemical properties of the fuel itself. The amount of the surfactant used is between the ranges of 0.5-5% by volume. Span series, Tween series, TritonX-100, sorbitan monooleate and polyethylene glycol sorbitan monooleate mixture, polyethylene glycol sorbitan monooleate and sorbitol sesquioleate mixture, sorbitan monolaurate, gemini, and detergent/liquid soap are the common surfactant types used in the literature (51, 52, 45, 55, 53, 54, 46, 47, 56, 57, 58, 59).

The parameters that affect the stability of the emulsion are emulsification technique, emulsification duration, stirring speed, amount of water used, and amount of surfactants used. There are four different ways to produce emulsions: jet mill, static mixer, homogeniser, and ultrasonication. Although these techniques are preferred by many researchers, there are some researchers who use membrane emulsification technique in order to improve productivity with the same particle size (60, 61). The proper water: surfactant: diesel ratio is important for the stability of the emulsion. It can be found by calculating the percentage of water settling in time. It can be calculated by using the formula given below (59, 62).

$$\text{Water settling\%} = \left[\frac{(H_2O)_i - (H_2O)_f}{(H_2O)_i} \right] * 100$$

Bidita et al. (63) have studied the physical and chemical characteristic of water-in-diesel emulsions. Their surfactant was TritonX-100. They have prepared the emulsions by using an ultrasonic processor under various processing conditions. In order to find the best water: surfactant: diesel ratio in emulsified fuel, they have changed both the surfactant ratio and the water ratio in diesel fuel. Volume fraction of water used was in the range of 0.1-0.5%. Volume fraction of surfactant used was in the range of 0.1-0.3% in 0.05% increment. They have also changed the ultrasonication amplitudes and time. They have used a scanning electron microscopy (SEM) for observing the surface morphology of emulsified fuels. According to their morphology results, emulsified fuels had lower volume of carbon and oxygen contents. Their results

on viscosity analysis show that the viscosity decreased up to a certain amount of water addition. After that point, as the amount of water kept being increased, the viscosity started to increase due to miscellization. The lower viscosity leads to better combustion efficiency compared to the neat diesel. They obtained a decrease in exhaust temperature for all emulsions compared to the neat diesel. The emission rates were also decreased.

Patil et al. (64) have aimed to prepare the most stable water-in-diesel emulsion in their research. They have used a high-speed mixing homogenizer in order to achieve that purpose. They have used the Span series (Span20, Span60, Span80, and Span85) and the Tween series (Tween20, Tween60, and Tween80) as the surfactants. They have mixed these surfactants together. They have checked for the stability of the emulsified fuel according to the absence of phase separation. They have changed the amount of water, the amount of surfactant, mixing time, and mixing speed in order to observe the effect of these parameters on the stability. According to their results, 5% of the mixture of Span80 and Tween80 with the HLB value of 9, 10% of water content, stirring speed of 5000 rpm for 20 min was the best conditions for the emulsion being stable for more than 25 days. Higher water content (>25%) affected negatively the stability behaviour of the emulsified fuel.

Hasannuddin et al. (65) have studied the stability of water-in-diesel emulsions. The type of surfactant, mixing speed, and mixing time were the main parameters in their experiment. They have used Span80 and different type of glycerines as surfactant. According to their results, as the amount of water content increased, the stability decreased. As the mixing time and speed increased, the stability increased.

Ghannam et al. (62) have studied the effect of the variables (water concentration, surfactant concentration, mixing time and speed) on the stability of water-in-diesel emulsions. They have changed these variables in order to observe the effects created by them. They have prepared the emulsions by using a laboratory high speed mixer. They have used Fann V.G. rotational viscometer and a Fischer Surface Tensiomat in order to measure viscosity and surface tension, respectively. Their surfactant was TritonX-100. According to their results, density increased when the water concentration increased. As the temperature increased, density and viscosity decreased. Viscosity decreased with the addition of water. The emulsion prepared with 0.2% surfactant, 10% water, stirring speed of 15000 rpm for 2 min stayed stable for one month. For higher water

concentrations (>20%), in order to obtain a stable mixture, the amount of surfactant increased to 2% and the stirring speed and time increased to 20000 rpm and 30 min, respectively.

2.2.2.3. Effect of Water-in-Diesel Emulsions on Spray Characteristics and Combustion

In water-in-diesel emulsions, water droplets are trapped into diesel by the help of surfactants. The effect of emulsified fuel on the injection properties have been studied by many researches (66, 56, 67, 57). When such a mixture is introduced into the hot combustion chamber, heat starts transferring through the droplets of the fuel. Since water has lower volatility, it starts evaporating earlier. As a consequence, the water molecules reach their superheated stage faster than the diesel creating vapour expansions breakup (38, 68). At this stage, two important phenomena show up: micro-explosion and puffing. In puffing, water leaves the droplet in a very fine size, whereas micro-explosion is a quick breakdown of the droplets. Micro-explosion causes the secondary atomization of droplets which ends up with the fast evaporation and enhanced air-fuel mixing (68, 57). Since it has a direct influence on the engine improvement, it is essential to understand the effecting parameters of the micro-explosion as well as the basics of the micro-explosion. Micro-explosion mechanism is represented in Figure 2.20 below.

Z.Sheng et al. (37) have focused on the micro-explosion phenomena of water-in-diesel fuel emulsion droplets in spray. According to their research, the droplet diameter, the ambient temperature, and the interaction of droplets were the most significant parameters on the combustion. Additionally, keeping the temperature of the injection nozzle at a certain level was very important for emulsions in order to avoid the evaporation of the water content before injection. Emulsion had the larger angle and larger area of the flame than the regular diesel fuel. Micro-explosion was more powerful and the flame angle was larger, as the pressure inside the cylinder reduced. As the cylinder temperature reduced, the micro-explosion lost its effect and became weaker.
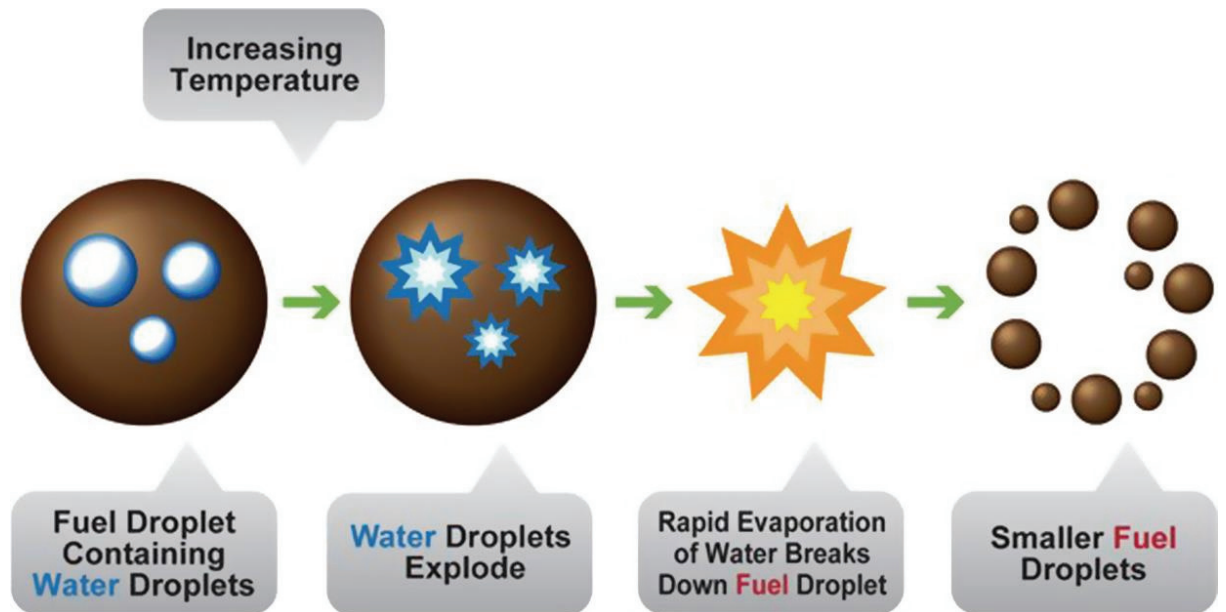
Figure 2. 20. Micro-explosion phenomenon (Source: (60))

Huo et al. (66) have investigated how spray and combustion characteristics are changed by using water-emulsified diesel. They have observed micro-explosion in a burning spray by using high speed camera. At high ambient temperature, they have obtained abnormal droplet explosion along the lift-off. Lift-off length is the distance between the lifted flame base and the orifice exit. Since the combustion of Ultra Low Sulphur Diesel (ULSD) never caused this droplet behaviour, it developed out of micro-explosion because of the boiling temperature difference between water and ULSD. According to their observations, at high ambient temperature and low injection pressure, glowing scattering droplets around lift-off in the burning flame of the emulsified fuel affected the primary breakup. It can be shown as a proof of the effect of the micro-explosion on the primary breakup. Additionally, as the injection pressure was increased, reduction in the puffing and glowing spots was observed. That is because of the competition between the micro-explosion delay time and primary breakup time. The higher injection pressure there is, the more severe primary breakup occurs. Thus, micro-explosion occurs slower than the primary breakup and affects only the secondary breakup.

Morozumi et al. (69) have investigated the effect of physical properties of emulsified fuel on the occurrence of micro-explosion. Based on their research, the influencing factors of micro-explosion were the volatility of the base fuel, type of

emulsion, and water content. As they increased the emulsifier content, the micro-explosion temperature and waiting time increased.

Although there are many researches both experimentally and numerically on the micro-explosion phenomena, it is still not clear what is actually happening inside the combustion chamber. Therefore, there are conflicting results with the existing literature (56, 70, 71, 72).

Lee et al. (67) have investigated how spray and combustion characteristics are affected by changing fuel properties. They have used light diesel fuel (Nisseki Mitsubishi Co.) which has less density, viscosity, surface tension, and boiling point than current diesel fuel (JIS No. 2 diesel fuel) as well as same cetane number and lower heating value than the current diesel fuel. The effect of the fuel properties on spray was examined. Experiment was run under the conditions of constant engine speed of 1500 rpm and varying the injection pressure by 60 and 80 MPa. According to their conclusion, due to the low density, the spray penetration of light diesel is weaker. Due to the low viscosity, atomization leads to evaporation which ends up with the reduction in soot formation. As increased injection pressure at the nozzle enhances momentum, liquid penetration distance becomes longer. Because of lower properties of the light diesel, atomization and mixture formation were advanced.

Huo et al. (66) have investigated how spray and combustion characteristics are changed by using water-emulsified diesel. They have observed micro-explosion in a burning spray by using high speed camera. They had a constant volume chamber which is able to simulate the real engine operation conditions. After they prepared the emulsions by applying stability test, they injected and combusted the emulsions in the chamber. Their base fuel was ULSD. The concentration of the emulsified diesel was 10% of water and 20% of water by volume. The experiment was run under the conditions of varying injection pressure of 70 MPa to 130 MPa with an increment of 20 MPa, and varying the ambient temperature by 800 K and 1200 K. As a result of their research, due to the low volatility of the water, longer liquid penetration was obtained for emulsified diesel in comparison with ULSD. Emulsified diesel tends to primary breakup because its higher viscosity and surface tension caused a thickened spray tip at the beginning of the combustion. As the ambient temperature increased to 1200 K, the physical properties of the fuel stayed in the background and emulsified fuels had similar

liquid penetration length with ULSD. At low ambient temperature of 800 K, longer penetration and longer ignition delay were obtained for emulsified fuel due to water addition. Thus, more air was able to inset allowing the reduction in emissions. It was vice-versa for the high ambient temperature of 1200 K.

Ochoterena et al. (56) have observed physical properties, spray behaviour and combustion characteristics of a water-in-diesel emulsion, a water-in-diesel micro emulsion and a conventional diesel fuel by an optical method. NMR diffusiometry was used in order to determine the size of the water droplets in the emulsion and micro emulsion. The Chalmers High Pressure and High Temperature Spray Rig was used in order to observe the spray characteristics. The injection pressure was 1200 bar. They have recorded that because of the volatility difference and the droplet size, spray penetration of the micro emulsion fuel was the longest, the emulsion fuel was following it, and the regular diesel fuel was at the end. The micro emulsion fuel had longest penetration because it contains higher amount of surfactant which results in lower volatility than the emulsion. Although a minimum flame lift-off distance was measured as the flame propagates in the up-stream direction near end of injection during combustion of either regular diesel fuel or the micro emulsion, for the emulsion fuel, flame lift-off distance remained constant. Because regular diesel fuel has more volatility, it was affected by the flame radiation and the hot air entrainment exerted on the spray more than the micro emulsion and the emulsion fuels. It resulted in narrower spray cone angle for regular diesel fuel. The widest spray cone angle was measured by the emulsion fuel at 42 nozzle diameters downstream the injector.

Ghojel et al. (57) have investigated experimentally the impact of high injection pressure and water content on the ignition delay and lift-off length of the spray on the combustion of water-in-diesel emulsions. Since the ignition delay and flame lift-off length determine a range of diesel engine operating characteristics, they are quite important parameters. The experiment was run under two different ambient conditions. The ambient temperature was set to be 1175 K and 1375 K, and the injection pressure was increased up to 100 MPa. The ignition delay is the time between the start of injection and the start of combustion. There are two different ways to determine the start of combustion: Pressure Ignition Delay (PID) and Luminous Ignition Delay (LID). PID can be determined by measuring the combustion chamber pressure with a quick response dynamic piezo-electric pressure sensor. LID can be determined by using a

high-speed camera which captures the start of injection and the bright spots. Based on their conclusion, the ignition delay of the emulsified fuel is always higher than the ignition delay of the standard diesel fuel. At low ambient temperature, the PID was higher than the LID. As the injection pressure was increased, the ignition delays decreased, and were getting closer to each other. At low ambient temperature, ignition delays increased with increasing the water content in the fuel. It was vice-versa at high ambient temperature. At high water content, ambient temperature had an important impact on the ignition delay. However, the injection pressure has a little impact on the ignition delay. This let more air get into the cylinder leading to leaner mixtures. As a result, soot formation inside the cylinder was reduced. At high ambient temperatures, the flame lift-off was decreased because of the higher vaporization rates of fuel.

Lif et al. (49) have investigated the effects of water content on the emissions and the combustion efficiency. According to their research, water content has two main effect on the combustion: 1) Decreased peak temperature in the cylinder resulting in a reduction in NO_x and PM, and 2) Micro-explosion phenomenon resulting in an improved combustion efficiency.

Suresh et al. (73) have studied the combustion and performance characteristics of water-in-diesel emulsion (0, 5, and 10% of water-in-diesel) in variable compression ratio (15 to 18), single-cylinder four-stroke diesel engine under varying loads. They have noted that, at low compression ratios, emulsified fuel ended up with the incomplete combustion. They have used Sorbitan Monolanrate with HLB value of 8.6 as a surfactant. They have prepared the emulsified fuel by adding desired amount of water and surfactant into the fuel mixing chamber drop by drop and stirred them at 15000 rpm for 30 minutes. The stability was checked by using a photonic circuit. According to their results, at no load condition, an increase in the peak pressure of the cylinder was recorded as the amount of water is increased. While they have reduced the compression ratio, the peak pressure of the cylinder was reduced due to lower overall cycle pressure. As they have increased the compression ratio, the net heat release rate was increased. The net heat release rate was reduced for the emulsified fuels compared to the base diesel. Water content in the base diesel led to reduction in the mean gas temperature. High ignition delay and increased combustion duration were observed with the increase in water concentration. By increasing load and increasing the water

concentration, they recorded a reduction in brake specific fuel consumption and an increase in the brake thermal efficiency.

Selim et al. (59) have investigated experimentally combustion study of stabilized water-in-diesel emulsions with different concentrations under different operating and design conditions. They have used Silent Crusher M homogenizer in order to produce water-in-diesel emulsions. The water concentration, the engine speed, load, fuel injection timing, and compression ratio were the variable parameters in their experiment. Triton X-100 has been used as surfactant. According to their results, spray pattern did not change with the water addition. As the water content increased, maximum pressure rise rate increased. As the engine speed reduced, the injection timing advanced, and compression ratio decreased, maximum pressure rise rate increased. In order to make the engine run steadily, they have increased the compression ratio while increasing the water content. They have obtained a slight decrease in brake power output and a slight increase in brake specific fuel consumption with the addition of water. However, they have noted that this situation can be tolerated when compared to the emission reduction rates.

2.3. Purpose of the Thesis

The purpose of this study is to investigate how spray characteristics of water-in-diesel emulsions change while concerning the different ambient conditions.

In order to comprehend the spray behaviour of water-in-diesel emulsions, neat diesel spray behaviour are going to be investigated. The experimental matrix includes different ambient pressures and different injection pressures. The experimental matrix is given in the Table 3.3. The experiments are going to be carried on a constant volume combustion chamber enhanced by fellow co-workers in Izmir Institute of Technology. The experiments are going to be recorded by the help of high-speed camera. While performing the experiments, an extra attention is going to be paid to the configuration of the camera due to the alignment and the angle of sight.

The outcome of the literature survey, the most stable water-in-diesel emulsion is going to be prepared. It is going to be used in this study as the main fuel. Emulsion is

going to be prepared by the help of a high-speed mixing homogenizer. As it is stated on the literature, the mixture of Span80 and Tween80 is going to be used as surfactant.

Since this study includes an image processing, Matlab based image processing code is going to be used in the data analysis.

In the present work, surfactants, which are Span80 and Tween80, are obtained from Croda Industrial Chemicals. Neat diesel is obtained from a local gasoline station. The amounts of surfactants, water, and diesel are decided according to the literature. Emulsion is prepared in Chemical Engineering Department by using a high-speed mixing homogenizer.

Eventually, the spray characterisation of water-in-diesel emulsion and neat diesel can be investigated and compared with each other. Spray angle and spray penetration are calculated and plotted for comparision purposes. Meanwhile, a quantitative comparision between neat diesel spray and emulsion spray is performed.

CHAPTER 3

METHODOLOGY

Chapter 3 involves a detailed explanation of constant volume combustion chamber, optical setup, Matlab algorithm, preparation of water-in-diesel emulsion, and experimental matrix.

3.1. Experimental Apparatus and Its Components

Constant Volume Combustion Chamber (CVCC) is a thick steel wall container used to study the spray characterisation and the fundamental aspects of spray combustion via optical access. The requirements of real engine-like conditions are to obtain high temperature (T) and high pressure (P) inside the combustion chamber. High T and high P conditions are the conditions of TDC. Because these conditions can be achieved easily in CVCC, it is commonly used among the researchers. The working principle of CVCC will be explained thereinafter. A schematic of CVCC used in this study is given in Figure 3.1. As it can be seen from the figure, it consists of gas supply system, ignition system, fuel supply system, injection system, vacuum system, high-speed optical system, and data acquisition module. Figure 3.2 depicts the experimental apparatus and its components.

Gas supply system is the system which supplies precombustion gases into the chamber. These are oxygen (O_2), nitrogen (N_2), argon (Ar), and acetylene (C_2H_2). They are introduced into the chamber by pipelines which are controlled by valves. The amount of the gases is adjusted by the general chemical formula of combustion process. To understand clearly the adjustment of the amount of the precombustion gases and precombustion process, first the chemistry behind the process is explained briefly.
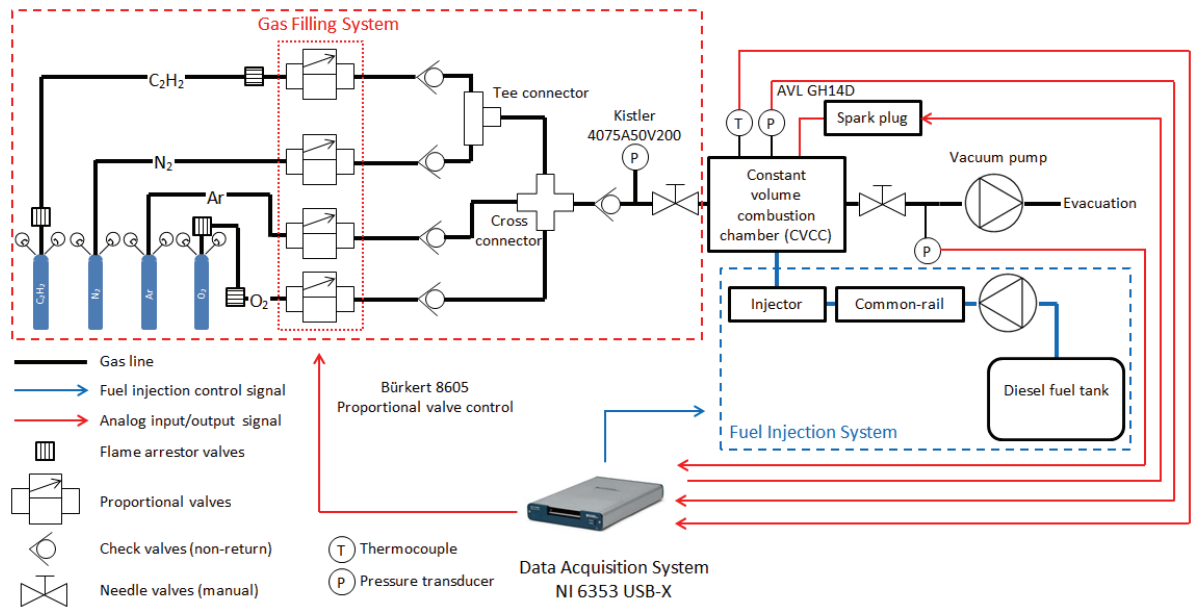
Figure 3. 1. Overall Experimental Setup

Figure 3. 2. Experimental Apparatus and Its Components

Chemical reactions are based on stoichiometry. Stoichiometry can be simply defined as the relationship between reactants and products. In chemical reactions, total number of atoms must be equal in the products as in the reactants, so that it is balanced. In order to balance a chemical reaction, stoichiometric coefficients must be added in front of the reactants and products. Equivalence is done by balancing the number of each element in both reactants and products. Stoichiometric equation of acetylene is given below.

$$C_2H_2 + 2.5(O_2 + 3.76N_2) \rightarrow 2CO_2 + H_2O + 9.4N_2$$
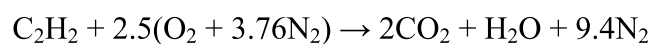
As it can be noticed, there are 2 carbon atoms, 2 hydrogen atoms, 5 oxygen atoms, and 9.4 nitrogen atoms on both sides of the equation. So, the total number of atoms in the reactants is equal to the number of atoms in the products. Both are 18.4.

Chemical reaction of acetylene is an example of combustion reaction. It is the reaction of hydrocarbon and oxygen to produce carbon dioxide and water. It is an exothermic reaction which means that it releases heat. In order to initiate combustion reaction, there must be an initiative high temperature heat source. There are two types of combustion: complete combustion and incomplete combustion. Complete combustion is also called as clean combustion. It is achieved when there is plenty of air. Thus, the fuel obtains enough oxygen for complete combustion. The products of complete combustion are water and carbon dioxide. The maximum amount of energy is released when complete combustion occurs. Incomplete combustion is also called as dirty combustion. It occurs when there is not enough supply of oxygen. Because the fuel does not find enough oxygen to react with, there are other products than water and carbon dioxide. Water is also produced. However, instead of carbon dioxide, carbon and carbon monoxide are produced. Pure amorphous carbon in powdery or flakey form is known as soot. Carbon monoxide is a toxic gas. Incomplete combustion is not preferable because of the negative effects of its products on both human health and environment, and it produces less energy.

To obtain real engine-like conditions inside CVCC, firstly a precombustion process is done. This process aims to adjust the oxygene level in the constant volume combustion chamber. It is the reaction of acetylene and air gases by the help of spark plugs. Spark plugs provide the initiative flame to initiate the combustion reaction. Air contains 78% Nitrogen, 21% Oxygen, and 1% Argon. When it comes to the precombustion of acetylene, the reaction given below is used.

$$aC_2H_2 + bO_2 + cN_2 + dAr \rightarrow (b\text{-}2.5a)\, O_2 + 2aCO_2 + aH_2O + cN_2 + dAr$$
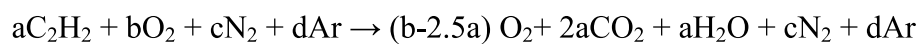
As it can be noticed from the reaction, total mol number of the products is '0.5a' less than total mol number of the reactants where 'a' is the coefficient of acetylene. 'a', 'b', 'c', and 'd' are the coefficients of C_2H_2, O_2, N_2, and Ar, respectively. The coefficients of acetylene and argon are determined by the researchers according to their needs. Total density inside the chamber also is determined by the researchers according to their chamber's design. In the products, oxygen concentration can be adjusted so that

there can be no oxygen left inside the chamber after the precombustion or there can be some oxygen left inside the chamber after the precombustion. The oxygen concentration can be varied between 0% and 21%. The amount of oxygen concentration by volume can be calculated by using Eq. (1) which is given below.

$$W_{O_2} = \frac{(b-2.5a)}{(0.5a+b+c+d)} * 100\%$$ (1)

Oxygen level can be controlled by using Eq. (1). The purpose of variable coefficient of oxygen is to be able to investigate the exhaust gas recirculation (EGR) effect on combustion process or to create evaporative conditions inside the chamber. EGR effect is the effect of amount of O_2 entrained on combustion. Fuel evaporation causes the hot entrained gases to cool down which results in shrinkage of the spray. This situation ends up with a difference in between the evaporative and non-evaporative conditions. The difference is that the penetration of vaporising spray lasts longer than the penetration of non-vaporising spray. In order to achieve evaporative conditions inside the chamber, oxygen concentration is adjusted that no oxygen is left as a product at the end of the combustion. When there is no oxygen left inside the chamber after precombustion, it means that evaporative conditions are achieved, and the spray injected after precombustion will not ignite but evaporate. When there is 21% oxygen left inside the chamber after precombustion, it means that the real engine-like combustion conditions are achieved, and the spray injected after precombustion will ignite as in the real engine.

In this experimental setup, the amount of acetylene and argon was kept constant at 5% and 1%, respectively. Partial pressures of reactants are calculated by using ideal gas equation which is shown in Eq. (2).

$$P = \frac{nRT}{V}$$ (2)

Actual total mol number of the reactants is calculated by the help of Eq. (3) which is given below.

$$x = \frac{\sum m}{d*V} = \frac{(a*M_{C_2H_2}+b*M_{O_2}+c*M_{N_2}+d*M_{Ar})}{d*V}$$ (3)

Actual mol number of the reactants is calculated individually by dividing their coefficients to the actual total mol number of the reactants. After calculating the actual mol number of the reactants, their partial pressure is calculated by using Eq. (2). All calculations are used to create a LabVIEW program for gas filling, so that the system can be controlled precisely.
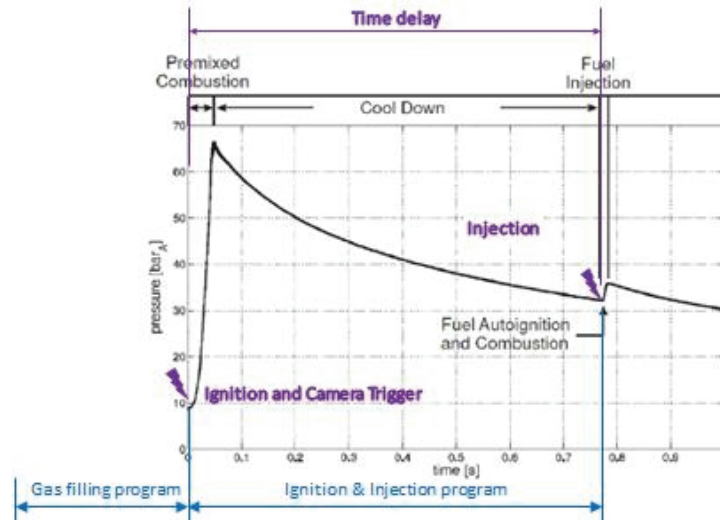
Figure 3. 3. Pressure-Time Graph

After the CVCC is filled up with the precombustion gases by using the gas filling LabVIEW program, precombustion takes place by using the spark plugs as initiative flame. Precombustion process is controlled by an ignition and injection program constituted in LabVIEW environment. Figure 3.3 represents the Pressure-Time graph of this process. As depicted in Figure 3.3, there is a time delay between the ignition and the injection, and they can be controlled by using the same program. When the desired in-cylinder conditions are obtained, the fuel spray is injected into the chamber by the help of fuel supply system and injection system. Fuel supply system used in this study consists of a high-pressure fuel pump. Injection system consists of an injector, and a common rail. These systems are controlled by the help of two valves: Pressure Control Valve (PCV) and Volume Control Valve (VCV). Fuel is pressurised by the high-pressure fuel pump. Fuel pump is accelerated by controlling these valves. VCV is used to control the amount of fuel entering the high-pressure fuel pump. The pressurised fuel is transferred to the common rail. The pressure inside the common rail is sensed by a fuel pressure sensor. PCV is used to control the common rail pressure for various operating ranges. The transferred fuel is then injected into the chamber by the

help of an injector. As it is mentioned, the amount and the pressure of the injected fuel are adjusted by using PCV and VCV. The injection duration is also defined in the LabVIEW ignition and injection program. After the injection, according to the oxygen left inside the chamber after precombustion, the combustion occurs. After the combustion, the system is vacuumed by a vacuum system. It is necessary to get rid of unwanted products of combustion. By the help of data acquisition module, the pressure and temperature data are collected and stored.

For non-evaporative spray analysis, the precombustion process is not performed. The ambient pressure is adjusted by supplying nitrogen into the chamber until the desired ambient pressure reached. For evaporative spray analysis, the precombustion process is performed so that there is no oxygen left inside the chamber after precombustion. The fuel spray only evaporates when such a condition is achieved.

Whole process is recorded by a high-speed camera through a Schlieren optical system. Schlieren optical system is composed of a light source, an optical lens, a mirror, a light filter, a knife-edge, and a high-speed camera and schematically shown in Figure 3.12. The trigger signal for high-speed camera is synchronised with the ignition signal. Before explaining the Schlieren setup used in this study, a brief introduction to Schlieren optical system is given in the following section.

3.2. Schlieren Optical System

Schlieren optical system is one of the optical systems that are used to visualize optical density. It has been first used by the German physicist August Toepler in 1864 in order to observe supersonic motion (93). With the advancing technology as time passes by, new methodologies for using Schlieren optical system has been arisen. These methodologies are of value in the fields of computer vision, biology, physics, and engineering (74, 75, 76, 77).

It detects changes in refractive index because it is susceptible to variations in refractive index. The changes in refractive index occurs due to fluctuations in pressure or in temperature. It means that it can separate compression waves from rapidly moving projectiles and air movements. Plane parallelism is also detected by changes in

refractive index. It is usually used to study small or medium size observation fields because it requires quite sensitive and fragile optical equipment. Since it does not obstruct the flow, it is beneficial and informative to use Schlieren optics to study fluid motion where density changes are important (78, 79).

3.2.1. Basic Principle of Schlieren

'Schlieren' is a German word, meaning 'streak'. It is defined as the points which are located in a translucent homogeneous medium where the refractive index varies from its nominal value. Snell's law forms the physical basis of Schlieren imaging. According to the Snell's law, light slows down proportional to refractive index when it interacts with matter. When considering homogeneous media such as in a vacuum, light moves uniformly at a constant speed. When considering inhomogeneous media such as fluids with density change, light does not move uniformly, it refracts which results in Schlieren. Air rising from the heaters, the turbulent wake of a flying projectile, inhomogeneity in salt solutions or in a mixture of two gases, and head and tail waves can be considered as examples of 'Schlieren' (79, 80).

In order to create Schlieren effect, many different optical systems have been defined by various researchers. Although there are different approaches in optical systems, all of them have the same main principle. The principle requires the incorporation of lenses, mirror, and a light source, to capture an accurate image of a sharp-edged stop lighted up by a condensing system. All components must have high precision to form a clear image. Additionally, the main lens and mirror must be as large as the visual field (79).

Figure 3.4 shows us the standard Schlieren setup. It basically consists of two lenses and one knife edge filter. To let all unbent light rays pass through a focal point, the Schlieren object has to be focused by a lens. In Figure 3.4, dashed lines represent the refracting rays, and one of them is filtered out by a cut-off plane. The difference between unbent and refracting rays can be seen more clearly in Figure 3.5. Refracting rays do not pass through the focal point. Further explanation is given in the following section.
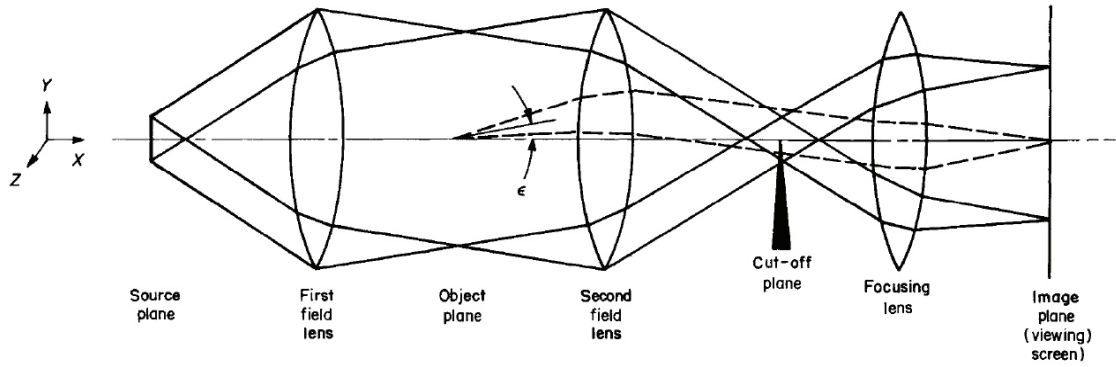
Figure 3. 4. Standard Schlieren Setup (Source: (81))
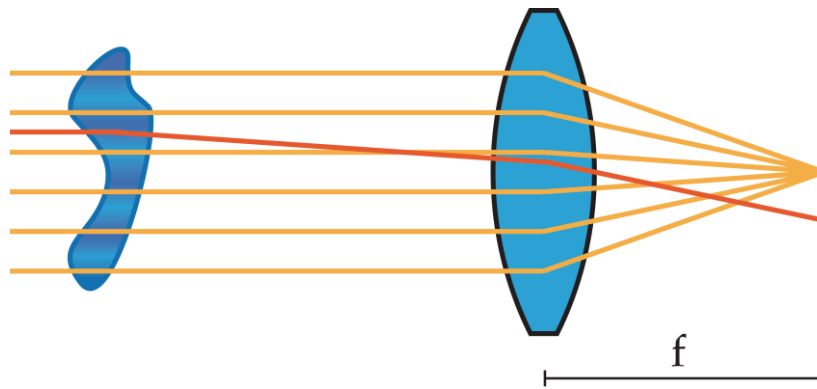
Figure 3. 5. Deviation of the Refracted Light Ray (Source: (81))

3.2.2. Optical Theory

As it is mentioned above, Snell's law forms the physical basis of Schlieren imaging. Deviations are occurred in the light propagation as a result of refraction and diffraction. In other words, they are caused by changes in refractive index. These deviations end up with inhomogeneity and result in Schlieren. There are 3 major concepts that affect the refractive index. These are pressure gradients, temperature differences, and variations of the chemical composition of the material. The changes in pressure gradients are hard to be seen by naked eye because they cause small variations at the refractive index. Only shock waves can be captured by naked eye due to the strong density gradient they owe. Temperature differences are the easiest to be observed because they cause the highest refractive index variations. A candle plume can be given

44

as an example of it. Sugar dilution in water can be given as an example of the variations of the chemical composition of the material (80, 81).

Further explanation about lens relations, refraction, and resolution improvements is given in the Appendix A.

3.2.3. Related Systems

It is possible to vary the Schlieren setup to visualise the refractive index variations. In order to form a basis, some of these different methods and mirror and lens systems are explained shortly.

3.2.3.1. Shadowgraphy

Shadowgraphy is the simplest optical technique to visualise the diffracted light. It projects the shadow of an object on to a projection screen. The image obtained by shadowgraphy is very similar to the human visualisation the image with the naked eye. Gas rising from a barbecue grill can be given as an example. A light source and a flat screen are the equipment for a basic shadowgraphy setup. The basic setup is represented in Figure 3.6. The magnitude of the shadowgrams, which are the images obtained by shadowgraphy, can be controlled by the object distance to the screen.
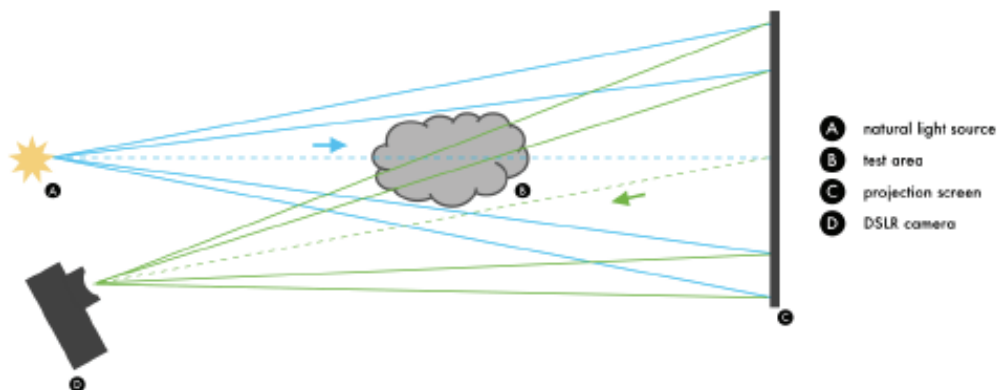
Figure 3. 6. Basic Shadowgraphy Setup (Source: (80))

Although Schlieren setup is designed to obtain an actual image rather than a shadow, shadowgrams are simpler and easier to be collected. Another advantage of the shadowgraphy is that it is flexible to be constructed and large scale or extremely sensitive Schlieren objects can be captured easily. According to the literature, shadowgraphy is useful to obtain more dramatic images of shock waves and turbulent flows. However, for gradual flow, it is not as precise as the Schlieren setup (82, 83).

3.2.3.2. Interferometry

Interferometry uses some basics of the visualization techniques. It provides more efficient and informative methods of measurement. It is used to measure small displacements, changes in refractive index, and surface irregularities in science and industry (84).

The basic interferometry setup is similar to the basic two-lens Schlieren setup. The difference between two of them is that knife-edge cut-off is not being used in the interferometry setup. Some sort of prism or fine wire is being used in order to stimulate the interference or diffraction in the Schlieren pattern in the interferometry setup, so that the image can be analysed.
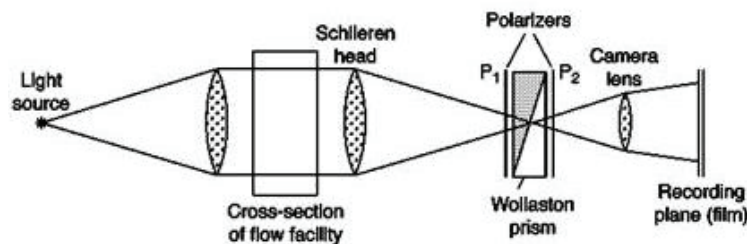
Figure 3. 7. Wollaston Prism Interferometer (Source: (85))

In Figure 3.7, Wollaston prism interferometer, which is one of the interferometry setups, is shown. It consists of a prism placed in between two polarizes. The images obtained by this technique are similar to the images captured by Schlieren setup (86).

Another example of interferometry setup is colour Schlieren interferometry. The difference between the basic two-lens Schlieren setup and the colour Schlieren setup is that a colour filter is being used in the colour Schlieren setup instead of knife-edge cut-

off. In order to get quantitative data from a Schlieren image, it uses particle-image velocimetry diagnostic techniques (87).

3.2.3.3. Background Oriented Schlieren

Background oriented Schlieren setup consists of a smaller number of precisely aligned optical components when compared to the basic Schlieren setup. It has three main components: a camera, a proper background, and a computer for post-processing. It captures the changes in the refractive index by comparing the differences between the stable background and the same background deflected by a flow. It uses Gladstone-Dale equation in order to analyse the captured images. Setup geometry and the distance between the object and the background are the parameters that affect the sensitivity of the background oriented Schlieren. Background oriented Schlieren setup has an advantage of depending only on the size and the detail of the selected stable background (88, 78, 89).

3.2.3.4. Hooke's Schlieren System

Hooke's Schlieren setup uses at least one convex lens or parabolic mirror to capture the Schlieren image. Hooke's Schlieren setup is given in Figure 3.7. According to the Figure 3.8, the setup consists of two candles and one convex lens. One of the candles is used for background illumination and placed to the imaging plane. The other candle is used as a source of a visualisation of hot air (81).
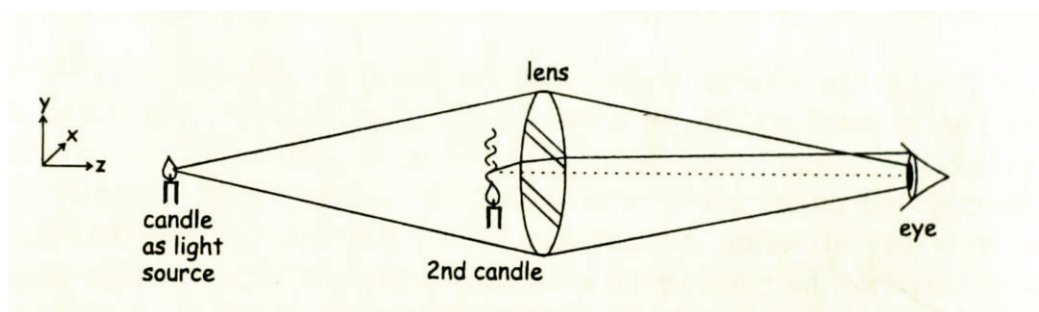
Figure 3. 8. Simple Hooke's Schlieren Setup (Source: (81))

3.2.3.5. Mirror and Lens Systems

The Schlieren setup can be done either by using the convex lens systems or by using the parabolic mirror systems. The combination of the lens and the mirror systems can be also applied as far as they do not cancel the advantages of one of the other.

The lens setup includes two main lenses. One lens is to collimate the light. The other lens is to focus the collimating light onto the filter plane. The setup must be centered on one axis. It is the advantage of the lens system to align all components on the same axis. It is needed to include additional optical components such as a point light source and a camera. An example of the lens system is given in Figure 3.9. Another example can be the Hooke's setup with a camera and a standard filter (81).
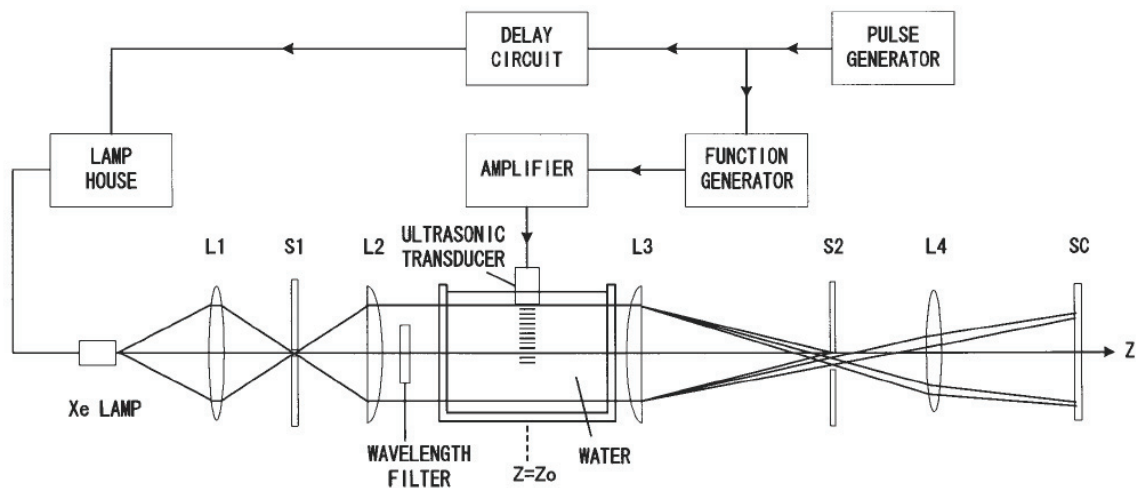
Figure 3. 9. Standard Lens Setup to Observe Ultrasonic Images (Source: (81))

In contrary to the lens setup, mirror setup cannot be aligned onto one axis because the light must not be reflected back from the origin. Typical z-shape setup is mostly used in mirror setup. Figure 3.10 shows us the typical z-shape mirror setup. Although it has an advantage of saving the setup area, it is much more difficult to arrange the mirror system (81).
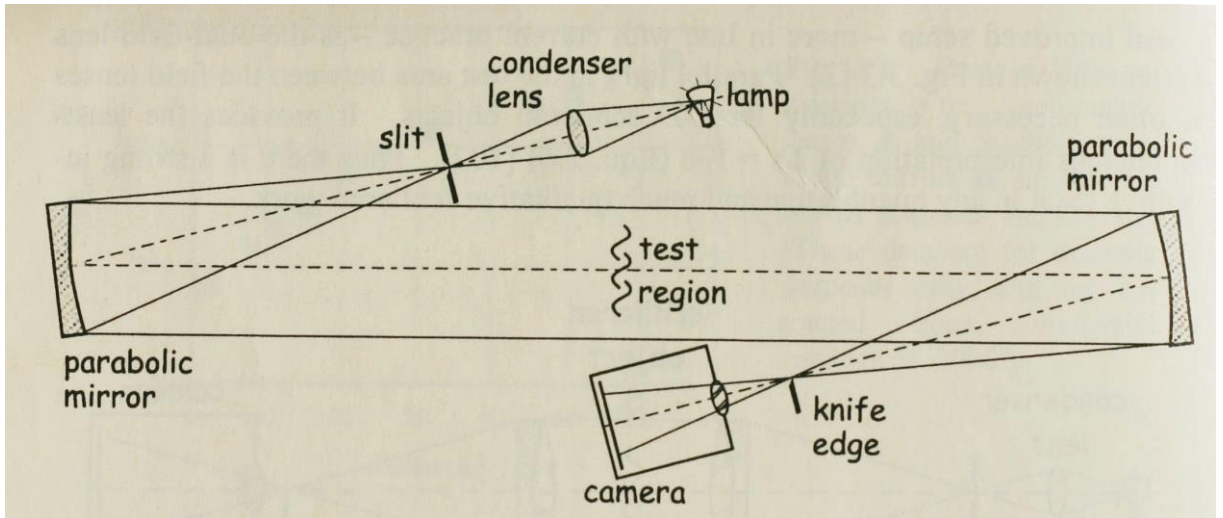
Figure 3. 10. Standard Mirror Setup (Source: (81))

Since geometrical properties are the same for mirrors, chromatic aberration does not occur. However, spherical aberration is unavoidable both for lenses and mirrors. Parabolic mirror is used in the setup because parabolic mirror is able to focus all parallel incoming light onto one point. Besides, off-axis aberration occurs in mirror setup. To prevent it, one-mirror setup can be applied as shown in Figure 3.11 (81).
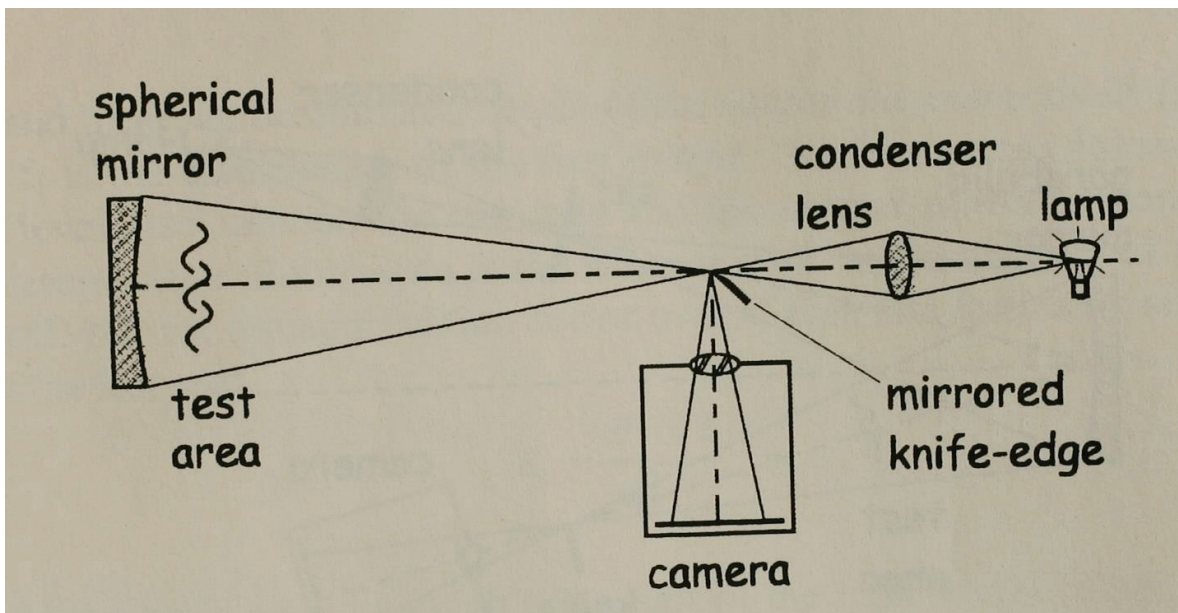
Figure 3. 11. One-Mirror Setup (Source: (81))

3.3. High-Speed Optical Setup Used in This Study

High-speed optical system used in this study consists of high-speed camera and schlieren optical components. The focused single pass schlieren setup has been used in this study. Figure 3.12 represents the schlieren setup visually.
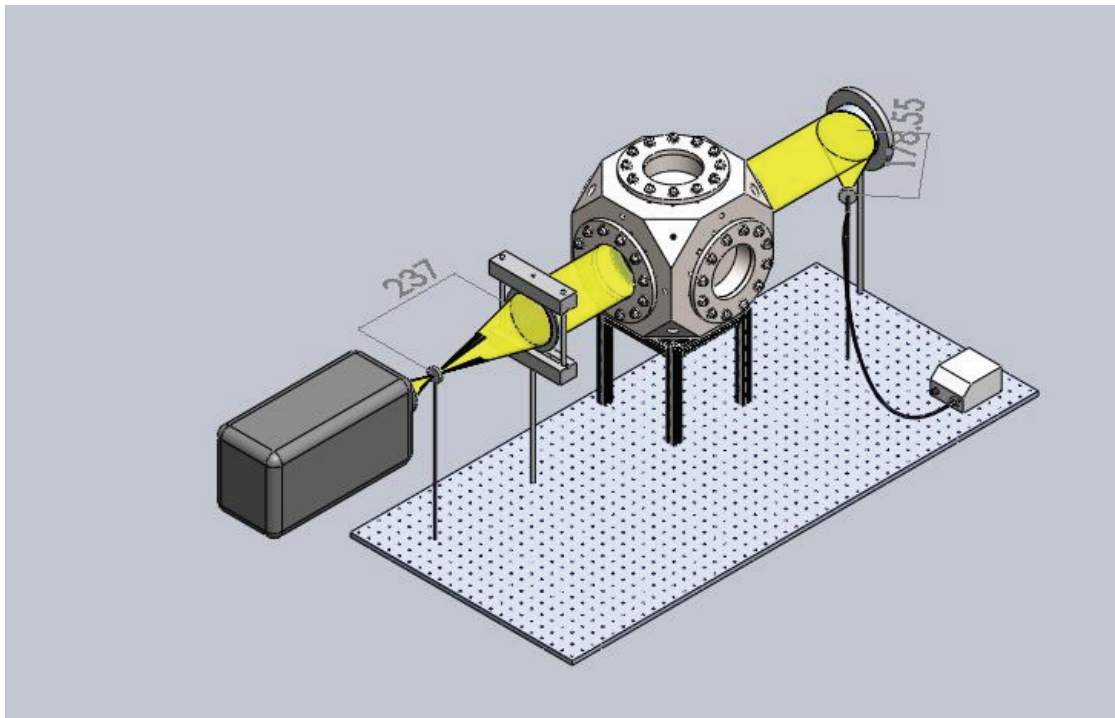
Figure 3. 12. Schlieren Setup

Schlieren optical components consists of a mirror, a high intensity illuminator, a pinhole, and a convex lens. A high intensity illuminator which goes through a pinhole is used as a light source. It is reflected to the test by the help of the mirror. The reflected light goes towards the test area and it is collected on the focal point of the convex lens. The high-speed camera is located on the focal point of the convex lens in order to obtain clear and sharp images. All system is controlled by data acquisition module which is controlled by LabVIEW ignition and injection program. Injection timing and injection pressure can be adjusted and high-speed camera is synchronised with injection timing signal.

3.4. Preparation of Water-in-Diesel Emulsion and Experimental Matrix

As it is depicted on the former sections, the mixture of two immiscible liquids is called as emulsion. Surface agents are used in order to disperse one liquid into the other one. In this study, two-phase emulsion has been used. Surfactants used in this study have been the mixture of Span80 and Tween80. Physical properties of the surfactants are given at the Table 3.1 below. Deionized water and diesel fuel have been used. Diesel has been purchased from a local gasoline station.

Table 3. 1. Physical Properties of the Surfactants

Surfactant	Physical State	Density (g/mL @25 ^{o}C)	HLB Value
Span 80	Liquid	0,994	4,3
Tween 80	Liquid	1,08	15

The volumetric water concentration of emulsion is 10%. The volumetric surfactant concentration of emulsion is 5%. The blend of Span80 and Tween80 has HLB value of 9. The volumetric concentrations of emulsion is given at the Table 3.2.

Table 3. 2. The Volumetric Concentrations of Emulsion

Water Concentration	Surfactant Concentration	Diesel Concentration
10	5	85

Emulsion has been prepared by using a high-speed homogenizer in two steps. Firstly, Span80 and Tween80 surfactants have been mixed with neat diesel. After that, certain amount of water has been included into the mixture of surfactant and neat diesel slowly with constant stirring at 800 rpm. By doing so, pre-emulsion has been prepared. Secondly, the stirring speed has been increased to 5000 rpm and pre-emulsion has been stirred at high speed for 20 minutes. The preparation of the emulsion has been done at

room temperature. Figure 3.13 represents the water-in-diesel emulsion prepared in this study. The emulsion has been stayed stable more than 50 days.

Figure 3. 13. Water-in-Diesel Emulsion

After preparing the emulsion, the experiments have been carried out by following the experimental matrix given at Table 3.3. The scheme of the study can be summarised as,

- After preparing the stable emulsion, preparation of optical setup
- Performing the experiments
- Analysing the results by using Matlab
- Examining the Matlab outcomes and comparing the effects of usage of water-in-diesel emulsion as fuel.

Table 3. 3. Experimental Matrix

NEAT DIESEL	Pv - Non-reactive cases		
Injection Pressure	5 bar	10 bar	15 bar
500	D_500_5	D_500_10	D_500_15
700	D_700_5	D_700_10	D_700_15
900	D_900_5	D_900_10	D_900_15

WATER-in-DIESEL	Pv - Non-reactive cases		
Injection Pressure	5 bar	10 bar	15 bar
500	W_500_5	W_500_10	W_500_15
700	W_700_5	W_700_10	W_700_15
900	W_900_5	W_900_10	W_900_15

3.5. Spray Angle and Spray Penetration Calculation via Matlab

Since the fundamental aims of this research is to measure spray penetration and spray angle, Matlab algorithm has been developed to measure spray penetration and spray angle. The algorithm is given in Appendix B.

The input is the video of the spray recorded by high speed camera. High speed camera captures 20000 frame per second. Shutter speed is set to 1/62000 seconds to obtain more clear videos. The camera resolution was 512*512.

In order to obtain the spray penetration measurement from the video, four images of the respective sequence have been taken before fuel injection. These images have been used for correction of the raw images taken from each complete injection. Background subtraction has been applied. After background subtraction, a threshold value has been calculated by using Otsu's threshold method. After thresholding, last pixel of each image has been defined and spray penetration has been calculated by using the formula for finding the distance between two points. In Figure 3.14, there is a representative picture to show how the penetration is measured. Since each video have

been taken from the same point of view, injector tip coordinates are selected as constant for all of them. The length of the line shown in Figure 3.14 gives the penetration length.

Figure 3. 14. Spray Penetration

In order to obtain the spray angle measurement, an angle measurement tool has been created in Matlab. Angle measurement tool creates 2 vectors according to the position of the injector tip. Figure 3.15 shows the vectors located on the image. After obtaining these vectors, end points of the vectors can be moved towards the desired point. The vectors should be tangent to the spray outline. Figure 3.16 represents the spray angle measurement by using angle measurement tool.
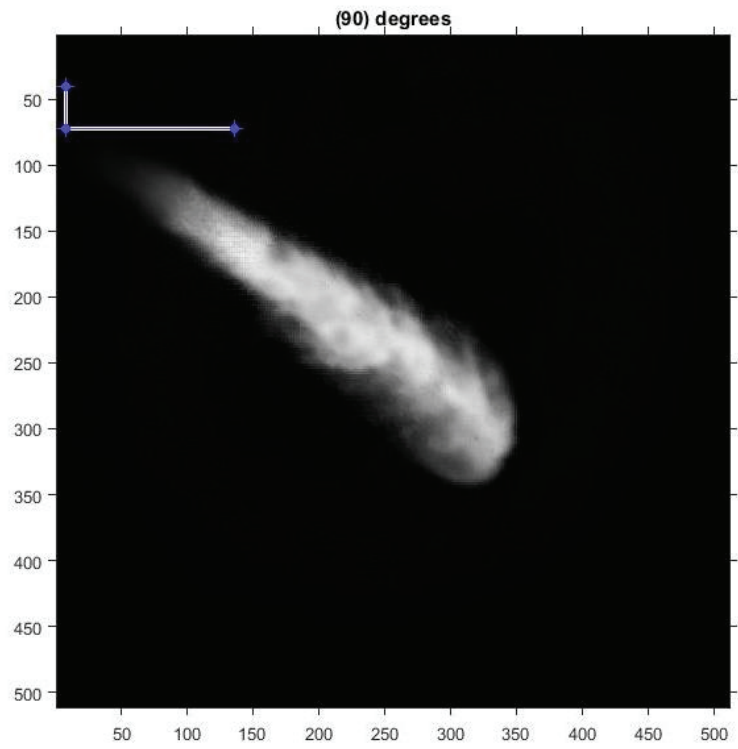
Figure 3. 15. Angle Measurement Vectors Located on the Image
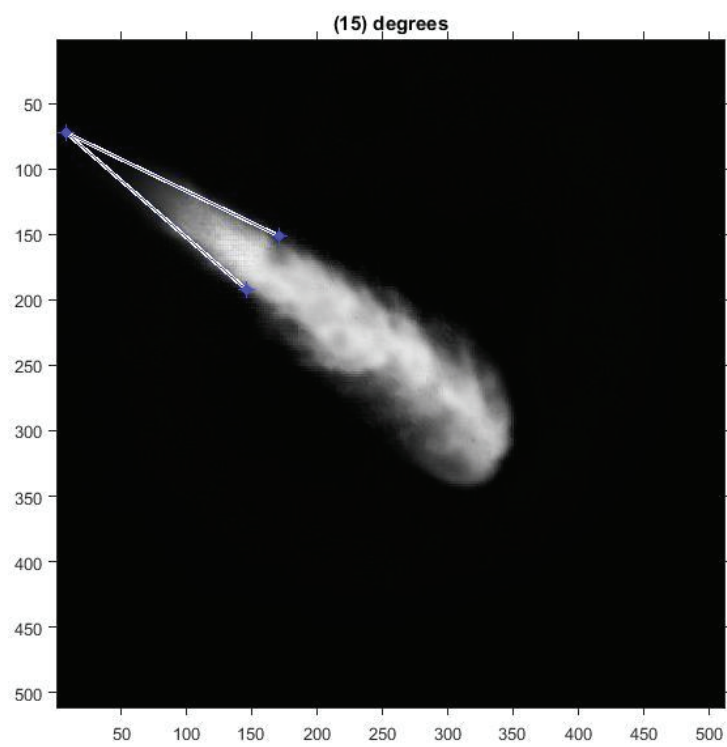
Figure 3. 16. Spray Angle Measurement

CHAPTER 4

RESULTS AND DISCUSSION

Combustion process is qualified by factors such as injection properties, spray angle, spray penetration, cylinder pressure, and atomization. Spray characteristics can be divided into two categories: spray angle and spray penetration. Before looking into these, brief information is given about spray propagation below.

4.1. Spray Propagation Due to Time Interval

Spray propagates differently under different conditions. This study investigates the spray characterisation of Water-in-Diesel Emulsion (WiDE) under different ambient pressures and injection pressures. In order to examine the progress of fuel sprays, neat diesel fuel and water-in-diesel emulsion fuel have been used in this study. After that, the differences among them have been investigated. Ambient pressure of constant volume combustion chamber has been changed from 5 bar to 15 bar with increments of 5 bar. Ambient pressure has been identified by filling the chamber with nitrogen. As mentioned, to obtain accurate pressure inside the chamber, gas filling system has controlled by PID and ambient pressure has been controlled by pressure sensors. Injection pressure has been changed from 50 Mpa to 90 Mpa with increments of 20 Mpa. In order to assure the repeatability of the tests, all experiments have been repeated two times. With the significance level of 0,1, confidence interval has been calculated as ±1,65 mm.

Visual comparison tables of diesel spray and WiDE spray are given below. As it can be noticed from the tables (Table 4.1 – Table 4.9), diesel spray propagates more slowly than WiDE spray for all conditions. Spray becomes smaller as the ambient pressure increases. Spray becomes wider as the injection pressure increases.

WiDE spray has better atomization due to lower volatility of water. It leads to longer and wider spray when compared to diesel spray. Spray angle and spray penetration are compared in detail at the following sections.

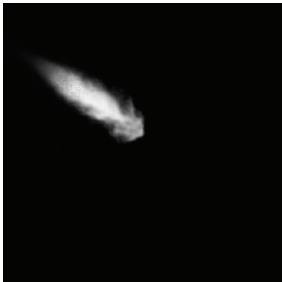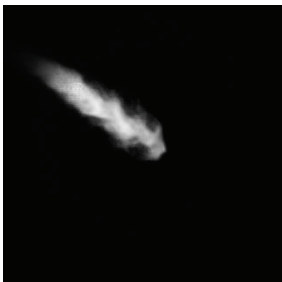Table 4. 1. Spray Under 5 bar Ambient Pressure with 50 Mpa Injection Pressure

5 Bar Ambient Pressure/ 50 MPa Injection Pressure		
Time	Diesel	WiDE
0,75 ms		
1,25 ms		
1,85 ms		

Table 4. 1. (cont.)
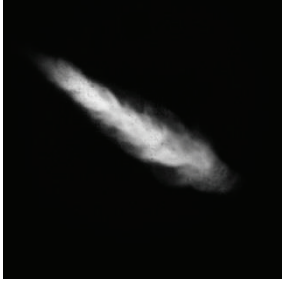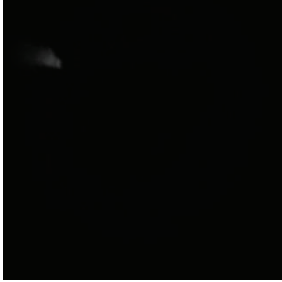
5 Bar Ambient Pressure/ 50 MPa Injection Pressure		
Time	Diesel	WiDE
2,2 ms		

Table 4. 2. Spray Under 5 bar Ambient Pressure with 70 Mpa Injection Pressure

5 Bar Ambient Pressure/ 70 MPa Injection Pressure		
Time	Diesel	WiDE
0,75 ms		
1,25 ms		

Table 4. 2. (cont.)

5 Bar Ambient Pressure/ 70 MPa Injection Pressure		
Time	Diesel	WiDE
1,85 ms		
2,2 ms		

Table 4. 3. Spray Under 5 bar Ambient Pressure with 90 Mpa Injection Pressure

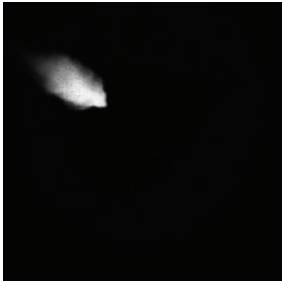| 5 Bar Ambient Pressure/ 90 MPa Injection Pressure		
Time	Diesel	WiDE
0,75 ms		

Table 4. 3. (cont.)

5 Bar Ambient Pressure/ 90 MPa Injection Pressure		
Time	Diesel	WiDE
1,25 ms		
1,85 ms		
2,2 ms		

Table 4. 4. Spray Under 10 bar Ambient Pressure with 50 Mpa Injection Pressure
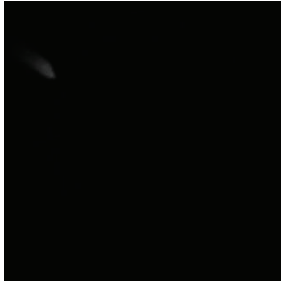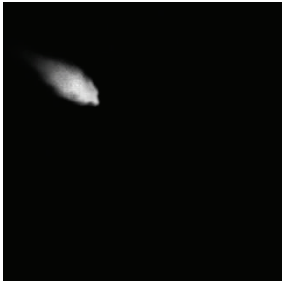
10 Bar Ambient Pressure/ 50 MPa Injection Pressure		
Time	Diesel	WiDE
0,75 ms		
1,25 ms		
1,85 ms		
2,2 ms		

Table 4. 5. Spray Under 10 bar Ambient Pressure with 70 Mpa Injection Pressure
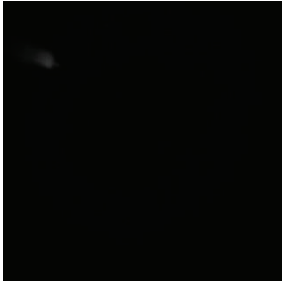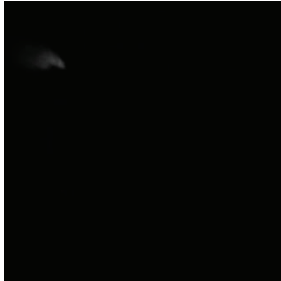
10 Bar Ambient Pressure/ 70 MPa Injection Pressure		
Time	Diesel	WiDE
0,75 ms		
1,25 ms		
1,85 ms		
2,2 ms		

Table 4. 6. Spray Under 10 bar Ambient Pressure with 90 Mpa Injection Pressure

10 Bar Ambient Pressure/ 90 MPa Injection Pressure		
Time	Diesel	WiDE
0,75 ms		
1,25 ms		
1,85 ms		
2,2 ms		

Table 4. 7. Spray Under 15 bar Ambient Pressure with 50 Mpa Injection Pressure
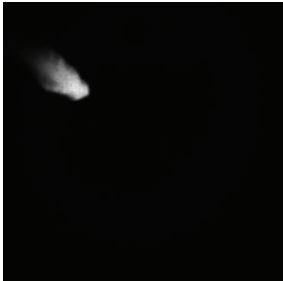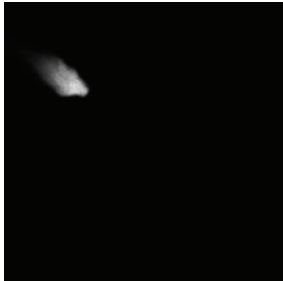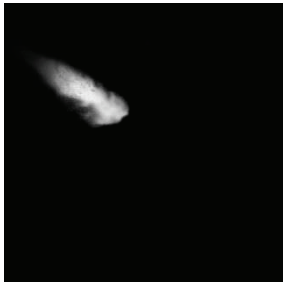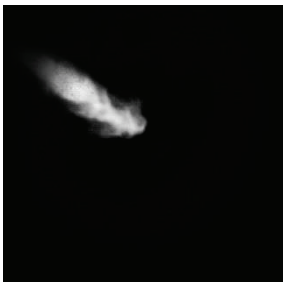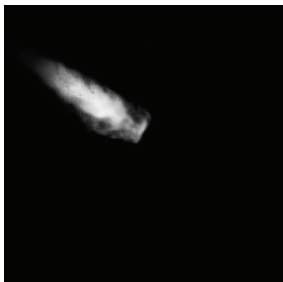
15 Bar Ambient Pressure/ 50 MPa Injection Pressure		
Time	Diesel	WiDE
0,75 ms		
1,25 ms		
1,85 ms		
2,2 ms		

Table 4. 8. Spray Under 15 bar Ambient Pressure with 70 Mpa Injection Pressure
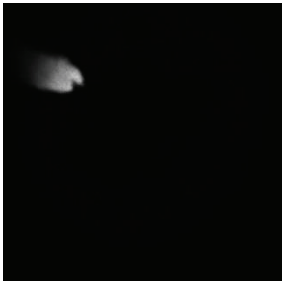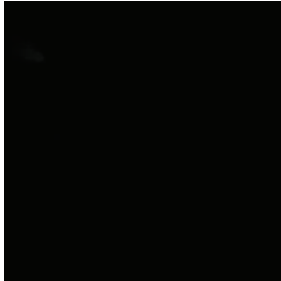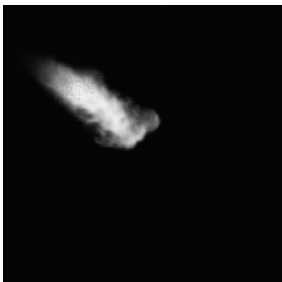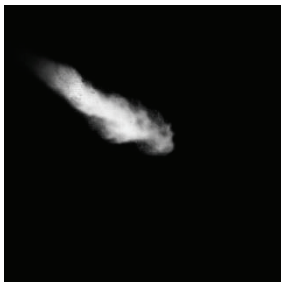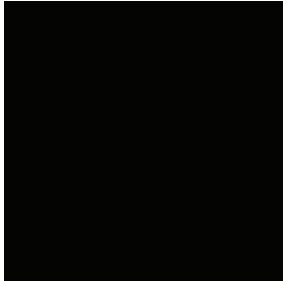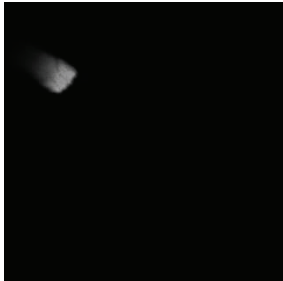
15 Bar Ambient Pressure/ 70 MPa Injection Pressure		
Time	Diesel	WiDE
0,75 ms		
1,25 ms		
1,85 ms		
2,2 ms		

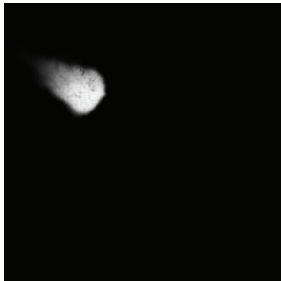Table 4. 9. Spray Under 15 bar Ambient Pressure with 90 Mpa Injection Pressure
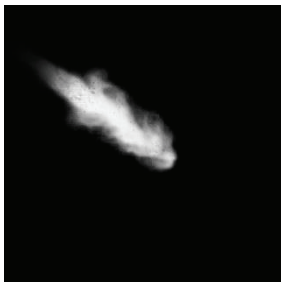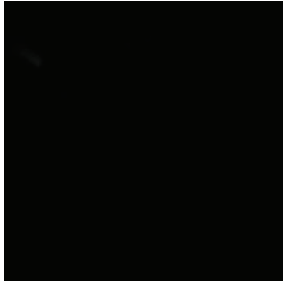
15 Bar Ambient Pressure/ 90 MPa Injection Pressure		
Time	Diesel	WiDE
0,75 ms		
1,25 ms		
1,85 ms		
2,2 ms		

4.2. Spray Penetration

Spray penetration is defined as the maximum distance starting from the injector to the spray tip. Injection pressure, in-cylinder pressure, fuel type, and nozzle geometry are the parameters that affect spray penetration. Spray penetration under different ambient pressures with different injection pressures compared at the graphs given below (Figure 4.1 – Figure 4.6).
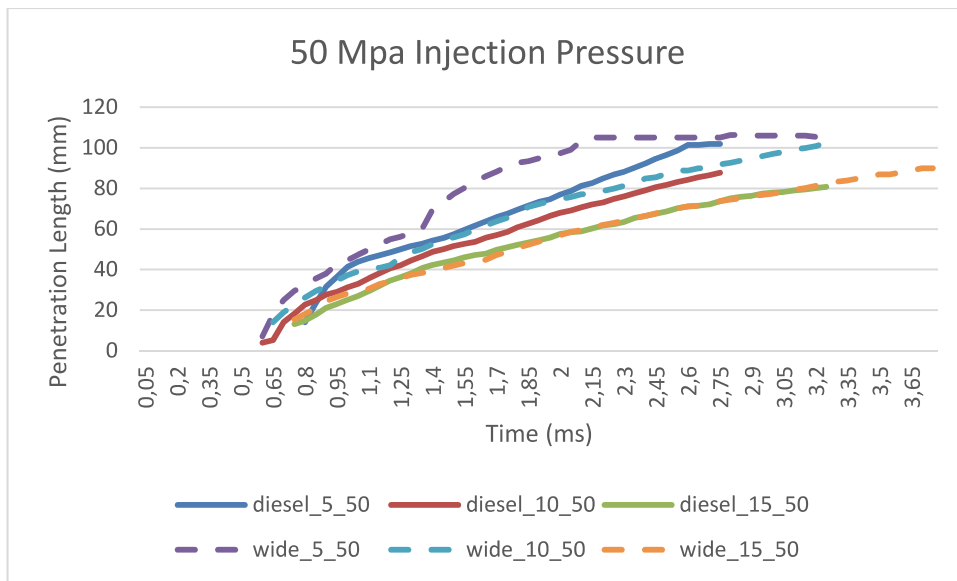
Figure 4. 1. Spray Penetration with Injection Pressure of 50 Mpa
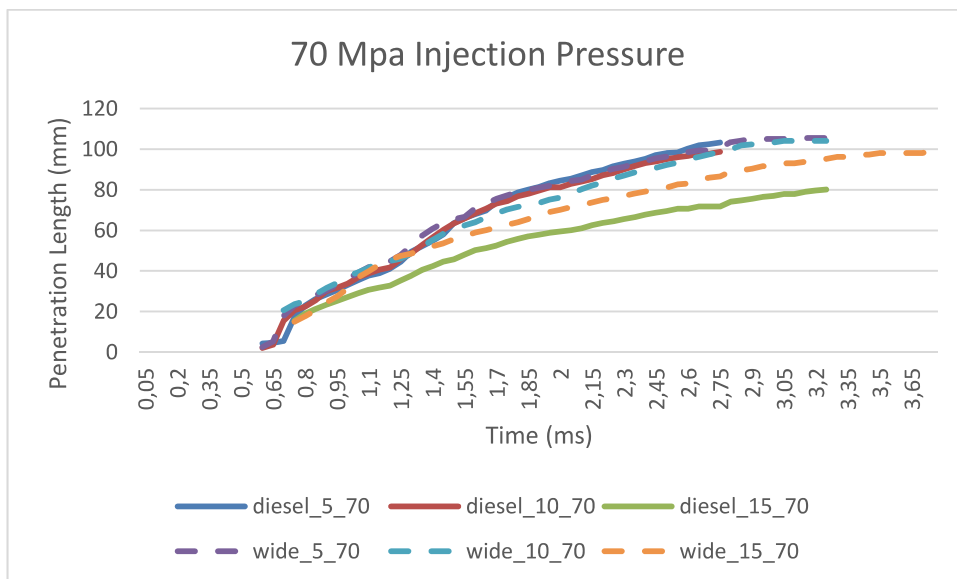
Figure 4. 2. Spray Penetration with Injection Pressure of 70 Mpa
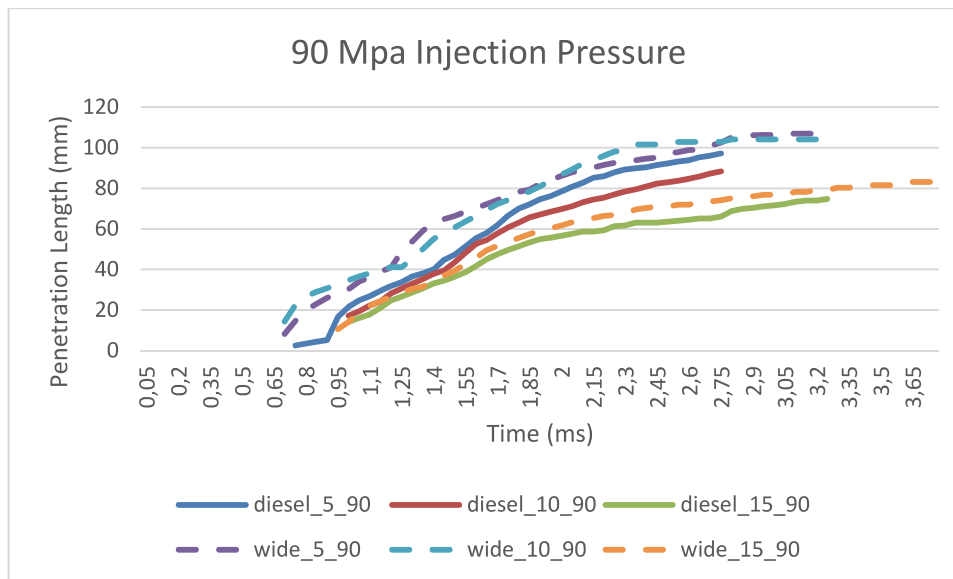
Figure 4. 3. Spray Penetration with Injection Pressure of 90 Mpa

Figure 4.1 represents how spray penetration changes according to different ambient pressures at 50 Mpa injection pressure. The longest spray has been observed with 5 bars of ambient pressure in order of WiDE and diesel. As it can be noticed from Figure 4.1, spray penetration lasts longer at higher ambient pressures. The reason of having longer penetration duration under higher ambient pressures is to obtain slower propagation due to high drag forces.

Figure 4.2 represents how spray penetration changes according to different ambient pressures at 70 Mpa injection pressure. As it is expected, WiDE has longer penetration length when compared to neat diesel fuel. When the injection pressure increased to 70 Mpa, penetration length increases due to better atomization. When viewed from the penetration time, the result aligns with the results of 50 Mpa injection pressure. As the ambient pressure increases, spray penetration lasts longer.

Figure 4.3 represents how spray penetration changes according to different ambient pressures at 90 Mpa injection pressure. As it is mentioned above, penetration duration increases when the ambient pressure increases. There against, the penetration length shortens when the injection pressure increased from 70 Mpa to 90 Mpa. WiDE has longer penetration than neat diesel due to the lower volatility of the water. When the fuel is injected with higher pressures, the liquid length of the spray becomes longer but penetration length becomes smaller. It is because of the better fuel atomization. Higher injection pressures lead better secondary atomisation, hence shorter penetration.

68

Figure 4. 4. Spray Penetration with Ambient Pressure of 5 Bar
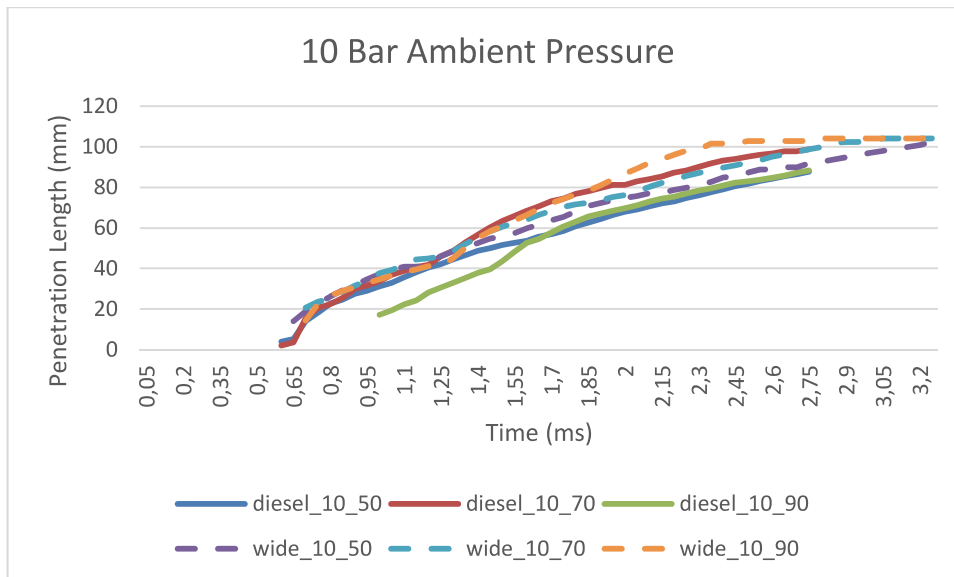
Figure 4. 5. Spray Penetration with Ambient Pressure of 10 Bar

Figure 4.4 represents how spray penetration changes according to different injection pressures at 5 bar ambient pressure. The longest sprays have been observed with 50 Mpa injection pressure in order of WiDE and diesel. The reason of obtaining longer penetration with the injection pressure of 50 Mpa is to have low injection pressure. When the injection pressure is not high enough, spray cannot propagate as it should. Secondary break-up becomes weaker, hence the atomization. That's why, spray penetrates longer when compared with the higher injection pressures.
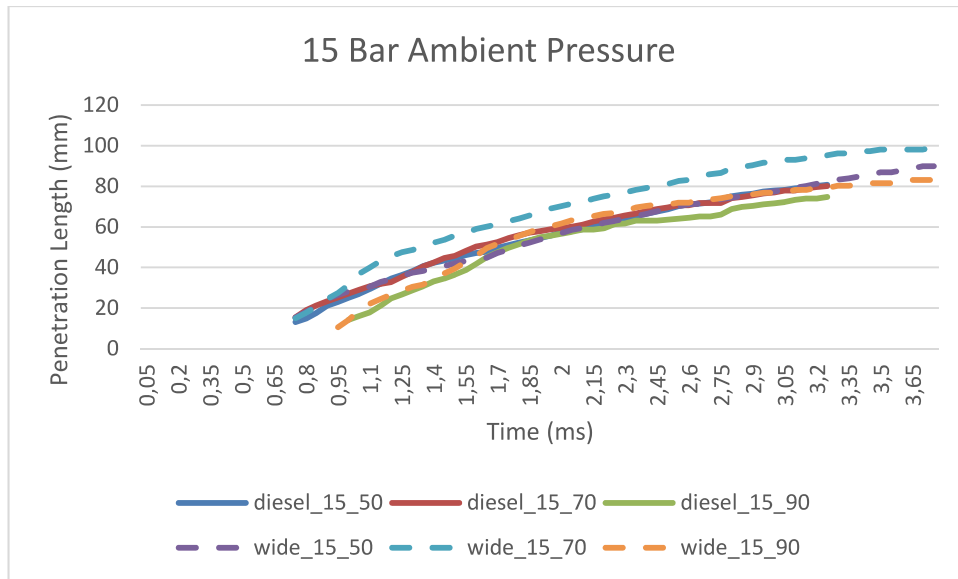
Figure 4. 6. Spray Penetration with Ambient Pressure of 15 Bar

Figure 4.5 represents how spray penetration changes according to different injection pressure at 10 bar ambient pressure. According to the Graph 4.5, WiDE spray penetrates longer as the injection pressure increases. However, diesel spray has the longest penetration with the injection pressure of 70 Mpa. As it is mentioned above, 50 Mpa injection pressure is very low to obtain real spray distribution performance. When compared 70 Mpa and 90 Mpa injection pressures, spray penetration of diesel fuel is longer with 70 Mpa injection pressure. It can be explained as the injection pressure increases, the evaporation after injection becomes faster. It results in smaller penetration. For general, WiDE spray is longer than neat diesel spray.

Figure 4.6 represents how spray penetration changes according to different injection pressure at 15 bar ambient pressure. As expected, due to the lower volatility and higher viscosity of WiDE, WiDE presented longer penetration when compared to neat diesel fuel. Spray penetration with 70 Mpa injection pressure is the longest both for neat diesel fuel and for WiDE. This is because of that the best spray atomization occurs with the injection pressure of 70 Mpa. When the injection pressure increases, spray starts evaporating near the nozzle. That's why, the penetration length is smaller for injection pressures higher than 70 Mpa.

(a) Spray penetration length at 800 bar   (b) Spray penetration length at 1000 bar

(c) Spray penetration length at 1200 bar
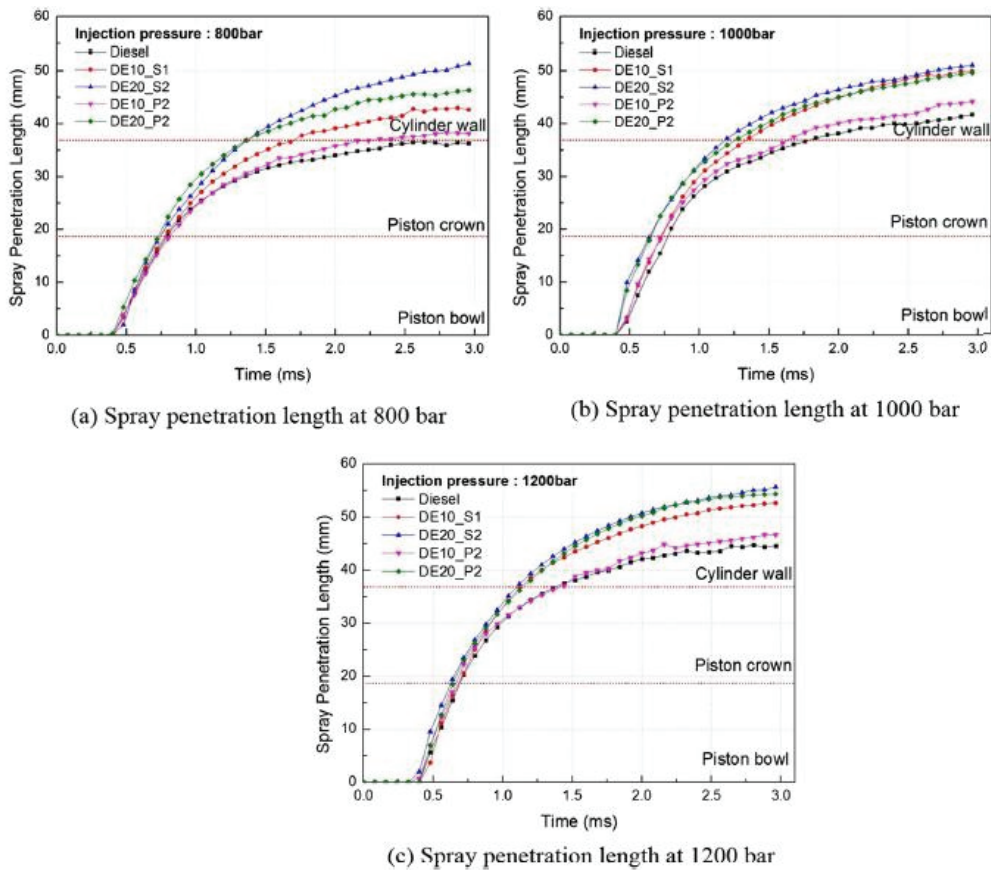
Figure 4. 7. Spray Penetration Lengths (Source: (60))

Park et al. investigated spray characterization of water emulsified fuels. Figure 4.7 depicts their spray penetration results according to the different injection pressures. They have ended up with longer spray penetration as the injection pressure increased. According to their results, emulsified fuel has longer penetration length than neat diesel fuel.

As it can be noticed, Park et al. have changed the injection pressure from 80 Mpa to 120 Mpa with increments of 20 Mpa. As it is mentioned previously, with the injection pressure of less than 70 Mpa, the spray cannot propagate as it should because of weaker atomization. When considering our results with the injection pressure of 70 Mpa and higher, they align with the results given in the literature.

These variations in penetration are caused by differences in volatility. Since water has lower volatility, it is expected to have longer penetration for WiDE. The results are generally aligned with the literature (56, 60, 66).

4.3. Spray Angle

Spray angle is defined as the angle between two tangent lines to the spray outline starting from the orifice exit of the nozzle. Spray angle under different ambient pressures with different injection pressures compared at the graphs given below (Figure 4.8 – Figure 4.13).
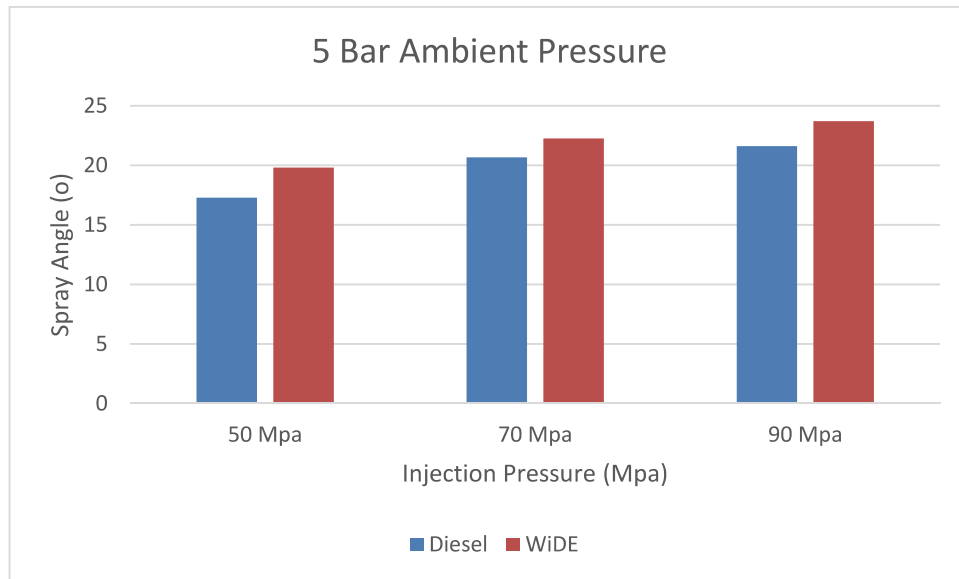

Figure 4. 8. Spray Angle witb Ambient Pressure of 5 Bar
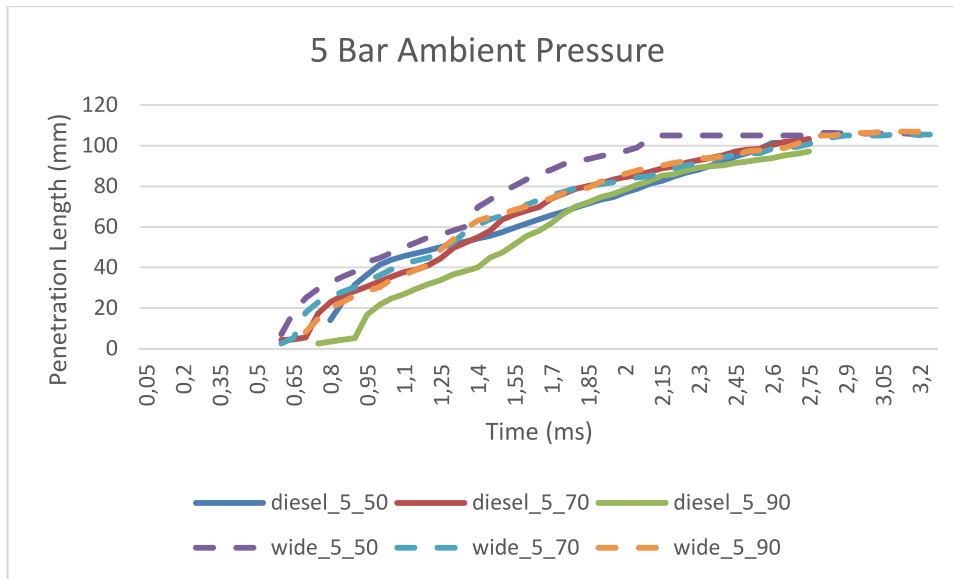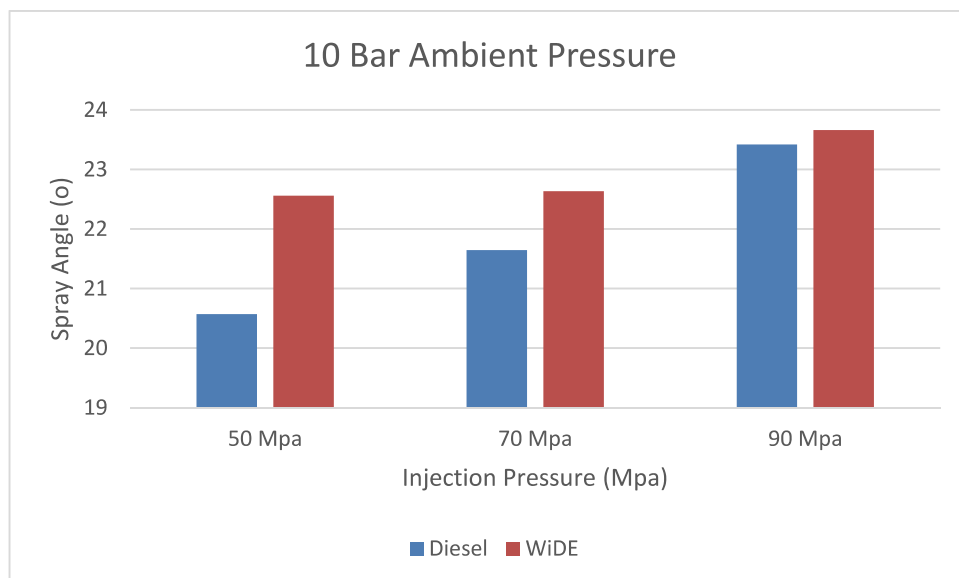

Figure 4. 9. Spray Angle with Ambient Pressure of 10 Bar
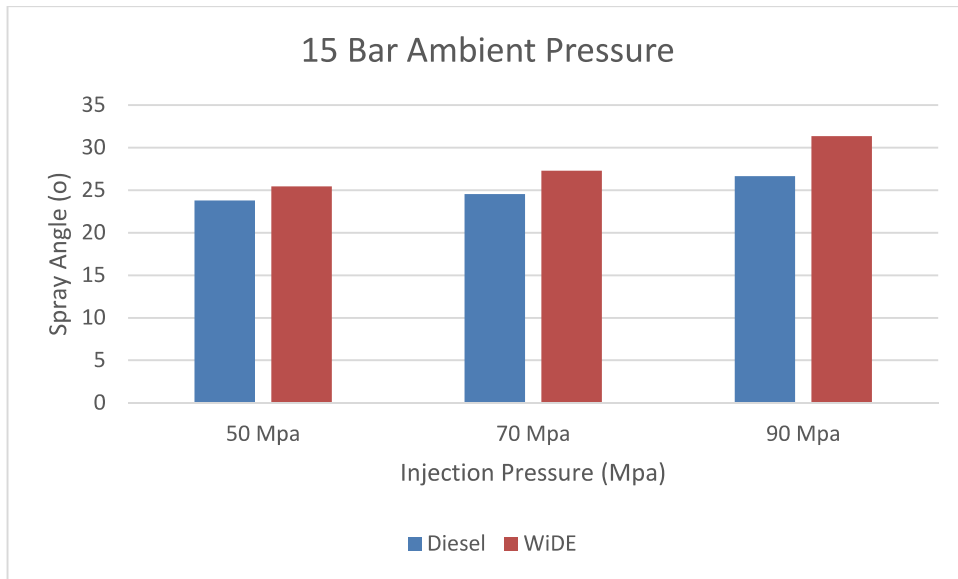
Figure 4. 10. Spray Angle with Ambient Pressure of 15 Bar

Figure 4.8 represents the spray angle change with different injection pressures under 5 bar ambient pressure. As it can be noticed from the graph, spray angle is wider for WiDE for all cases. Spray angle becomes wider as the injection pressure increases due to the secondary atomization. As the injection pressure increases, atomization starts near the nozzle resulted in wider spray angle.

Figure 4.9 represents the spray angle change with different injection pressures under 10 bar ambient pressure. As a result of better atomization, spray angle is wider for higher injection pressures.

Figure 4.10 represents the spray angle change with different injection pressures under 15 bar ambient pressure. As expected, the widest spray angle occurs for WiDE with 90 Mpa injection pressure.

Figure 4.11 represents the spray angle change with 50 Mpa injection pressure under different ambient pressures. From the graph, when the ambient pressure increases, spray angle gets wider. Higher ambient pressure means higher drag forces. When spray reacts with these drag forces, it starts evaporating. This scenario results in wider spray angle.
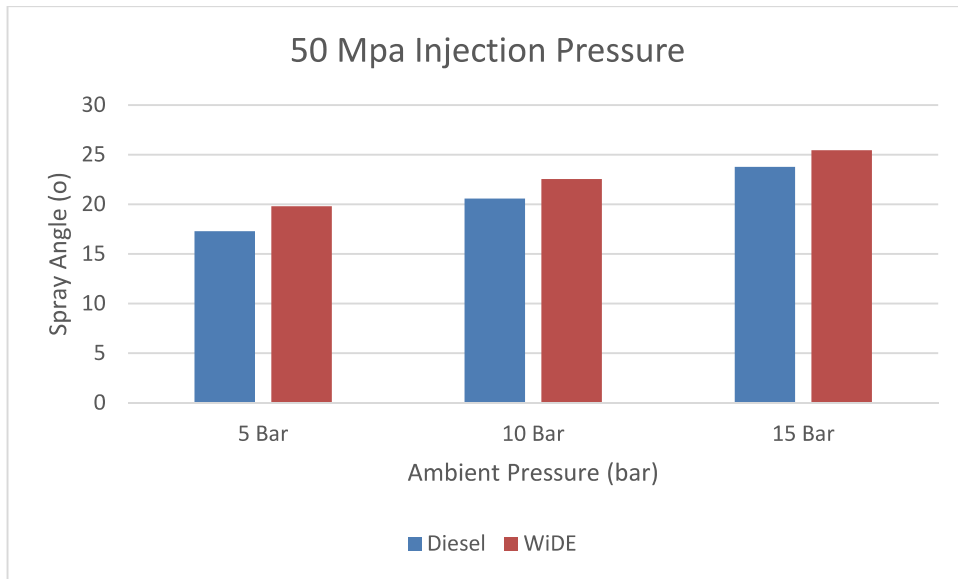
Figure 4. 11. Spray Angle with Injection Pressure of 50 Mpa
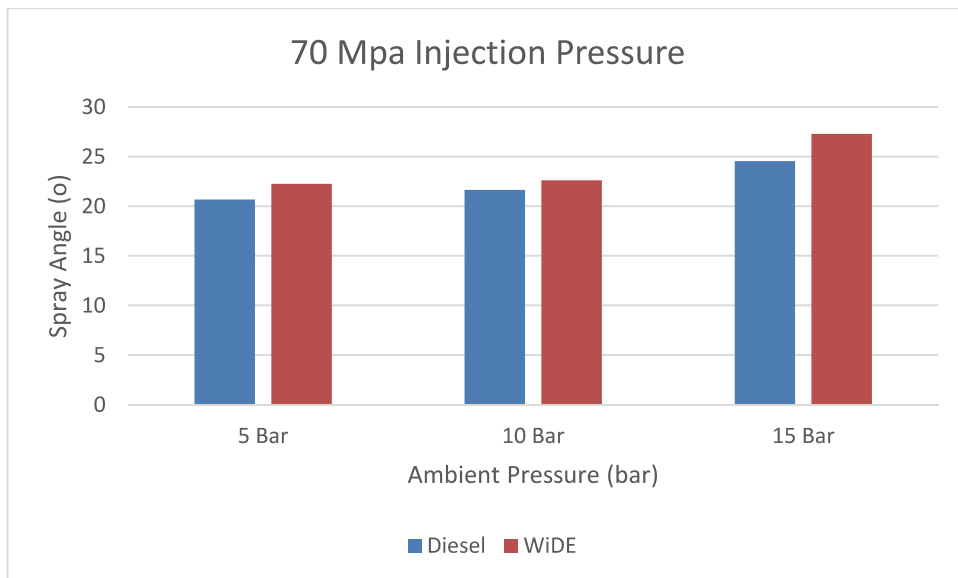
Figure 4. 12. Spray Angle with Injection Pressure of 70 Mpa

Figure 4.12 represents the spray angle change with 70 Mpa injection pressure under different ambient pressures. It is observed that WiDE has wider spray angle when compared to neat diesel spray. Besides, as the ambient pressure increases, angle of the spray increases.
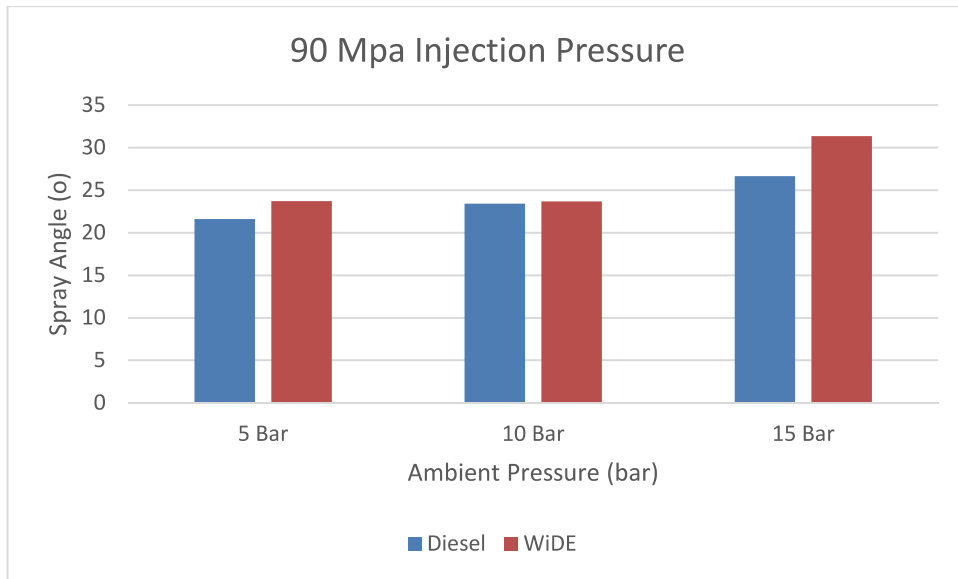
Figure 4. 13. Spray Angle with Injection Pressure of 90 Mpa

Figure 4.13 represents the spray angle change with 90 Mpa injection pressure under different ambient pressures. As expected, the result aligns with the results of other injection pressures. Higher ambient pressures lead wider spray angle.

According to the spray angle investigation, results shows that spray angle becomes wider as the injection pressure and ambient pressure increases. WiDE has wider spray angle when compared to the neat diesel. The reason of that the lower volatility of the water. The results align with the literature (56, 60, 66).

4.4. Future Works

Since water-in-diesel emulsions are still under investigation and new trend for alternative fuel types, there are wide range of investigation area for them. For the future works, this study can be extended as follows:

- Different emulsions can be produced by changing the water content. After that, emulsions can be compared with each other in order to obtain the better water concentration.
- There are 2 more types of emulsions: micro-emulsions and nano-emulsions. One of them can be included in the future study.

- Since the most important phenomena in emulsions is micro-explosions, optical system can be enhanced to observe micro-explosions in WiDE spray.

- Fuel characteristics such as viscosity, density, etc. can be a focus of future study.

- Emulsions can be investigated under microscope in order to observe the water droplets trapped in diesel. By doing so, SMD can be calculated.

- Water-in-biodiesel emulsions can be a part of the future investigations.

- Emulsions can be prepared by using different surfactants. So that, surfactant effect on emulsions can be understood clearly.

- Combustion characteristics can be investigated for the future works.

CHAPTER 5

CONCLUSION

The focus of the study was to investigate one of the most important spray characteristics, spray penetration depth for water-in-diesel emulsions. Through this study, water-in-diesel emulsions and their spray penetration depth have been investigated and compared with neat diesel fuel.

In order to achieve the purpose of the study, water-in-diesel emulsion with 10% of water content has been produced. Before starting the experiments, stability check of the emulsion has been done. The emulsion used in this study stayed stable more than 50 days. After that, experiments have been started confidently.

In order to observe the spray, a CVCC and high-speed optical system have been used. Spray investigation has been completed under various ambient pressures and various injection pressures. Ambient pressure has been varied from 5 bar to 15 bar with an increment of 5 bar. Injection pressure has been varied from 50 Mpa to 90 Mpa with an increment of 20 Mpa. All experiments have been recorded by using a high-speed camera.

The results have been investigated by using a Spray Angle and Spray Penetration Calculation Matlab algorithm developed for this study. For spray characterisation, spray angle and spray penetration have been calculated by the help of Matlab algorithm.

According to the results, water-in-diesel emulsion had 11% longer and wider spray when compared to neat diesel spray. The confidence interval of the penetration results was ±1,65 mm. Due to the lower volatility of the water, spray tended to be longer and wider. The reason of having enhanced spray for emulsions is that water content in diesel led to better atomization as a result of micro-explosion and puffing. This situation results in better air-fuel mixing for combustion and decreases the in-cylinder temperature. That's why, using water-in-diesel emulsion as a fuel leads to cleaner exhaust gas.

To sum up, spray cannot propagate as it should for the injection pressures lower than 70 Mpa. That's why, the longest sprays have been obtained for the injection pressure of 50 Mpa. When the injection pressure becomes higher than 70 Mpa, the fuel started evaporating near the nozzle due to cavitation. That's why, spray penetration has become smaller. As a result, 70 Mpa is the proper injection pressure for investigation of spray penetration. Spray penetration has become smaller as the ambient pressure increased due to higher drag forces caused by the pressure. Spray angle has become wider as injection pressure and ambient pressure increased.

To sum up, this research shows us that the usage of WiDE as fuel resulted in higher penetration length and wider spray angle. It leads to better fuel-air mixing which results in cleaner combustion. Because of the volatility difference between water and diesel, better atomization is obtained. It leads to a decrease in cylinder temperature, hence NO_x formation.

This research aligns with the literature and supports the results found in the literature. Since it is still not clear what is really happening inside the engine, this topic is under investigation. That's why, it is important to find out close results to the literature.

This research has claimed that a stable emulsion can be produced. Spray characteristics characterize the combustion efficiency. This research shows that the most proper injection pressure to achieve better atomisation is 70 Mpa. It is assumed that better atomisation leads to better fuel/air mixing and lower emission rates.

REFERENCES

(1)   Roy. Ci engine combustion by Akhileshwar Nirala
        https://www.slideshare.net/akhileshroy96/ci-engine-combustion-by-akhileshwar-
        nirala (accessed May 23, 2019).

(2)   https://www.quora.com/Provided-the-fuel-is-injected-after-air-compression-
        why-cant-gasoline-engines-be-designed-at-the-same-high-compression-rates-as-
        diesel-engines (accessed May 23, 2019).

(3)   https://www.researchgate.net/profile/Sohel_Anwar/publication/258401046
        (accessed May 23, 2019).

(4)   Hamza. Fuel Injection and Spray Formation
        https://www.slideshare.net/AhmedHamza43/fuel-injection-and-spray-formation
        (accessed May 24, 2019).

(5)   Hsu, B. Practical Diesel-Engine Combustion Analysis; Society of Automotive
        Engineers: Warrendale, 2002.

(6)   Spray characteristics https://en.wikipedia.org/wiki/Spray_characteristics
        (accessed May 23, 2019).

(7)   Diesel Fuel Injector Nozzles
        https://www.dieselnet.com/tech/engine_fi_nozzle.php#saet (accessed May 23,
        2019).

(8)   Types of Nozzle in IC Engine: Pintle Nozzle, Single Hole Nozzle, Multihole
        Nozzle, Pintaux Nozzle - mech4study
        http://www.mech4study.com/2017/03/types-of-nozzle-in-ic-engine.html
        (accessed May 23, 2019).

(9)   Baumgarten, C. Mixture Formation in Internal Combustion Engines; Springer:
        Berlin, 2010.

(10) Schugger, C.; Renz, U. Experimental Investigations on the Primary Breakup Zone of High Pressure Diesel Sprays from Multi-Orifice Nozzles. In Iclass-Europe 2003; Sorrento, Italy, 2003.

(11) Blessing, M., König, G., Krüger, C., Michels, U. et al. Analysis of Flow and Cavitation Phenomena in Diesel Injection Nozzles and Its Effects on Spray and Mixture Formation; SAE Technical Paper 2003-01-1358, 2003.

(13) https://www.globalspec.com/learnmore/manufacturing_process_equipment (accessed May 23, 2019).

(13) Kadocsa, A.; Tatschl, R.; Kristóf, G. Analysis of Spray Evolution In Internal Combustion Engines Using Numerical Simulation. Journal of Applied Mathematics and Computational Mechanics 2007, 85-100.

(14) Payri, R.; Salvador, J.; Gimeno, J.; De la Morena, J. Analysis of Diesel Spray Atomization by Means of a Near-Nozzle Field Visualitation Teqnique. Atomization and Sprays 2011, 21, 753-774.

(15) Frs, L. On The Instability of Jets. London Mathematical Society 1878, 10, 4-13.

(16) Yuen, M. Non-Linear Capillary Instability of A Liquid Jet. Journal of Fluid Mechanics 1968, 33, 151-163.

(17) Nayfeh, A. Nonlinear Stability of a Liquid Jet. Physics of Fluids 1970, 13, 841.

(18) Rutland, D.; Jameson, G. Theoretical Prediction of the Sizes Of Drops Formed In The Breakup Of Capillary Jets. Chemical Engineering Science 1970, 25, 1689-1698.

(19) Reitz, R.; Bracco, F. Mechanisms of Breakup of Round Liquid Jets. 1986.

(20) Wierzba, A. Deformation and Breakup of Liquid Drops In A Gas Stream At Nearly Critical Weber Numbers. Experiments in Fluids 1990, 9, 59-64.

(21) Liu, Z.; Hwang, S.; Reitz, R. Breakup Mechanisms and Drag Coefficients of High-Speed Vaporizing Liquid Drops. Atomization and Sprays 1996, 6, 353-376.

(22) Krzeczkowski, S. Measurement of Liquid Droplet Disintegration Mechanisms. International Journal of Multiphase Flow 1980, 6, 227-239.

(23) Gavaises, M. Effect of Fuel Injection Processes on The Structure Of Diesel Sprays. SAE International Journal of Engines 1997.

(24) Hiroyasu, H.; Shimizu, M.; Arai, M. Breakup Length of A Liquid Jet And Internal Flow In A Nozzle. Iclass-91 1991.

(25) Soteriou, C., Andrews, R., and Smith, M. Direct Injection Diesel Sprays and the Effect of Cavitation and Hydraulic Flip on Atomization. SAE Technical Paper 950080, 1995.

(26) Tamaki, N.; Shimizu, M.; Hiroyasu, H. Enhancement of the Atomization of a Liquid Jet by Cavitation in a Nozzle Hole. Atomization and Sprays 2001, 11, 14.

(27) Shi, H.; Kleinstreuer, C. Simulation and Analysis of High-Speed Droplet Spray Dynamics. Journal of Fluids Engineering 2007, 129, 621.

(28) Anastopoulos, G.; Zannikou, Y.; Stournas, S.; Kalligeros, S. Transesterification Of Vegetable Oils With Ethanol And Characterization Of The Key Fuel Properties Of Ethyl Esters. Energies 2009, 2, 362-376.

(29) Hannab, M.; Maa, F. Biodiesel Production: A Review. Elsevier 1999, 70, 1-15.

(30) Biofuels - Biofuel Information - Guide to Biofuels http://biofuel.org.uk/ (accessed May 23, 2019).

(31) Taha, A.; Abdel-salam, T.; Vellakal, M. Alternative Fuels for Internal Combustion Engines: An Overview of the Current Research. International Energy and Environment Foundation 2013, 279-306.

(32)   Murugesan, A.; Umarani, C.; Subramanian, R.; Nedunchezhian, N. Bio-Diesel As An Alternative Fuel For Diesel Engines—A Review. Renewable and Sustainable Energy Reviews2009, 13, 653-662.

(33)   Payri, F.; Payri, R.; Salvador, F.; Martínez-López, J. A Contribution to The Understanding Of Cavitation Effects In Diesel Injector Nozzles Through A Combined Experimental And Computational Investigation. Computers & Fluids 2012, 58, 88-101.

(34)   Som, S.; Longman, D.; Ramírez, A.; Aggarwal, S. A Comparison of Injector Flow and Spray Characteristics of Biodiesel with Petrodiesel. Fuel 2010, 89, 4014-4024.

(35)   Dernotte, J.; Hespel, C.; Foucher, F.; Houillé, S.; Mounaïm-Rousselle, C. Influence of Physical Fuel Properties On The Injection Rate In A Diesel Injector. Fuel 2012, 96, 153-160.

(36)   Battistoni, M.; Grimaldi, C. Numerical Analysis of Injector Flow and Spray Characteristics from Diesel Injectors Using Fossil and Biodiesel Fuels. Applied Energy 2012, 97, 656-666.

(37)   Sheng, H.; Zhang, Z.; Wu, C. Study of Atomization and Micro-Explosion of Water-In-Diesel Fuel Emulsion Droplets in Spray within A High Temperature, High Pressure Bomb. 1990.

(38)   Yahaya Khan, M.; Abdul Karim, Z.; Hagos, F.; Aziz, A.; Tan, I. Current Trends In Water-In-Diesel Emulsion As A Fuel. The Scientific World Journal 2014, 2014, 1-15.

(39)   Wamankar, A.; Satapathy, A.; Murugan, S. Experimental Investigation Of The Effect Of Compression Ratio, Injection Timing & Pressure In A DI (Direct Injection) Diesel Engine Running On Carbon Black-Water-Diesel Emulsion. Energy 2015, 93, 511-520.

(40)   Ghojel, J.; Honnery, D.; Al-Khaleefi, K. Performance, Emissions And Heat Release Characteristics of Direct Injection Diesel Engine Operating on Diesel Oil Emulsion. Applied Thermal Engineering 2006, 26, 2132-2141.

(41)   Abu-Zaid, M. Performance Of Single Cylinder, Direct Injection Diesel Engine Using Water Fuel Emulsions. Energy Conversion and Management 2004, 45, 697-705.

(42)   Vellaiyan, S.; Amirthagadeswaran, K. The Role of Water-In-Diesel Emulsion and Its Additives on Diesel Engine Performance and Emission Levels: A Retrospective Review. Alexandria Engineering Journal 2016, 55, 2463-2472.

(43)   Park, J.; Huh, K.; Lee, J. Reduction of Nox, Smoke and Brake Specific Fuel Consumption with Optimal Injection Timing and Emulsion Ratio of Water-Emulsified Diesel. Proceedings of the Institution of Mechanical Engineers, Part D: Journal of Automobile Engineering 2001, 215, 83-93.

(44)   Lin, C. The Fuel Properties of Three-Phase Emulsions as an Alternative Fuel for Diesel Engines⋆. Fuel 2003, 82, 1367-1375.

(45)   Lin, C.; Chen, L. Comparison Of Fuel Properties and Emission Characteristics Of Two- And Three-Phase Emulsions Prepared By Ultrasonically Vibrating And Mechanically Homogenizing Emulsification Methods. Fuel 2008, 87, 2154-2161.

(46)   Lin, C.; Wang, K. Diesel Engine Performance and Emission Characteristics Using Three-Phase Emulsions As Fuel. Fuel 2004, 83, 537-545.

(47)   Lin, C.; Chen, L. Emulsification Characteristics of Three- And Two-Phase Emulsions Prepared By The Ultrasonic Emulsification Method. Fuel Processing Technology 2006, 87, 309-317.

(48)   Chen, G.; Tao, D. An Experimental Study of Stability of Oil–Water Emulsion. Fuel Processing Technology 2005, 86, 499-508.

(49)   Lif, A.; Holmberg, K. Water-In-Diesel Emulsions And Related Systems. Advances in Colloid and Interface Science 2006, 123-126, 231-239.

(50)   Tarlet, D.; Bellettre, J.; Tazerout, M.; Rahmouni, C. Prediction Of Micro-Explosion Delay Of Emulsified Fuel Droplets. International Journal of Thermal Sciences 2009, 48, 449-460.

(51)   Tran, T.; Ghojel, J. Impact Of Introducing Water Into The Combustion Chamber Of Diesel Engines On Emissions-An Overview. In Asia Pacific Conference on Combustion 2005; Adelaide University, 2005; pp. 33-36.

(52)   Watanabe, H.; Suzuki, Y.; Harada, T.; Matsushita, Y.; Aoki, H.; Miura, T. An Experimental Investigation of the Breakup Characteristics of Secondary Atomization Of Emulsified Fuel Droplet. Energy 2010, 35, 806-813.

(53)   Abu-Zaid, M. An Experimental Study of the Evaporation Characteristics of Emulsified Liquid Droplets. Heat and Mass Transfer 2003, -1, 1-1.

(54)   Han, Y.; Lee, K.; Min, K. A Study On The Measurement Of Temperature And Soot In A Constant-Volume Chamber And A Visualized Diesel Engine Using The Two-Color Method. Journal of Mechanical Science and Technology 2009, 23, 3114-3123.

(55)   Nadeem, M.; Rangkuti, C.; Anuar, K.; Haq, M.; Tan, I.; Shah, S. Diesel Engine Performance And Emission Evaluation Using Emulsified Fuels Stabilized By Conventional And Gemini Surfactants. Fuel 2006, 85, 2111-2119.

(56)   Ochoterena, R.; Lif, A.; Nydén, M.; Andersson, S.; Denbratt, I. Optical Studies Of Spray Development And Combustion Of Water-In-Diesel Emulsion And Microemulsion Fuels. Fuel 2010, 89, 122-132.

(57)   Ghojel, J.; Tran, X. Ignition Characteristics Of Diesel−Water Emulsion Sprays In A Constant-Volume Vessel: Effect Of Injection Pressure And Water Content. Energy & Fuels 2010, 24, 3860-3866.

(58)   Yatsufusa, T.; Kumura, T.; Nakagawa, Y.; Kidoguchi, Y. Advantage Of Using Water-Emulsified Fuel On Combustion And Emission Characteristics. 2009.

(59)   Selim, M.; Ghannam, M. Combustion Study Of Stabilized Water-In-Diesel Fuel Emulsion. Energy Sources, Part A: Recovery, Utilization, and Environmental Effects 2009, 32, 256-274.

(60)   Park, S.; Woo, S.; Kim, H.; Lee, K. The Characteristic Of Spray Using Diesel Water Emulsified Fuel In A Diesel Engine. Applied Energy 2016, 176, 209-220.

(61)   Attia, A.; Kulchitskiy, A. Influence Of The Structure Of Water-In-Fuel Emulsion On Diesel Engine Performance. Fuel 2014, 116, 703-708.

(62)   Ghannam, M.; Selim, M. Stability Behavior Of Water-In-Diesel Fuel Emulsion. Petroleum Science and Technology 2009, 27, 396-411.

(63)   Bidita, B.; Aien, N.; Suraya, A.; Mohd Salleh, M.; Idris, A. Effect Of Experimental Variables On The Combustion Characteristics Of Water-In-Diesel Emulsion Fuels. Journal of Dispersion Science and Technology 2014, 35, 185-192.

(64)   Patil, H.; Gadhave, A.; Mane, S.; Waghmare, J. Analyzing The Stability Of The Water-In-Diesel Fuel Emulsion. Journal of Dispersion Science and Technology 2014, 36, 1221-1227.

(65)   Hasannuddin, A.; Ahmad, M.; Zahari, M.; Mohd, S.; Aiman, A.; Aizam, S.; Wira, J. Stability Studies Of Water-In-Diesel Emulsion. Applied Mechanics and Materials 2014, 663, 54-57.

(66)   Huo, M.; Lin, S.; Liu, H.; Lee, C. Study On The Spray And Combustion Characteristics Of Water–Emulsified Diesel. Fuel 2014, 123, 218-229.

(67)   Lee, S.; Tanaka, D.; Kusaka, J.; Daisho, Y. Effects Of Diesel Fuel Characteristics On Spray And Combustion In A Diesel Engine. JSAE Review 2002, 23, 407-414.

(68)   Hagos, F.; A.Aziz, A.; Tan, I. Water-In-Diesel Emulsion And Its Micro-Explosion Phenomenon-Review. In 2011 IEEE 3rd International Conference on Communication Software and Networks; 2011.

(69)   Morozumi, Y.; Saito, Y. Effect Of Physical Properties On Microexplosion Occurrence In Water-In-Oil Emulsion Droplets. Energy & Fuels 2010, 24, 1854-1859.

(70)   Tarlet, D.; Bellettre, J.; Tazerout, M.; Rahmouni, C. Prediction Of Micro-Explosion Delay Of Emulsified Fuel Droplets. International Journal of Thermal Sciences 2009, 48, 449-460.

(71)   Fu, W.; Hou, L.; Wang, L.; Ma, F. A Unified Model For The Micro-Explosion Of Emulsified Droplets Of Oil And Water. Fuel Processing Technology 2002, 79, 107-119.

(72)   Fu, W.; Gong, J.; Hou, L. There Is No Micro-Explosion In The Diesel Engines Fueled With Emulsified Fuel. Chinese Science Bulletin 2006, 51, 1261-1265.

(73)   Vellaiyan, S.; K S, D. Combustion And Performance Characteristics Of Water-In-Diesel Emulsion Fuel. Energy Sources Part A Recovery Utilization and Environmental Effects 2015.

(74)   Dalziel, S.; Hughes, G.; Sutherland, B. Whole-Field Density Measurements By 'Synthetic Schlieren'. Experiments in Fluids 2000, 28, 322-335.

(75)   Gopal, V.; Klosowiak, J.; Jaeger, R.; Selimkhanov, T.; Hartmann, M. Visualizing The Invisible: The Construction Of Three Low-Cost Schlieren Imaging Systems For The Undergraduate Laboratory. European Journal of Physics 2008, 29, 607-617.

(76)   Hargather, M.; Settles, G. Natural-Background-Oriented Schlieren Imaging. Experiments in Fluids 2009, 48, 59-68.

(77)   Atcheson, B.; Heidrich, W.; Ihrke, I. An Evaluation Of Optical Flow Algorithms For Background Oriented Schlieren Imaging. Experiments in Fluids 2008, 46, 467-476.

(78)   Richard, H.; Raffel, M. Principle And Applications Of The Background Oriented Schlieren (BOS) Method. Measurement Science and Technology 2001, 12, 1576-1585.

(79)   Taylor, H.; Waldram, J. Improvements In The Schlieren Method. Journal of Scientific Instruments 1933, 10, 378-389.

(80)   Amrita, M. Principles and Techniques of Schlieren Imaging Systems. Columbia University Computer Science Technical Reports, cucs-016-13 2013.

(81)   Degen, N. An Overview On Schlieren Optics And Its Applications Studies On Mechatronics. ETH-Zürich 2012.

(82)   Gordon, W.; Ramesh, R.; Wolfgang, H. Hand-Held Schlieren Photography With Light Field Probes. 2011 IEEE International Conference on Computational Photography (ICCP) 2011.

(83)   Settles, G. Schlieren And Shadowgraph Techniques; Springer: [Place of publication not identified], 2013.

(84)   Interferometry https://en.wikipedia.org/wiki/Interferometry (accessed May 24, 2019).

(85)   http://heli-air.net/2016/04/21/wollaston-prism-interferometer/] (accessed May 24, 2019).

(86)   Davies, T. Schlieren Photography—Short Bibliography And Review. Optics & Laser Technology 1981, 13, 37-42.

(87)   Settles, G. Colour-Coding Schlieren Techniques For The Optical Study Of Heat And Fluid Flow. International Journal of Heat and Fluid Flow 1985, 6, 3-15.

(88)   Atcheson, B.; Heidrich, W.; Ihrke, I. An Evaluation Of Optical Flow Algorithms For Background Oriented Schlieren Imaging. Experiments in Fluids 2008, 46, 467-476.

(89)   Meier, G. Computerized Background-Oriented Schlieren. Experiments in Fluids2002, 33, 181-187.

(90)   Lens (optics) https://en.wikipedia.org/wiki/Lens_(optics) (accessed May 30, 2019).

(91)   Create Angle Measurement Tool Using ROI Objects- MATLAB & Simulink https://www.mathworks.com/help/images/create-angle-measurement-tool-using-roi-objects.html (accessed May 30, 2019).

(92)   https://www.researchgate.net/profile/Nachida_Bourabaa/publication/320762946
         (accessed Jun 10, 2019).

(93)   Schlieren photography https://en.wikipedia.org/wiki/Schlieren_photography
         (accessed Jun 10, 2019).

APPENDIX A

THE REFERENCE SECTION

A.1   Lens Relations

Most of the lenses can be classified as spherical lenses. Surfaces of the spherical lenses comprise of surfaces of spheres. These surfaces can be convex, concave, or planar. Axis of the lens is the line that connects the centers of the spheres. Unless the lens is manufactured to be shaped differently, the axis of the lens passes through the physical surface of the lens.

Another type of the lenses is toric lenses. They are also called as sphero-cylindrical lenses. Surfaces with two different radii of curvature in two orthogonal planes form the surfaces of toric lenses. They are used to fix the astigmatism in someone's eye.

If the surfaces of the lenses are neither in spherical shape nor in cylindrical shape, they are called as aspheric lenses. They help to capture images with less aberration when compared to the other lenses. However, they are difficult and expensive to be produced.

Lenses are classified according to the curvature of the two optical surfaces. If both surfaces are convex, the lens is called as biconvex lens. It the radius of curvature of the surfaces are equal to each other, the lens is called as equiconvex. If both surfaces are concave, the lens is called as biconcave lens. If one of the surfaces is flat, the lens is called as plano-convex or plano-concave. The meniscus lens consists of one convex surface and one concave surface. It is mostly used as corrective lens. Figure 5 represents us the type of the lenses visually (90).
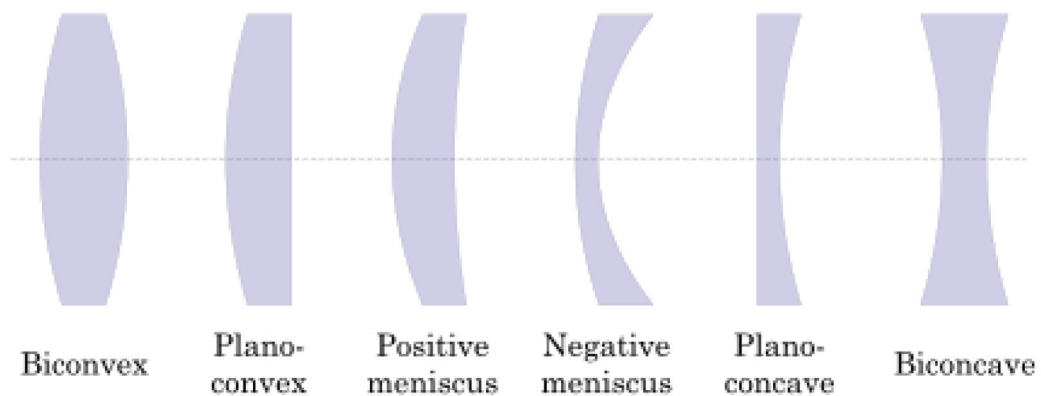
Figure A. 1. Types of Simple Lenses (Source: (90))

Since convex lenses and parabolic mirrors are being used in Schlieren, the general information about convex lenses is given briefly. A converging lens illustration is given at Figure 6.
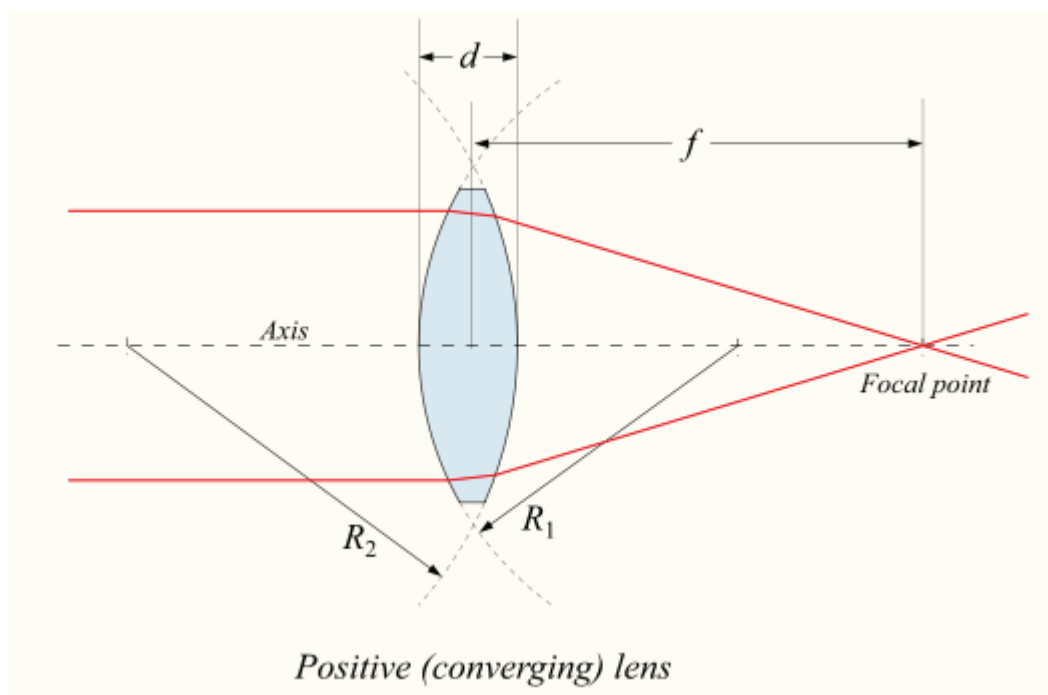
Figure A. 2. Convex Lens (Source: (90))

A converging lens, whether it is biconvex or plano-convex, collapses the collimated beam of light to a focus point behind the lens. The distance between the lens and the focus point is called as the focal length of the lens. It is depicted with f in diagrams and equations. Focal length is the characteristic specification of the lenses.

Focal length can be calculated by using Lensmaker's equation and it is defined by the following formula:

$$\frac{1}{f} = (n-1)\left[\frac{1}{R_1} - \frac{1}{R_2} + \frac{(n-1)d}{nR_1R_2}\right]$$ (1)

Where:

f: Focal Length of the Lens,

n: Refractive Index of the Lens Material,

R_1: Radius of the Curvature of the Lens Surface Closer to the Light Source,

R_2: Radius of Curvature of the Lens Surface Farther from the Light Source, and

d: Thickness of the Lens.
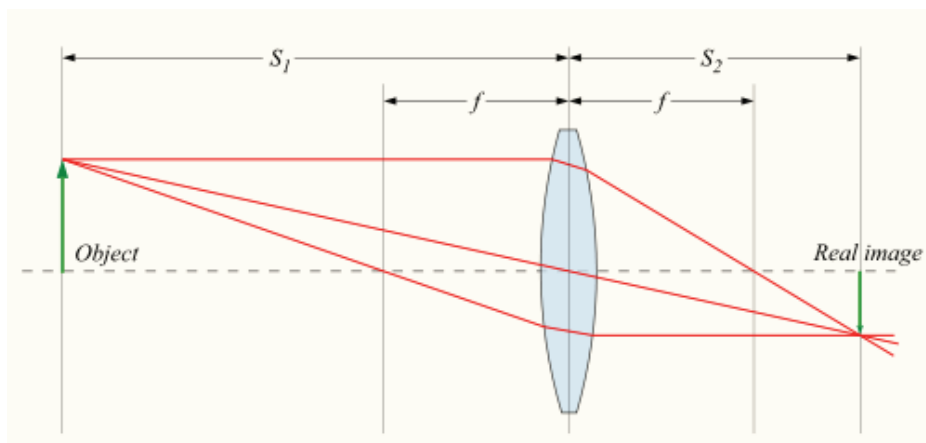

Figure A. 3. Imaging Properties of a Convex Lens (Source: (90))

Figure 7 shows us how image formation occurs in lenses. Imaging properties of a lens can be calculated by using the following formula.

$$\frac{1}{S_1} + \frac{1}{S_2} = \frac{1}{f}$$ (2)

Where:

S_1: The Distance from the Object to the Lens,

S_2: The Distance from the Lens to the Image, and

f: Focal Length of the Lens.

In order to obtain a real image, the distance from the object to the lens should be larger than the focal length of the lens. If it is smaller than the focal length of the lens, a virtual image is obtained behind the lens.

The lenses should be designed carefully to minimize the imperfections of the images. These imperfections are called as aberration. There are many types of aberration that affect the image quality such as spherical aberration and chromatic aberration (81,90).

A.2   Refraction

Refraction is the basic physical effect which makes the Schlieren visible. That's why it is important to understand refraction clearly. A simple light-ray deflection is shown in Figure 8.
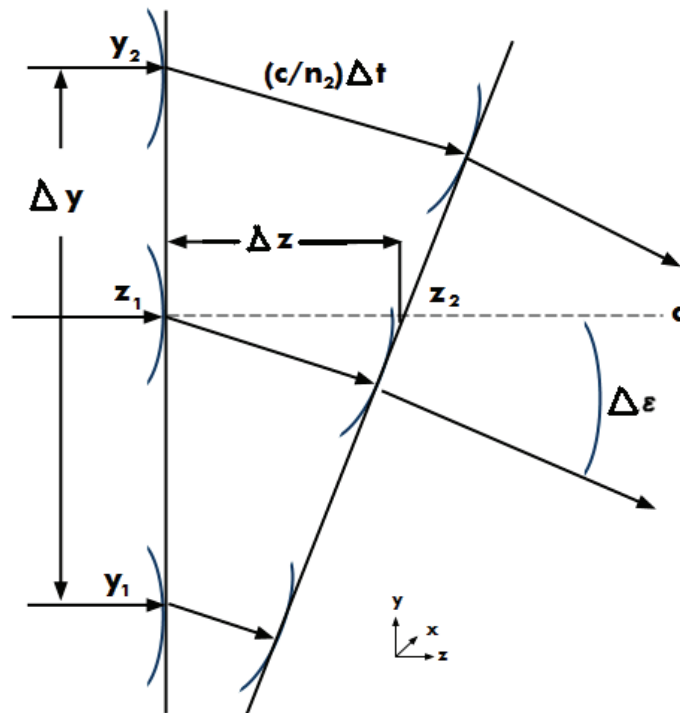

Figure A. 4. Light-Ray Deflection (Source: (80))

Schlieren light refraction can be presented simply by assuming a negative vertical refractive-index gradient, and no gradient neither in the x-direction nor z-direction.

$$\delta n / \delta y < 0 \tag{3}$$

A vertical planar light wave becomes shifted after moving through a Schlieren object as shown in Figure 8. It travels a differential distance in a differential time, $\Delta z / \Delta t$, and it is refracted through the differential angle, $\Delta \varepsilon$. The refractive index is a dimensionless number, and it is used to understand how fast light propagates through an object. It is described as the proportion of the speed of light in a vacuum to the local light speed.

$$n = \frac{c}{\vartheta} \tag{4}$$

Where:

n: Refractive Index,

c: Speed of Light in a Vacuum, and

ϑ: Local Light Speed.

From Figure 8, it can be noticed that $\Delta \varepsilon$ is found by using the following formula.

$$\Delta \varepsilon = \frac{c/n_2 - c/n_1}{\Delta y} \Delta t \tag{5}$$

After combining Eq. (5) with $\Delta t = \Delta z \frac{n}{c}$ and simplifying the equation, the following expression is obtained.

$$\Delta \varepsilon = \frac{n}{n_1 n_2} \frac{(n_1 - n_2)}{\Delta y} \Delta z \tag{6}$$

If all finite differences approach to zero, Eq. (6) becomes as follows.

$$\frac{d\varepsilon}{dz} = \frac{1}{n} \frac{dn}{dy} \tag{7}$$

Where:

$$d\varepsilon = \frac{dy}{dz} \tag{8}$$

Then, Eq. (7) becomes as follows.

$$\frac{\delta^2 y}{\delta z^2} = \frac{1}{n}\frac{\delta n}{\delta y} \tag{9}$$

Eq. (9) represents us the relation between the curvature of a refracted ray and the refractive-index gradient. By integrating the ray curvature of light rays in optical inhomogeneity in the appropriate directions, Schlieren images are found as a result of the following expression.

$$\varepsilon_y = \frac{1}{n}\int \frac{\delta n}{\delta y} \delta z \tag{10}$$

All of these expressions can be modified to find the component of the 2D gradient in the x-direction by replacing the y's with x's.

According to Eq. (9), refractive index does not affect directly the ray deflection. The gradient of the refractive index affects the ray deflection. In addition to this, Eq. (9) and Eq. (10) tell us that the light ray deflections are refracted towards the regions of higher refractive index (80, 81).

A.3   Resolution Improvements

In order to extract useful information from the images, resolution improvements can be applied. It is important to obtain higher quality Schlieren images. To achieve that, one needs to focus on spatial resolution, dynamic range, and noise level.

Spatial resolution refers to the clearness of lines in an image. Since the sensitivity of a system that contains extremely large or small object is highly affected by the spatial resolution level. In such a system, as the spatial resolution increases, the sensitivity of the system decreases. That's why, a more powerful and larger LED should be chosen as a light source so that the spatial resolution can be increased without affecting the sensitivity of the system. Another way to increase the spatial resolution is to use a sharp-focus or multi-source Schlieren system (80). Dynamic range refers to

difference in luminescence values. In order to adjust the dynamic range of the system, the image should be cut-off by a knife-edge or a colour filter before being captured (80). Noise cannot be avoidable in Schlieren imaging. Besides, as the spatial resolution increases, noise level increases. To reduce noise level while increasing the spatial resolution, a pulsed laser can be used to capture multiple images. After that, the images can be superimposed (80).

APPENDIX B

MATLAB ALGORITHM USED IN THIS STUDY

B.1   Matlab Algorithm for Spray Penetration

```matlab
clc, clear all;
vid=VideoReader('500bar_C1S0001.avi');
newVid=VideoWriter('NewVid_diesel_5_500');
a=vid.NumberOfFrames;
for i=1:a
    b=read(vid,i);
    c=rgb2gray(b);
    c1=rgb2gray(read(vid,1));
    d=imsubtract(c1,c);
    open(newVid);
    writeVideo(newVid,d);
end
close(newVid);
vid2=VideoReader('NewVid_diesel_5_500.avi');
newVid2=VideoWriter('diesel_5_500_pcalc');
f=[];
for j=1:a
    k=rgb2gray(read(vid2,j));
    level=graythresh(k);
    l=im2bw(k,0.1);
    [x y]=find(l, 1, 'last');
    m=insertMarker(k, [y x]);
    open(newVid2);
    writeVideo(newVid2,m);
    f=[f,((((sqrt((8-y).^2+(72-x).^2)))/47.297)*10)];
end
f=transpose(f);
xlswrite('diesel_5_500_pcalc',f);
close(newVid2);
```

B.2   Matlab Algorithm for Angle Measurement Tool

It is obtained from Mathworks (Sourcce: (91)).

```matlab
function my_angle_measurement_tool(im)
% Create figure, setting up properties
figure('Name','My Angle Measurement Tool',...
    'NumberTitle','off',...
```

```matlab
        'IntegerHandle','off');

% Display image in the axes % Display image
imshow(im)
axis on
% Get size of image.
m = size(im,1);
n = size(im,2);


% Get center point of image for initial positioning.
midy = 72;
midx = 8;


% Position first point vertically above the middle.
firstx = midx;
firsty = midy - ceil(m/16);
lastx = midx + ceil(n/4);
lasty = midy;


% Create a two-segment right-angle polyline centered in the image.
h = impoly(gca,[firstx,firsty;midx,midy;lastx,lasty],'Closed',false);
api = iptgetapi(h);
initial_position = api.getPosition()


% Display initial position
updateAngle(initial_position)


% set up callback to update angle in title.
api.addNewPositionCallback(@updateAngle);
fcn =
makeConstrainToRectFcn('impoly',get(gca,'XLim'),get(gca,'YLim'));
api.setPositionConstraintFcn(fcn);
%


% Callback function that calculates the angle and updates the title.
% Function receives an array containing the current x,y position of
% the three vertices.
function updateAngle(p)
% Create two vectors from the vertices.
% v1 = [x1 - x2, y1 - y2]
% v2 = [x3 - x2, Y3 - y2]
v1 = [p(1,1)-p(2,1), p(1,2)-p(2,2)];
v2 = [p(3,1)-p(2,1), p(3,2)-p(2,2)];
% Find the angle.
theta = acos(dot(v1,v2)/(norm(v1)*norm(v2)));
% Convert it to degrees.
angle_degrees = (theta * (180/pi));
% Display the angle in the title of the figure.
title(sprintf('(%1.0f) degrees',angle_degrees))
```

B.3   Matlab Algorithm for Angle Measurement

```matlab
clc,clear all;
a=imread('frame43.jpg');
my_angle_measurement_tool(a);
```